Development of a large animal model for percutaneous vertebroplasty for *in vivo* evaluation of a new injectable cement

Maria Teresa Carvalho Oliveira

Tese apresentada à Universidade de Évora
para obtenção do Grau de Doutor em Ciências Veterinárias

ORIENTADORES: *Professora Doutora Joana Margarida Ferreira da Costa Reis*
Professor Doutor José Alberto Caeiro Potes

ÉVORA, JUNHO DE 2017

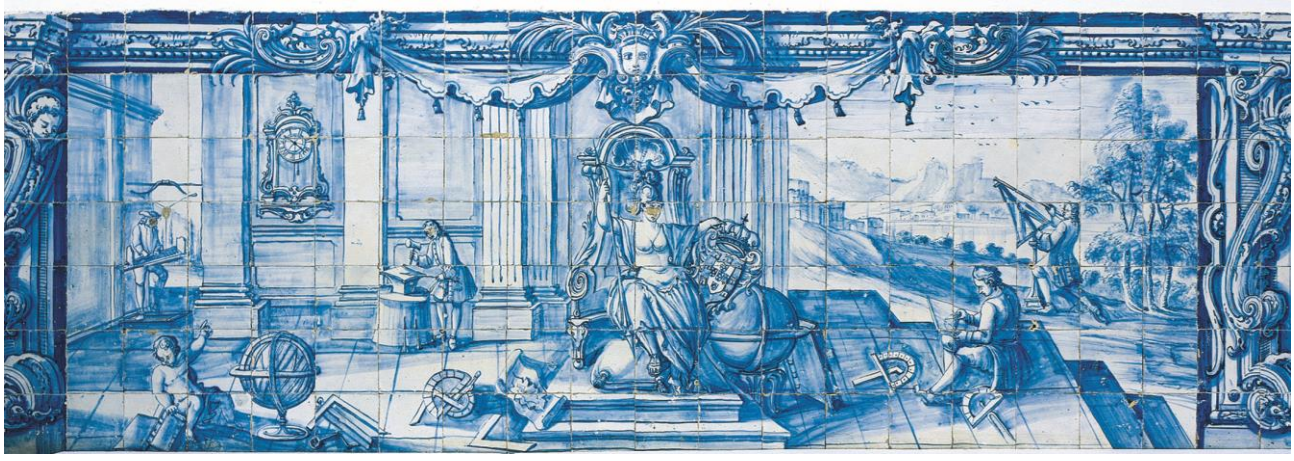

INSTITUTO DE INVESTIGAÇÃO E FORMAÇÃO AVANÇADA

Para ser grande, sê inteiro: nada

Teu exagera ou exclui.

Sê todo em cada coisa. Põe quanto és

No mínimo que fazes.

Assim em cada lago a lua toda

Brilha, porque alta vive.

Ricardo Reis

À memória dos meus avós

Aos meus amores

À minha família

Agradecimentos

O desenvolvimento e a execução deste trabalho não teriam sido possíveis sem o auxílio precioso de algumas pessoas e instituições. A todos, desde já, o meu muito obrigada.

O meu mais profundo agradecimento à minha orientadora, Professora Doutora Joana Reis, pela confiança que depositou continuamente em mim, até quando a mesma em mim teimava em falhar. Pela motivação e orientação constantes ao longo destes anos, dando-me sempre asas para voar.

Ao meu orientador, Professor Doutor José Potes, por toda a generosa e filantropa transmissão de conhecimentos, quer no âmbito deste projeto, quer no restante da minha actividade profissional, enquanto médica veterinária.

O meu agradecimento à Universidade de Évora, que apoiou financeiramente o meu trabalho através de uma bolsa individual de doutoramento, por sua vez suportada pela Comissão Europeia, ao abrigo do Sétimo Programa-Quadro, através do projeto RESTORATION – RESORBABLE CERAMIC BIOCOMPOSITES FOR ORTHOPAEDIC AND MAXILLOFACIAL APPLICATIONS–, ao abrigo da ação "SME-targeted Collaborative project", grant agreement NMP.2011.2.1-1.

Agradeço à Professora Doutora Maria Cristina Queiroga a ajuda preciosa nos trabalhos decorrentes do projeto, quer fosse nas cirurgias, quer no tratamento das ovelhas internadas no Hospital Veterinário. Mais agradeço todo o auxílio prestado na correção dos artigos publicados, uma e outra vez.

Ao Professor Doutor José Lopes de Castro agradeço toda a inestimável amizade e companheirismo demonstrados desde os primeiros dias de convivência. Muito obrigada pela sua entusiástica disponibilidade para todas as tarefas que lhe propúnhamos, mesmo quando se

afiguravam fora da sua área técnica. Obrigada ainda pela partilha de saberes e sabores da alma, uma constante ao longo destes anos.

Ao Professor Doutor Alfredo Franco Pereira, o meu muito obrigada por todo o auxílio prestado e transmissão de conhecimentos no tratamento e bem-querer das nossas "amigas", ao longo de todo este projeto. Não tenho qualquer dúvida que o seu trabalho, conjuntamente com o trabalho do Professor Lopes de Castro, foi fundamental para o sucesso inolvidável deste projeto.

Ao Professor Doutor Kenneth Dalgarno, da Universidade de Newcastle, e à Doutora Sarrawat Rehman, da JRI Orthopaedics, pela pronta disponibilidade que demonstraram para nos auxiliar nos testes mecânicos efetuados no decorrer do estudo *ex vivo*, tendo que, para isso, abandonar o conforto dos seus lares e famílias e vir até Portugal.

À Professora Doutora Chiara Vitale-Brovarone, do Politécnico de Turim, e ao Doutor Antonio Manca, da Unidade Radiológica do Instituto Oncológico Candiolo de Turim, pela amabilidade que tiveram em corrigir em tempo recorde o artigo "Novel mesoporous bioactive glass/calcium sulphate cement for percutaneous vertebroplasty and kyphoplasty: *in vivo* study", só assim tornando possível a entrega desta tese "a tempo e horas".

Ao Professor Doutor António Ramos, na representação do TEMA, da Universidade de Aveiro, por se ter disponibilizado para nos auxiliar na execução dos testes mecânicos das vértebras, abrindo-nos a porta da sua "casa" e acompanhando-me nesta minha aprendizagem.

Ao Professor Doutor António Completo, o meu agradecimento pelo convite dirigido à Professora Doutora Joana Reis e, posteriormente, estendido à minha pessoa, para a submissão do capítulo "Bone: functions, structure and physiology", inserido num livro, neste momento em fase de edição, intitulado de "The bone tissue computational mechanics - Biologic behaviour, remodelling algorithms and numerical applications".

O meu agradecimento também ao Pedro Pinto, pelos “rabiscos” perfeitos com que brindou este trabalho. Fê-los de maneira tão eficaz e célere que até se afigurou fácil.

À Dra. Sónia Lucena, por toda a amizade e companheirismo demonstrados no início desta aventura.

Aos colegas do Hospital Veterinário da Universidade de Évora e alunos que se encontravam em atividades hospitalares/ complementares, o meu muito obrigada por todo o auxílio prestado nas cirurgias e tratamentos dos animais.

À Leonor Pinho e à Margarida Costa, o meu eterno obrigada. Nunca me esquecerei dos nossos anos no HVUÉ, das nossas estórias, das nossas alegrias e tristezas, convivências e divergências, e todos os ingredientes que constroem relações duradouras.

O meu desmedido agradecimento ao João Fragoso e à Ana Bota por toda a amizade, companheirismo, motivação e ajuda disponibilizados desde sempre, quer no âmbito do projeto, quer fora dele. Vocês fazem parte da minha família de Évora.

O meu eterno obrigada às minhas amigas de coração, que mesmo longe estão perto, sempre à distância de um telefonema, e que são sempre as primeiras a quem recorro nos momentos mais difíceis. À Susana, minha companheira de viagem, obrigada pela paciência para ouvires os meus dilemas quando por vezes os teus se afiguram gigantes. À Ana Isabel, minha amiga desde sempre, que admiro enquanto mãe e profissional, e que continua a ser uma das minhas referências quando volto à minha terra-mãe. À minha prima Marta, pelo exemplo de força de mulher que é e dá. Todas lutamos e almejamos por vidas melhores, mais justas e plenas.

À minha família, de sangue e de coração, que em tempos de necessidade são os primeiros a acudir.

Aos meus pais, que fizeram de mim quem eu sou, e cujo apoio familiar foi imprescindível para me dar a serenidade de espírito suficiente e permitir abraçar uma empreitada deste tamanho. Sem eles, nada disto era possível.

À minha amada irmã, por toda a paciência e ajuda na correção de boa parte destes escritos.

Aos meus amores pequeninos, que sem quererem ou pedirem, se viram privados da mãe, mais do que, por vezes, a própria desejava. Amo-vos daqui até à Lua e voltar.

Ao Artur, o meu porto seguro, desde sempre e para sempre.

Nota: O conteúdo da presente tese foi parcialmente publicado ou submetido para publicação. Como tal, os capítulos 2, 3, 4, 5 e 6 encontram-se formatados de acordo com as normas de formatação e de referenciação bibliográfica das respetivas publicações. A indexação das secções, figuras e tabelas dos capítulos supracitados aparece de acordo com a ordem original, precedida pelo número do capítulo correspondente.

Index

List of figures

List of tables

Abbreviations

ADHR	Autosomal dominant hypophosphatemic rickets
ALP	Alkaline phosphatase
AOI	Area of interest
ASBMR	American Society for Bone and Mineral Research
BAr	Bone area
BCIS	Bone cement implantation syndrome
BMC	Bone mineral content
BMD	Bone mineral density
BMP	Bone morphogenetic protein
BMU	Basic multicellular unit
BRU	Bone remodelling unit
BSP	Bone sialoprotein
BS/BV	Specific surface
BTM	Bone turnover marker
BV/TV	Relative bone volume
Ca^{2+}	Calcium ions
CaS	Calcium sulphate
CHv	Caudal hemivertebra
CNS	Central nervous system
COX-2	Cyclooxygenase-2
CSR	Calcium-sensing receptor
CSH	α-Calcium sulphate hemihydrate
CTGF	Connective tissue growth factor
DAB	Diaminobenzidine
DGAV	Direcção Geral de Alimentação e Veterinária
ECG	Electrocardiograma
ECM	Extracellular matrix
EISA	Evaporation-induced self-assembly
FELASA	Federation of European Laboratory Animal Science Associations
FGF23	Fibroblast Growth Factor 23
GABA	Gamma-aminobutyric acid

GH	Growth hormone
HA	Hydroxyapatite
HVUE	Hospital veterinário da Universidade de Évora
IGF	Insulin-like growth factor
KP	Kyphoplasty
MAR	Mineral apposition rate
MBG	Mesoporous bioactive glass
M-CSF-1	Macrophage colony stimulating factor-1
Micro-CT	Micro-computed tomography
MSC	Mesenchymal stem cells
NSAID	Non-steroidal anti-inflamatory drug
NO	Nitric oxide
ODF	Osteoclast differentiation factor
OPG	Osteoprotegerin
OPN	Osteopontin
PFF	Pulsating fluid flow
PG	Proteoglycan
PGE2	Prostaglandin E2
Pi	Phosphorus ions
PMMA	Polymethylmethacrylate
PKP	Percutaneous kyphoplasty
PTH	Parathormone
PVP	Percutaneous vertebroplasty
RANK	Receptor activator of nuclear factor-κB
RANKL	Receptor activator of nuclear factor κB ligand
RESTORATION	Resorbable Ceramic Biocomposites for Orthopaedic and Maxillofacial Applications
ROI	Region of interest
Rt-PCR	Reverse transcription-polymerase chain reaction
Runx2	Runt-related transcription factor 2
SBF	Simulated body fluid
SMC	Smooth muscle cell
SPARC	Secreted protein acidic and rich in cysteine
TbN	Trabecular number

TbSp	Trabecular separation
TbTh	Trabecular thickness
TGF	Transforming growth factor
TIO	Tumour-induced osteomalacia
TIVA	Total intravenous anaesthesia
TRAP	Tartrate-resistant acid phosphatase
TSH	Thyroid stimulating hormone
TV	Tissue volume
T3	Triiodothyronine
T4	Thyroxine
VBH	Vertebral body height
VCF	Vertebral compression fracture
VOI	Volume of interest
[1,25$(OH)_2$D]	1,25 dihydroxyvitamin D_3 [1,25$(OH)_2D_3$]
2D	Two-dimensional
3D	Three-dimensional

Abstract

The present work aimed to test *in vivo* a new biomaterial for vertebral augmentation.

Vertebral compression fractures not healing with conservative management are treated through minimally invasive surgical techniques. Presently, most of the cements used in percutaneous bone interventions are based on a polymeric non-resorbable matrix. However, they can present some complications. Calcium suphate-based cements are effective bone substitutes. Disadvantages include their limited shear and compressive strength.

To go beyond the state of the art, a new bioactive calcium sulphate-based cement was developed – Spine-Ghost. To test the suitability of the injectable cement for percutaneous vertebroplasty, a preclinical study was mandatory.

A new large animal model for percutaneous vertebroplasty was developed in sheep. In the *ex vivo* model, bone defects were created in the cranial hemivertebrae through a bilateral modified parapedicular approach, and mechanical tests were performed. The *ex vivo* model is reproducible, and safe under physiological loads.

In the *in vivo* study, two groups of Merino sheep were defined (n=8): a) the control group, injected with a commercial ceramic cement; and b) the experimental group, injected with Spine-Ghost. Of the first interventioned animals, two presented cardiorespiratory distress during the cement injection, and one had mild neurologic deficits in the hindlimbs. All sheep survived and completed the 6-month implantation period.

After sacrifice, the samples were assessed by micro-computed tomography, histological, histomorphometric, and immunohistological studies. There was no evidence of cement leakage into the vertebral foramen. No signs of infection or inflammation were observed. Most importantly, there was cement resorption and new trabecular bone formation in the bone defects of all sheep.

The model of percutaneous vertebroplasty is considered suitable for preclinical *in vivo* studies, mimicking clinical application.

Spine-Ghost proved to be an adequate material for percutaneous vertebroplasty, with a biological response identical, if not superior, to the one elicited by the available commercial control.

Desenvolvimento de modelo animal superior para vertebroplastia percutânea para avaliação *in vivo* de um novo cimento injetável.

Sumário

O trabalho aqui apresentado teve por objetivo a avaliação *in vivo* de um novo biomaterial injetável para vertebroplastia a cifoplastia percutâneas.

As fraturas de compressão vertebral com indicação cirúrgica são tratadas com recurso a técnicas minimamente invasivas. Presentemente, a maioria dos cimentos utilizados baseiam-se numa matriz polimérica não reabsorvível. Podem, no entanto, causar algumas complicações. Os cimentos à base de sulfato de cálcio são substitutos ósseos eficazes, cujas desvantagens incluem resistência limitada a esforços de corte e compressão.

Um novo cimento bioativo de sulfato de cálcio – Spine-Ghost – foi desenvolvido. Para testar a sua aplicabilidade na vertebroplastia percutânea, tornou-se imperativo um estudo pré-clínico.

Para o efeito, um novo modelo animal para vertebroplastia percutânea foi desenvolvido em ovinos e sujeito a ensaios mecânicos. No modelo *ex vivo*, foram criados bilateralmente dois defeitos ósseos interligados, nas hemivértebras craniais, através de uma abordagem parapedicular modificada. O modelo *ex vivo* é reprodutível e seguro sob cargas fisiológicas.

No estudo *in vivo*, definiram-se dois grupos de ovelhas Merino (n=8): a) grupo controlo, injetado com cimento comercial de base cerâmica; b) grupo experimental, injetado com Spine-Ghost. Nos primeiros animais intervencionados, dois apresentaram alterações cardiorrespiratórias durante a injeção de cimento, e um défices neurológicos ligeiros nos membros pélvicos. Todos os animais sobreviveram e completaram o período de implantação de 6 meses.

Após a ocisão, as amostras foram avaliadas por microtomografia computorizada, histologia, histomorfometria e imunohistoquímica. Não se observou derrame de cimento para o canal vertebral, nem sinais de infeção ou inflamação. Ademais, verificou-se a reabsorção do cimento e a neoformação de tecido ósseo trabecular no interior dos defeitos ósseos, em todos os animais.

O modelo de vertebroplastia percutânea é considerado adequado para estudos pré-clínicos, mimetizando a aplicação clínica.

O Spine-Ghost demonstrou ser um biomaterial adequado para vertebroplastia percutânea, com uma resposta biológica idêntica, se não superior, à elicitada pelo controlo comercial.

Chapter 1

Introduction

1. Introduction

1.1. Context and objectives

Presently, it's reasonable to discuss biomedical research in an integrated, transdisciplinary way. The contemporary "One medicine – One health" concept implies that multidisciplinary teams of medical doctors, veterinarians, engineers, biologists, among other experts (Cook & Bal, 2014), share the responsibilities and synchronise local and global activities to address health problems at the animal-human-environment interfaces, either these problems concern the whole population or the individual, since a better understanding and a more adequate control of animal health (often through environmental management) potentially lead to less human risks (Kaplan *et al.*, 2008). The collaboration between the specialists from the different scientific areas is the vital key that will result in a better health for humans and animals in a near future.

The improvement of the living conditions and the aging of the world population, along with the evolution of medicine, led to the necessity of new approaches to pathologies and the development of novel therapeutics. Likewise, the evolution of animal healthcare and welfare and the subsequent raise of the life span of our pets and domestic animals triggered the increase of disorders commonly associated with geriatrics. These diseases occasionally can be compared with some human conditions, considering the interspecies similarities. Conditions like cancer, diabetes, asthma, orthopaedic disorders – like osteoarthritis and osteoporosis –, cardiovascular diseases, and neurologic diseases – like dementia – are thoroughly studied in companion animals, as well as in other species. These studies can be of benefit to both animal and human health, in the sense that they can generate longer, healthier lives for all species.

The testing of innovative biomaterials – for clinical application in orthopaedic surgery and other areas – in living and sentient animal models in direct benefit to the human race, must be the subject of careful planning and consideration, given the ethical conflict that arises. There are several currents of thought within the international scientific community, either for or against the use of animals. For example, the "Medical Research Modernization Committee" believes that animal testing is mainly driven by economic interests. Moreover, it says that animal testing should not be considered a valid method for medical research due to the anatomical, physiological and pathological differences between human and non-human (Anderegg, 2002). Bearing this in mind, in order to deepen the knowledge in bone structure and physiology, and responding to an invitation made by Professor Joana Reis, Chapter 2 was written. Nonetheless, numerous evidences show that animal testing is inexorable and an

important way to advance in science, by allowing the observation of the *in vivo* processes that otherwise would not be evaluated (Paul, 2001). This theme is succinctly approached in Chapter 3, in a small paper that was presented orally and published in the Proceedings of the "VI Congresso Nacional de Biomecânica".

In accordance to the previous insights, the present doctoral research work was integrated in a multidisciplinary European project – Resorbable Ceramic Biocomposites for Orthopaedic and Maxillofacial Applications [RESTORATION] – led by the University of Newcastle Upon Tyne, United Kingdom. This project involved several consortium partners, each with different tasks – from the development of the biomaterials, through the *in vitro* testing and the *in vivo* testing in the small animal model, until the *in vivo* testing in the large animal model.

The project's research team from the University of Évora, coordinated by Professor Joana Reis, was responsible for the development and application of the large animal models and ulterior biomaterials testing. Encompassing the different models, a total of 40 Merino sheep were intervened. All animals were daily assessed and taken care by members of the research team, for over 6 months. After the sacrifice of the animals, the samples were collected and processed for ulterior analysis. This work is the result of multiple tasks, such as sheep handling and care, surgery planning and performance, postoperative animal care, and bone samples processing and evaluation. For confidentiality reasons imposed on the Consortium partners, in this thesis the only shown data are those relative to vertebroplasty, even though this was just one of the models developed. Nevertheless, other surgical models were implemented and biomaterials assessed.

The entire project was designed and developed respecting the prevailing European legislation for the protection of animals used for scientific purposes – Directive 2010/63/EU (Official Journal of the European Union, 2010) –, and the Federation of European Laboratory Animal Science Associations [FELASA] guidelines (Mähler *et al.*, 2014), which follows the 3R's recommendations of replacement, reducing and refinement of animals. Consortium partners' local laws were also respected; hence, the work regarding the large animal models was developed under the Portuguese law decree – Decreto-Lei nº 113/2013 (Diário da República, 2013).

Accordingly, researchers are advised to minimize the use of animals through Replacement – e.g. with computational models, *in vitro* studies, studies in invertebrates –; Reducing – e.g. with proper study's experimental design, pilot tests, *ex vivo* studies, and the use of non-invasive techniques of diagnostic, like ultrasonography, fluoroscopy, radiology and

fluorochromes, which allows the collection of data from the same animal at different experimental time points –; and methodology Refinement, in such a way that the pain, suffer and anxiety inflicted to the animals are reduced to minimum levels. At this time, it is important to refer the responsibility of all the team researchers, as well as their experience and technical knowledge as imperative requisites to be able to recognize the distinct behaviours of each chosen experimental species and to prevent and minimize the negative impact over the individuals, not only acting when the distress or pain are installed, but also assuming a proactive attitude and avoiding unnecessary noxious stimulus or manipulations.

In consideration of the foregoing, it is within the 3R's concepts that the veterinarian role assumes utmost importance in basic science's research, through the development of new better models and other refinement techniques, in a synergy with the other researchers – e.g. physicians, engineers, and biologists –, which help to minimize the animal usage. This way, in addition to contribute to the progress of medicine, the veterinarian guarantees the best health care to the experimental animals. Therefore, it is of utter importance the investment in veterinary science as a mean to a general medical benefit, diminishing the gap between animal models and clinical trials and profiting every species (Cook *et al.*, 2010; Vainio, 2012; Baird *et al.*, 2013).

Finally, the ultimate purpose of the project was to evaluate, in a controlled *in vivo* study, the bone response to a novel resorbable calcium sulphate injectable bone cement, developed by one of the consortium partners for application in percutaneous vertebroplasty. As in the clinical context, the biomaterial was to be injected in a vertebral body defect through a minimally invasive procedure. Considering the difficulties and limitations found in previous techniques and studies (Zhu *et al.*, 2011; Galovich *et al.*, 2011; Benneker *et al.*, 2012; Verron *et al.*, 2014), the development of a new reproducible and feasible preclinical model for percutaneous vertebroplasty in sheep was mandatory. The use of sheep is largely accepted due to its translational features regarding the human species, besides its availability, low cost, easy handling and good homogeneity when selected for age, race and gender. In addition, sheep are considered a good model for orthopaedic research due to its anatomical similarities when compared to the human model, when it comes to the size, weight, skeletal structure, bone remodelling and biomechanical behaviour of the bone, also consenting the use of some of the same prosthetic material (Alini *et al.*, 2008; Li *et al.*, 2015; Wancket *et al.*, 2015). Chapter 4 presents an article describing the development of the *ex vivo* model and chapter 5 the *in vivo* application of the previously developed model for the novel biomaterial testing.

In the past two decades, the development of bone fillers and cements as bone substitutes for trauma and orthopaedic surgery saw an exponential growth due to the overall gratifying results (Kopylov *et al.*, 1996; Goodman *et al.*, 1998; Wolfe *et al.*, 1999; Jubel *et al.*, 2004; Cassidy *et al.*, 2003; Poitout, 2016).

Up to date, most of the cements used in orthopaedic surgery are based on a polymeric matrix – polymethylmethacrylate (PMMA) (Magnan, 2013; Puoci, 2015). These cements have been thoroughly used and investigated over the years, mainly for its immediate effect and safety, but they also present some limitations, such as high polymerization temperatures, low bioactivity, bioinertia, absence of resorbability, and high elastic modulus. These properties are related to the – relatively rare – complications that have been documented with the use of PMMA. For instance, the high polymerization temperatures potentially induce inflammation and/or necrosis of the neighbour structures; likewise, the formation of new healthy tissue is hindered by the cement's the low bioactivity. Another syndrome, known as Bone Cement Implantation Syndrome (BCIS), is described as a possible complication of PMMA injection during total hip arthroplasty and vertebroplasty/kyphoplasty. It occurs around the cement injection, secondary to medullary fat embolism, and is characterized by hypoxia and/ or hypotension, with or without unexpected loss of consciousness and ultimately death. Finally, subsequent fractures of the contiguous vertebrae are also described as complications, due to the cement's high elastic modulus (Becker *et al.*, 2014; Puoci, 2015).

Synthetic ceramics are widely known and are proved to be safe and effective in bone substitution, since they are highly biocompatible, resorbable, and osteoconductive, displaying mechanical properties similar to those of the cancellous bone, with reduced Young's Modulus, and a low risk of infection or donor site morbidity (Campana *et al.*, 2014). They also present low setting temperatures and short setting times. Some disadvantages include their limited shear and compressive strength, when compared to those of the normal bone (Campana *et al.*, 2014; Gupta *et al.*, 2015). To overcome these limitations, ceramics are most of the times combined with other composites (Campana *et al.*, 2014). Numerous different formulations are commercially available, like different-sized granules, blocks, and injectable pastes. Furthermore, currently there is an investment in developing new composites that can act as delivery vehicles for cells, growth factors and antibiotics into fractures (Waselau *et al.*, 2007; Larsson *et al.*, 2011; Campana *et al.*, 2014).

Calcium sulphate-based injectable ceramics present themselves as good alternatives to PMMA, concerning vertebroplasty/kyphoplasty. Calcium sulphate offers an effective, low cost gap filler, by allowing vascular ingrowth and by being resorbable, thus allowing new bone

formation (Kumar *et al.*, 2013); it's also known for being osteoconductive and osteoinductive. Disadvantages include the – sometimes – too fast resorption (6-8 weeks) and secondary inflammatory reaction (Larsson *et al.*, 2011; Kumar *et al.*, 2013; Campana *et al.* 2014). Subsequently calcium sulphate, like other ceramics, is widely used mixed with other biomaterials.

To progress beyond the state of the art in terms of available calcium sulphate cements for percutaneous vertebroplasty, a novel bioactive injectable cement for percutaneous vertebroplasty was developed – Spine-Ghost (Vitale-Brovarone *et al.*, 2015). Spine-Ghost was implanted into a sheep vertebral defect model. The performance was compared to a commercial biphasic cement – Cerament™|Spine Support. Cerament™'s application for vertebral compression fractures (VCFs) has been well documented (Marcia *et al.*, 2014). Spine-Ghost supported new bone formation into the vertebral body defect, while slowly biodegraded, suggesting it allows a safe and unpainful medical recovery, thus reducing pain and morbidity. Chapter 6 presents the final *in vivo* study and the biological response to the biomaterial.

1.2. References

Anderegg, C. (2002). "A critical look at animal experimentation", Medical Research Modernization Committee.

Baird, A. W., Rathbone, M. J., & Brayden, D. J. (2013). Human: Veterinary Technology Cross Over. In Long Acting Animal Health Drug Products (pp. 359-375). Springer US.

Benneker, L. M., Gisep, A., Krebs, J., Boger, A., Heini, P. F., & Boner, V. (2012). Development of an *in vivo* experimental model for percutaneous vertebroplasty in sheep. *Veterinary and Comparative. Orthopaedics and Traumatololy V.C.O.T., 25* (3), 173-177.

Cassidy, C., Jupiter, J. B., Cohen, M., Delli-Santi, M., Fennell, C., Leinberry, C., Husband, J., Ladd, A., Seitz, W. R., & Constanz, B. (2003). Norian SRS cement compared with conventional fixation in distal radial fractures. A randomized study. *Journal of Bone and Joint Surgery. American volume, 85*(11), 2127–2137.

Cook, J. L., Kuroki, K., Visco, D., Pelletier, J. P., Schulz, L., & Lafeber, F. P. J. G. (2010). The OARSI histopathology initiative–recommendations for histological assessments of osteoarthritis in the dog. *Osteoarthritis and cartilage*, *18*, S66-S79.

Cook, J. L., & Bal, B. S. (2014). The Clinical Biomedical Research Advances Achievable Utilizing One Health Principles. In Confronting Emerging Zoonoses (pp. 233-239). Springer Japan.

Decreto-Lei nº 113/2013, de 7 de Agosto. Diário da República, 1.ª série — N.º 151. Ministério da Agricultura, do mar, do ambiente e do ordenamento do território, Lisboa.

Directive 2010/63/EU. (2010). *Official Journal of the European Union*, L276/33-79, ISSN 1725-2601.

Galovich, L. A., Perez-Higueras, A., Altonaga, J. R., Gonzalo Orden, J. M., Barba, M. M., & Morillo, M. C. (2011). Biomechanical, histological and histomorphometric analyses of calcium phosphate cement compared to PMMA for vertebral augmentation in a validated animal model. *European Spine Journal*, *20*(3), 376-382.

Goodman, S. B., Bauer, T. W., Carter, D., Casteleyn, P. P., Goldstein, S. A., Kyle, R. F., Larsson, S., Stankewich, C. J., Swiontkowski, M. F., Tencer, A. F., Yetkinler, D. N., &

Poser, R. D. (1998). Norian SRS cement augmentation in hip fracture treatment. Laboratory and initial clinical results. *Clinic Orthopaedics and Related Research, 348*, 42–50.

Gupta, A., Kukkar, N., Sharif, K., Main, B. J., Main, B. J., Albers, C. E., & El-Amin Iii, S. F. (2015). Bone graft substitutes for spine fusion: A brief review, *World Journal of Orthopaedics*, *6*(6), 449-456.

Jubel, A., Andermahr, J., Mairhofer, J., Prokop, A., Hahn, U., & Rehm, K. E. (2004). Use of the injectable bone cement Norian SRS for tibial plateau fractures. Results of a prospective 30-month follow-up study. *Der Orthopäde*, *33*(8), 919–927.

Kaplan, B., Kahn, L. H., & Monath, T. P. (2008). The brewing storm. *Veterinaria italiana*, *45*(1), 9-18.

Kopylov, P., Jonsson, K., Thorngren, K. G., & Aspenberg, P. (1996). Injectable calcium phosphate in the treatment of distal radial fractures. *The Journal of hand surgery (British and European Volume)*, *21*(6):768–771.

Larsson, S., & Hannink, G. (2011). Injectable bone-graft substitutes: current products, their characteristics and indications, and new developments. *Injury*, *42*, S30-S34.

Li, Y., Chen, S. K., Li, L., Qin, L., Wang, X. L., & Lai, Y. X. (2015). Bone defect animal models for testing efficacy of bone substitute biomaterials. *Journal of Orthopaedic Translation*, *3*(3), 95-104.

Kumar, C. Y., Nalini, K. B., Jagdish Menon, D. K. P., & Banerji, B. H. (2013). Calcium sulfate as bone graft substitute in the treatment of osseous bone defects, a prospective study. *Journal of clinical and diagnostic research: JCDR*, *7*(12), 2926-2928.

Magnan, B., Bondi, M., Maluta, T., Samaila, E., Schirru, L., & Dall'Oca, C. (2013). Acrylic bone cement: current concept review. *Musculoskeletal surgery*, *97*(2), 93-100.

Mähler, M., Berard, M., Feinstein, R., Gallagher, A., Illgen-Wilcke, B, Pritchett-Corning K, Raspa M (2014). FELASA recommendations for the health monitoring of mouse, rat, hamster, guinea pig and rabbit colonies in breeding and experimental units. *Laboratory Animals*, 0023677213516312.

Marcia, S., Boi, C., Dragani, M., Marini, S., Marras, A., Piras, E., Anselmetti, G., & Masala, S. (2012). Effectiveness of a bone substitute (CERAMENT^{TM}) as an alternative to PMMA in percutaneous vertebroplasty: 1-year follow-up on clinical outcome, *European Spine Journal, 21*(1), 112–118.

Paul, E.F., Paul, J. (eds.) (2001). "Why Animal Experimentation Matters: The Use of Animals in Medical Research", Transaction Publishers.

Vainio, O. (2012). Translational animal models using veterinary patients–An example of canine osteoarthritis (OA). *Scandinavian Journal of Pain, 3*(2), 84-89.

Verron, E., Pissonnier, M. L., Lesoeur, J., Schnitzler, V., Fellah, B. H., Pascal-Moussellard, H., Pilet, P., Gauthier, O., & Bouler, J. M. (2014). Vertebroplasty using bisphosphonate-loaded calcium phosphate cement in a standardized vertebral body bone defect in an osteoporotic sheep model. *Acta biomaterialia, 10*(11), 4887-4895.

Vitale-Brovarone C., Pontiroli L., Novajra G., Tcacencu I., Reis J., Manca A. (2015). Spine-Ghost: a new bioactive Cement for Vertebroplasty. *Key Eng Mat, 631*, 43-47.

Wancket, L. M. (2015). Animal Models for Evaluation of Bone Implants and Devices Comparative Bone Structure and Common Model Uses. *Veterinary pathology, 52*(5), 842-850.

Waselau, M., Samii, V. F., Weisbrode, S. E., Litsky, A. S., & Bertone, A. L. (2007). Effects of a magnesium adhesive cement on bone stability and healing following a metatarsal osteotomy in horses. *American Journal of Veterinary Research, 68*(4), 370-378.

Wolfe, S. W., Pike, L., Slade, J. F. III, & Katz, L. D. (1999). Augmentation of distal radius fracture fixation with coralline hydroxyapatite bone graft substitute. *The Journal of hand surgery, 24*(4):816–827.

Zhu, X.S., Zhang, Z.M., Mao, H.Q., Geng, D.C., Zou, J., Wang, G. L., Zhang, Z. G., Wang, J. H., Chen, L., & Yang, H. L. (2011). A novel sheep vertebral bone defect model for injectable bioactive vertebral augmentation materials. *Journal of Materials Science: Materials in Medicine 22*(1), 159-164.

Chapter 2

Bone: functions, structure and physiology

Accepted for publication in July 2016 as a chapter of the book "The bone tissue computational mechanics - Biologic behaviour, remodelling algorithms and numerical applications", in the book series entitled: Lecture Notes in Computational Vision and Biomechanics, Springer.

Bone: functions, structure and physiology

Maria Teresa Oliveira[1] and Joana da Costa Reis[2]

Abstract The bone is reviewed regarding its functions, regulation, morphological structure and physiology; addressing how complex, how responsive to external and internal stimuli, and how intimately intertwined with other organs it is. From embryogenesis to endocrine regulation and bone remodelling, an overall view is presented. Special emphasis is given to how cell structure and tissue organization contribute to the response to mechanical stimuli.

1. Introduction

Bones are dynamic structures. They vary in shape, size and number, and are divided in axial and appendicular skeleton. Through life they are subjected to loads and strains that induce their shape, with old matrices being replaced by newly formed ones. This process is important for maintaining bone volume and strength. In the case of fractures, bones are capable of healing, as long as stability and alignment are assured.

It is the entanglement of environment, cell-to-cell interactions and cell-extracellular matrix interactions that direct and model osteogenesis, bone repair and remodelling.

Mechanical forces are essential in early embryonic development. There is evidence that morphogenesis is regulated through fluid flow mechanisms and by cellular contractility. Cells generate tensional forces through contraction of actin-myosin cytoskeleton filaments, which are transmitted through cadherin-mediated adhesion sites to neighbour structures, these being either cells or extracellular matrix. Cohesivity determines morula contraction and the definition of multiple layers - with the development of endoderm, mesoderm and ectoderm in the blastula - and thus early embryo shaping (Oster et al., 1983; Takeichi, 1988; de Vries et al., 2004;

[1] Maria Teresa Oliveira
Universidade de Évora, Largo dos Colegiais, Évora, email: teresoliveira@uevora.pt

[2] Joana da Costa Reis
Universidade de Évora, Largo dos Colegiais, Évora, email: jmfcr@uevora.pt

Ingber, 2006). The stress-dependent changes in cytoskeletal conformation and cell shape act locally to regulate cell phenotype, of utter importance are interactions with the extracellular matrix (Ingber, 2006). Unidirectional fluid flow, dependent on the specialized motor protein complex dynein, determines organ lateralization and asymmetry, by causing differences in key molecules expression (such as the TGF-family signalling molecules) (Collignon et al., 1996, Okada et al., 1999; Cartwright et al., 2004, Nakamura et al., 2006). Lateralization may also depend on fluid shear, in the embryo, by acting on a group of non-motile cilia, coupled to calcium channels; fluid shear may cause the intracellular calcium concentrations to rise and initiate the cascade of events responsible for lateralization (McGrath et al., 2003).

The mechanical environment is also determinant for vasculogenesis, angiogenesis (Schmidt et al., 2007; le Noble et al., 2008; Patwari and Lee, 2008), and neuronal development (Bray, 1979; Dennerll et al., 1989; Anava et al., 2009).

The embryo mesoderm is constituted by spindle or star-shaped cells called mesenchymal stem cells (MSCs). MSCs are the most pluripotential cells in the organism, giving rise to different tissues such as the connective tissue, muscle, cardiovascular tissue and the entire skeletal system. Bone, cartilage, tendons and ligaments develop through mechanisms of proliferation, migration and differentiation, but also apoptosis (Carter and Beaupré, 2001).

For a long time, bone was generally regarded as a less interesting organ, but we are only now starting to address how complex it is in its functions, its responsiveness to external and internal stimuli, and its intimate intertwining with other organs.

2. And yet it moves

2.1 Bone functions

Bone or osseous tissue is the most rigid and resilient tissue of the body. Constituted by dense connective tissue, it's the primary tissue of the skeleton, thus providing structure, support, and protection to vital organs, like the brain (skull), the spinal cord (vertebrae), and the heart and lungs (ribs and sternum). Moreover, the vertebrae participate in the spine shock absorbance – providing adequate load cushioning for the intervertebral disks (fibrocartilaginous joints) –, whilst long bones, along with the joints, enable body movement – providing levers for the muscles.

Additionally, bones act as the major source of blood, since haematopoiesis occurs in their medullary cavity. In infants, the bone marrow of all long bones is capable of this synthesis. As a person gets older, part of the red marrow turns into yellow fatty marrow, no longer capable of haematopoiesis. Functional red marrow in adults is restricted to the vertebrae and the extremities of femur and tibia.

Bones also have an important role as:

- Mineral storage: mostly calcium (Ca^{2+}), phosphate (Pi), and magnesium; it plays an important metabolic role, regulating mineral homeostasis (Bélanger et al., 1968; Zallone et al., 1983; Teti & Zallone, 2009), a process mediated by many hormones.
- Growth factor storage: insulin like growth factors 1 and 2 (IGF-1 and IGF-2), transforming growth factor-beta (TGF-β), acidic and basic fibroblast growth factor, platelet-derived growth factor, and bone morphogenetic proteins have been isolated from bone matrix (Mohan & Baylink, 1991). Osteoblasts have been shown to produce many of these growth factors and their production is regulated by systemic hormones and local mechanical stress (Baylink et al., 1993).
- Adipose tissue storage (yellow bone marrow as a fatty acid/ energy reserve) (Rosen et al., 2009; Krings et al., 2012; Suchacki et al., 2016).
- Acid-base balance, as it buffers the blood against excessive pH changes by absorbing or releasing alkaline salts (Green & Kleeman, 1991; Arnett et al., 2003; Bushinsky & Krieger, 2015).
- Heavy metal and other foreign elements storage, after detoxification from the blood, that are, later on, excreted (Roelofs-Iverson et al., 1984; Sharma et al., 2014).
- Endocrine organ, as it produces two known circulating hormones:
    a. Fibroblast Growth Factor 23 (FGF23): produced mainly by osteocytes (Rhee et al., 2011), but also by osteoblasts (Masuyama et al., 2006), acts on the kidney to inhibit 1α-hydroxylation of vitamin D and promote phosphorus excretion in urine (Shimada et al., 2004; Fukumoto & Martin, 2009; Haussler et al., 2012). FGF23 also inhibits phosphorus absorption in the intestine, thus regulating inorganic phosphate metabolism and mineralization (Feng et al., 2006). It is now acknowledged that the serum calcium concentration regulates FGF23 production (David et al., 2013), thus making FGF23 into a calcium-phosphorus regulatory hormone (Lopez et al., 2011; Rodriguez-Ortiz et al., 2012). Hence, FGF23 excess or deficiency results in several abnormalities of phosphate metabolism. Excess FGF23 inhibits renal phosphate reabsorption and 1,25 dihydroxyvitamin D_3 [$1,25(OH)_2D$] production, leading to hypophosphatemia and suppression of circulating $1,25(OH)_2D$ levels and, ultimately, rachitic changes in bone (Fukumoto & Yamashita, 2007), such as happens in autosomal dominant hypophosphatemic rickets and osteomalacia (ADHR) and in the paraneoplastic syndrome called tumour-induced osteomalacia (TIO). In contrast, reductions in FGF23 cause the syndrome of tumoral calcinosis (Shimada et al., 2001), characterized by hyperphosphatemia, increased $1,25(OH)_2D$ and soft tissue calcifications (Lyles et al., 1988; Fukumoto & Yamashita, 2007). An obligate FGF23 coreceptor was identified –Klotho– (Urakawa et al., 2006). Klotho is required to activate FGF

receptors and their signalling molecules. Secreted Klotho suppresses, by itself, activity of insulin, insulin-like growth factor-1 (IGF-1) (Kurosu et al., 2005), Wnt (Liu et al., 2007), and TGF-β1 (Doi et al., 2011) by interacting with these growth factors or their receptors. The resulting FGF23-Klotho axis represents a specialized system responsible for the external and internal Ca^{2+} e P_i balance in the bone, intestine and kidney. FGF23-Klotho axis works under parathormone regulation, since parathormone directly promotes FGF23 expression by osteocytes (Quarles et al., 2012), whereas balance is sought by FGF23 inhibiting action on parathyroid glands (Ben-Dov et al., 2007; Krajisnik et al., 2007).

b. Osteocalcin: a protein produced by osteoblasts in bone, major regulator of insulin secretion by direct action over the pancreatic β-cell, and increasing sensitivity of peripheral tissues, e.g. muscles and liver, enhancing glucose uptake and energy expenditure, thus intervening in glycaemia regulation (Lee & Karsenty, 2008; Ferron et al., 2008; Ferron et al., 2010; Fulzele et al., 2010); it also acts on adipocytes to increase adiponectin, thus reducing fat deposition (Ribot et al., 1987; Reid et al., 1992). Furthermore, studies on clinical diabetes have shown that blood osteocalcin levels are significantly lower in diabetics, when compared to non-diabetic controls, and that these levels are inversely related to fat mass and blood glucose (Kindblom et al., 2009; Pittas et al., 2009). Lastly, osteocalcin shows some influence in male fertility, by enhancing testosterone production by Leydig cells in the testes (Oury et al., 2011).

2.2 Regulation of bone metabolism (modelling/ remodelling)

Bone functions, like (re)modelling and fracture repair, are accomplished by four types of cells: osteoblasts, bone lining cells, osteocytes and osteoclasts. These processes are regulated locally by cytokines and growth factors, and systemically by hormones, neuropeptides and other mediators (Harada and Rodan, 2003; Karsenty et al., 2009).

2.2.1 Parathormone (PTH), Vitamin D and calcitonin:

The regulation of the bone mineral metabolism (calcium and phosphorus) results from the interplay between parathormone (PTH), calcitonin, FGF23 and vitamin D. PTH is released from the parathyroid glands in response to low levels of extracellular ionized calcium, through the presence of specific cell-surface calcium-sensing receptor (CSR) on the glands. High levels of PTH cause the increase of the number of osteoclasts, and resorption of bone matrix, with consequent release of calcium phosphate and increasing calcaemia. Inversely, low levels of PTH cause the elevation of osteoblast numbers. It also acts over osteoblasts' receptors, thus stimulating osteoblasts to stop synthetizing collagen, and to inhibit the secretion of stimulating factor by osteoclasts (Calvi et al., 2003). At renal level PTH, stimulated

by low plasma calcium, inhibits phosphate reabsorption and accelerates its excretion, stimulates calcium reabsorption, and upregulates a hydroxylase enzyme (CYP27B1), thus stimulating the final step of $1,25(OH)_2$ vitamin D_3 synthesis (Murayama et al., 1998).

Circulating hormonal metabolite, 1α,25-dihydroxyvitamin D_3 ($1,25(OH)_2D_3$) originates an activated complex that enhances several physiological functions, including intestinal calcium and phosphate absorption, bone phosphate and calcium resorption, and renal calcium and phosphate reabsorption, which results in a rise in the blood calcium and phosphate, required for bone passive mineralization of unmineralized bone matrix to occur (Haussler et al., 1998; Saini et al., 2013). Additionally, $1,25(OH)_2D_3$ stimulates differentiation of osteoblasts and the expression of several bone proteins, like bone-specific alkaline phosphatase, osteocalcin, osteonectin, osteoprotegerin, and other cytokines; and influences the proliferation and apoptosis of other skeletal cells, including hypertrophic chondrocytes (Clarke, 2008).

Calcitonin is produced by parafollicular cells of the thyroid, in direct relationship to extracellular calcium, through the same sensor that regulates the production of PTH. It inhibits matrix resorption, promotes calcium and phosphate excretion, thus reducing calcium and phosphate serum levels; calcitonin has an inhibiting effect over osteoclast mobility and over the secretion of proteolytic enzymes through its receptor on osteoclasts (Boissy et al., 2002; Hadjidakis & Androulakis, 2006).

2.2.2 Growth hormone (GH):

Growth hormone, or somatotropin, is produced in the anterior hypophysis, stimulates growth in general, particularly over the epiphyseal cartilage (Isaksson et al., 1982). It stimulates certain organs, as the liver and the skeleton, to synthetize somatomedins that have effect over growth, like insulin-like growth factor 1 (IGF-1) and 2 (IGF-2). Thus, GH stimulates bone formation in two ways: 1) via a direct interaction with GH receptors on osteoblasts and 2) via an induction of endocrine and autocrine/paracrine IGF-1 (Ohlsson et al., 1998).

According to Ohlsson et al. (1998), GH action in bone remodelling follows a "biphasic model": initially it increases bone resorption with a concomitant bone loss, which is followed by a phase of increased bone formation. When bone formation is stimulated more than bone resorption (transition point), bone mass is increased. A net increase of bone mass will be seen after 12–18 months of GH treatment in GH deficient adults.

Moreover, a recent study developed in rats showed that GH increased bone growth, by increasing both periosteal and endocortical bone formation, bone mineral content (BMC) and bone mineral density (BMD), and that the administration of GH along with PTH increases bone growth and bone formation, decreases bone resorption, and has a synergistic effect on increasing bone density and bone mass (Guevarra et al., 2010).

2.2.3 Sexual hormones and steroids (oestrogen and testosterone):

Oestrogen is an important regulator of skeletal development and homeostasis, both via direct and indirect effects over the skeleton (Turner et al., 1994; Prince et al., 1994). Indirectly it influences, for example, the calcium intestinal absorption (Liel et al., 1999; ten Bolscher et al., 1999) and secretion (Draper et al., 1997), and the calcium renal excretion; oestrogen also influences the secretion of PTH (Väänänen et al., 2005; Robinson et al., 2009). On the other hand, the mechanisms by which oestrogen acts directly on bone tissue are not completely understood. Nevertheless, it's now acknowledged that oestrogen maintains bone homeostasis by inhibiting osteoblast and osteocyte apoptosis (Tomkinson et al., 1997; Kousteni et al., 2002; Emerton et al., 2010). Moreover, oestrogen inhibits the osteoclast formation and activity as well as induces osteoclast apoptosis, thus indirectly preventing excessive bone resorption (Hughes et al., 1996; Rodan & Martin, 2000; Faloni et al., 2007; Faloni et al., 2012; Khosla et al., 2012).

Androgens are also important to bone homeostasis, in both sexes. It has been shown that they stimulate bone formation in the periosteum, through several effects on osteoblasts and osteoclasts, and by influencing the differentiation of pluripotent stem cells toward distinct lineages (Wiren & Marcus, 2010). Similarly, to the loss of oestrogen, the loss of androgen influences the rate of bone remodelling by removing restraining effects on osteoblastogenesis and osteoclastogenesis, and creates an imbalance between resorption and formation, as it prolongs the lifespan of osteoclasts and shortens the lifespan of osteoblasts. Likewise, androgens maintain cancellous bone mass and integrity, regardless of age or gender (Compston et al., 2001; Vanderschueren et al., 2004).

2.2.4 Thyroid hormones:

Thyroid hormones (T3 and T4) levels influence bone growth during early development as well as adult bone turnover and maintenance. They act both indirectly, by enhancing the effects of growth hormone over tissues, and directly, by stimulating bone resorption and formation. Hypothyroidism causes impaired bone formation and growth retardation; inversely, thyrotoxicosis is an established cause of secondary osteoporosis. Osteoclastic receptors for thyroid hormone have been demonstrated (Abu et al., 1997). Thus, bone turnover is increased by thyroid hormones, which is confirmed by increased biochemical markers of bone turnover, such as osteocalcin and bone-specific alkaline phosphatase (Harvey et al., 1991; El Hadidy et al., 2011; Waring et al., 2013), and therefore bone loss can occur (Britto et al., 1994; Hadjidakis & Androulakis, 2006). Recent studies also suggest a potential direct effect of thyroid stimulating hormone (TSH) on bone (Abe et al., 2003) and TSH receptors have been found on osteoblasts and osteoclasts. Furthermore, recombinant TSH showed antiresorptive effects in ovariectomized rats (Abe et al., 2003; Sun et al., 2008) and lower TSH levels – with no apparent association with free T4 levels – have been related with hip fracture risk, supporting the idea that TSH effect on the skeleton may be independent from free T4 (Waring et al., 2013). Finally, abnormal thyroid hormone signalling has been recognized as an osteoarthritis' risk factor (Bassett & Williams, 2016).

2.2.5 Leptin ("satiety" hormone):

Leptin is produced mainly in adipose tissue, influences bone metabolism via direct signalling from the central nervous system (CNS). It inhibits osteoclast generation (Holloway et al., 2002), promotes the decrease in cancellous bone and increase in cortical bone, thus enhancing bone enlargement (Ducy et al., 2000; Elefteriou et al., 2004; Hamrick & Ferrari, 2008); it also increases osteoblast number and activity, acting primarily through the peripheral pathways (Turner et al., 2013). Another study showed that leptin increases bone mineral content and density, especially at the lumbar spine (Mantzoros et al., 2011). Leptin also increases the expression of IGF-1 receptor and IGF-1 receptor messenger RNA (mRNA) within the chondrocytes and the progenitor cell population, thus acting as a skeletal growth factor with a direct peripheral effect on skeletal growth centre; it also induces chondrocytes proliferation and differentiation through specific leptin binding sites (Maor et al., 2002). Leptin is also a key up regulator of FGF23 secretion (Tsuji et al., 2010) and it has recently been described as a direct enhancer of parathormone secretion (Lopez et al., 2016).

2.2.6 Bone Morphogenetic Proteins (BMPs):

BMPs are group of 15 growth factors also known by cytokines, which belong to the transforming growth factor β (TGF-β) superfamily, with the ability to induce the formation of bone (Urist et al., 1965) and cartilage (Kobayashi et al., 2005). Bone formation is a very complex process wherein BMPs play the major role in the regulation of osteoblast lineage-specific differentiation and later bone formation (Beederman et al., 2013). Alterations in BMPs activity are often associated to a great variety of clinical pathologies, like skeletal and extra-skeletal anomalies, autoimmune, cancer, and cardiovascular diseases (Rahman et al., 2015). BMPs crosstalk with several other major signalling pathways, e.g. Wnt, Akt/mTOR, miRNA, among others, having Runx2 as a key integrator (Lin & Hankenson, 2011; Rahman et al., 2015). Among all BMPs, several authors refer to BMP9 as one of the most potent BMPs in inducing osteogenic differentiation of MSCs, both *in vitro* and *in vivo* (Kang et al., 2004; Kang et al., 2007; Beederman et al., 2013); moreover, TGF-β and GH are known to act synergistically with BMP9 to enhance bone formation (Li et al., 2012; Huang et al., 2012; Rahman et al., 2015). In addition to BMP9, other BMPs also have shown the ability to induce osteogenesis *in vivo*, such as BMP2, BMP6 and BMP7 (Franceschi et al., 2000; Jane et al., 2002; Cheng et al., 2003), with recombinant human-BMP2 and -BMP7 already being commercialized with the purpose of enhancing bone healing (Carreira et al., 2014). Contrariwise, BMP3 is known to be a negative regulator of bone formation (Kang et al., 2004).

2.2.7 Insulin and insulin-like growth factors (IGF-1 and IGF-2):

IGF-1 stimulates chondrocyte proliferation in the growth plate, thus playing a crucial role in longitudinal bone growth (Lupu et al., 2001). It is also involved in the formation of trabecular bone, which is essential to bone mineralization (Zhang et al., 2002). Insulin and IGF-1 have shown to be anabolic agents in osteoblast and bone development, mainly through the activation of Akt and ERK signalling

pathways; also, IGF-1, but not insulin, was capable of inducing osteoblasts *in vivo* proliferation (Zhang et al., 2012). IGF-1 inhibits the gene expression of osteocalcin, a marker for differentiating osteoblasts, whilst insulin enhances it. Furthermore, insulin indirectly enhances Runx2 expression, which is a regulator of osteoblast differentiation, by inhibiting the expression of Runx2 inhibitor Twist2 (Fulzele et al., 2010; Zhang et al., 2012). A study with insulin-deficient type I diabetic mice showed that these mice presented a decreased expression of Runx2 and the Runx2-regulated genes, like osteocalcin and collagen type I, and a secondary decrease in bone formation. Bone loss was restored after insulin treatment, which increased Runx2 expression and the expression of related genes (Fowlkes et al., 2008).

Likewise, IGF-2 potentiates BMP-9-induced osteogenic differentiation and bone formation (Chen et al., 2010) through PI3K/AKT signalling. Moreover, a recent study in mice aortas showed that IGF-2 induces the expression of miR-30e, in a feedback loop, which is a major down-regulator of osteogenic differentiation in MSCs and smooth muscle cells (SMCs) (Ding et al., 2015).

2.3 Bone structure and mechanical properties

Bone mechanical properties depend on mineralization degree, porosity, composition and organization of solid matrix. Therefore, the mechanical behaviour of a whole bone is highly dependent on its properties at a microscale (Rho et al., 1998).

Bone is composed of 70% inorganic component (of which 95% is hydroxyapatite and 5% are impurities impregnated in hydroxyapatite), 22% to 25% of organic component (of which 94-98% is mainly collagen type I and other non-collagen proteins and 2%-6% are cells) and 5 to 8% is water (Sommerfeldt & Rubin, 2001).

Mature, lamellar bone is morphologically classified in two different types: cortical or compact and cancellous bone. Cortical and cancellous bone types differ in structure and functional properties.

The typical structure of a long bone such as the femur or the humerus comprises the shaft, or diaphysis, and the extremities, or epiphysis (Fig. 1). The diaphysis consists of a cylinder of compact bone surrounding the central medullary cavity, lined by a thin layer of connective tissue, the endosteum.

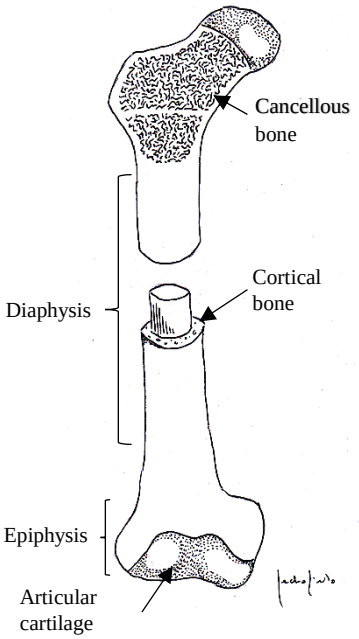

Fig. 1 Illustration of a long bone structure, showing the distribution of two different types of lamellar bone: cancellous and cortical compact bone.

The epiphysis consists of cancellous bone surrounded by a layer of cortical bone. Within the porous chambers of cancellous bone lays red bone marrow. A layer of dense connective tissue called periosteum covers the outer surface of the bone, except for the areas of articulation, covered with hyaline cartilage. The periosteum is highly vascular and is responsible for appositional bone growth (Van De Graaff, 2001).

Cortical bone (Fig. 2) is a porous mineralized tissue and accounts for approximately 80% of the skeletal mass. It is formed by tightly packed collagen fibrils, forming concentric lamellae. Each lamella is 2 – 3 μm thick and is arranged in several discrete layers of parallel fibrils, each layer having a different orientation of fibrils (Weiner et al., 1999). Apatite crystals (mainly carbonated apatite) are deposited within and around these fibrils. The lamellae form cylinders containing a hollow central tube wherein blood vessels and nerves run. The ensemble is called Haversian system or osteon and it is the microstructural unit of cortical bone. Blood vessels form a three-dimensional network, from the centre of the osteon (Haversian canals) and penetrating the cortical bone layer perpendicularly (Volkman's channels) (Meyer & Wiesmann, 2006). In between the osteons are remnants of incomplete osteons, known as interstitial systems or interstitial bone.

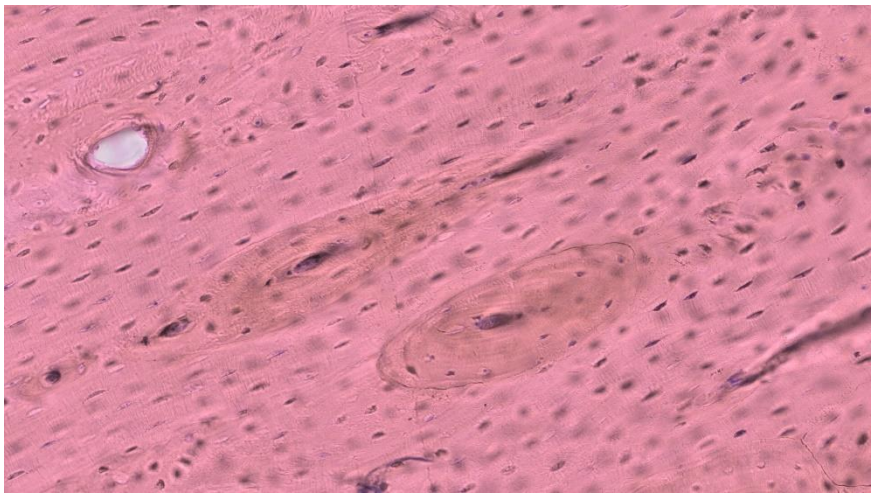

Fig. 2 Microphotograph of cortical bone in vertebrae (undecalcified bone section of sheep vertebra, Giemsa-Eosin, 20x magnification; slide digitalized using Nanozoomer SQ, Hamamatsu Photonics, Portugal). Haversian systems are evident, along with organized fibrils. Osteocytes are visible in their lacunae, in between lamellae.

Cancellous (or trabecular) bone has a more loosely organized structure and higher porosity. The lamellae are organized in a parallel manner, forming trabeculae in a flattened and spongy-like network (Fig. 3). Trabeculae are covered by osteoblasts and bone-lining cells. Osteoblasts actively depose extracellular matrix (ECM) and bone-lining cells are in an inactive state.

The metabolic rate of trabecular bone is higher than that of cortical bone, and so are the remodelling phenomena. The trabecular network is a light structure, of uttermost importance for load transfer through the bone. This can be clearly seen in epiphyses and metaphysis of long bones, but also in vertebrae and ribs; trabeculae are orientated according to routine load bearing direction (Carter & Beaupré, 2001; Currey, 2003).

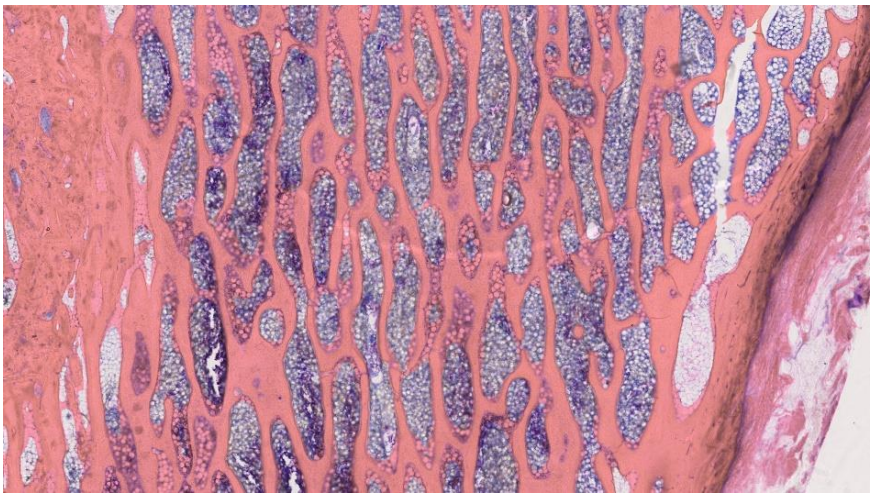

Fig. 3 Image of vertebral trabecular bone (undecalcified bone section of sheep lumbar vertebra, Giemsa-Eosin, 1.25x magnification; slide digitalized using Nanozoomer SQ, Hamamatsu Photonics, Portugal). The picture illustrates the sponge-like structure of cancellous bone.

The bone exhibits a stress-strain response of sequential elastic and plastic responses. The slope of the elastic region is called the elastic or Young's modulus, and is a measure of the intrinsic stiffness of the material.

Bone can withstand a maximum level of stress, corresponding to a maximum strain, before a fracture occurs. In its elastic region, no permanent damage is caused to the bone structure; if the stress increases, a gradual transition to a plastic response occurs. Elastic and plastic regions of the stress-strain curve are separated by the yield point. Post-yield deformations are permanent and may include lesions at cement lines, cracks and trabecular fractures. Crack formation and growth is a mean to dissipate energy. In the elastic phase of the curve energy builds up, whilst in the plastic region the energy levels are lowered by damage to the bone structure, and ultimately, by fracture. Generally speaking, the higher bone mineral density, the higher the stiffness. However, a higher Young's modulus corresponds to less ductility and higher brittleness (Turner, 2006). Long bones, as other natural composite tubular structures, combine great strength and fatigue resistance against axial compression forces with minimum weight. However, much of the strain measured in bone is due also to bending moments (Sommerfeldt et al., 2001). Normal loading of long bones combines compressive and bending efforts, causing in humans a large variation of strains, up to 400 to 2000 μstrains or even as high as 4000 μstrains (Duncan & Turner, 1995; Burr et al., 1996; Sommerfeldt et al., 2001). Strains are local deformations and 1 μstrain corresponds to 1 μm deformation per meter of length (Duncan & Turner, 1995).

However, due to difficulties to measure bone mechanical properties at a microstructural level, in the various possible directions, further knowledge about the actual strains bone cells are subjected to and able to sense *in vivo* is necessary.

Both cancellous and compact bone show anisotropic behaviour, i.e. the Young's modulus depends on the direction of the load, due to the deliberate direction of lamellae (Heinonen et al., 1995; Carter & Beaupré, 2001). In long bones, fundamental for load bearing and leverage, stiffness along the long axis was favoured. Vertebral bodies function like shock absorbers and flexibility was preferred and achieved through the cancellous porous architecture (Carbonare et al., 2005).

Woven or primary bone is present in growth, fracture healing and in certain diseases (like Paget's disease). Cells and ECM are laid randomly. During intramembranous, endochondral or rapid appositional bone growth, woven bone is formed. In large animals (whether reptiles, birds or mammals), woven bone with large vascular canals is rapidly deposited in the subperiosteal region. The canals are lined with osteoblasts that slowly will deposit lamellae, until the canal has a reduced diameter; the resulting structure is a primary Haversian system or osteon. The random distribution of its components explains woven bone's isotropy.

2.4 The bone matrix

The mineral phase comprises most of bone mass, but the organic component is essential for normal function. The collagen network is coated by hydroxyapatite crystals.

Structure and biomechanical properties of the bone depend on collagen. Three long peptide sequences, arranged helicoidally, constitute the collagen I molecule. Collagen goes through several enzymatic modifications whilst still within the osteoblast (Young, 2003). Further cross-linking within and between collagen molecules occurs after leaving the cell. Diseases such as osteogenesis imperfecta are caused by collagen chain mutations (Young, 2003; Bodian et al., 2009). As reviewed ahead in this chapter, the triple tropocollagen units are aligned in fibrils, displaying a permanent dipole moment. Therefore, collagen acts as a piezoelectric and pyroelectric material, and as an electromechanical transducer (Fukada & Yasuda, 1964; Noris-Suárez et al., 2007). The piezoelectric properties of collagen and the native polarity of the molecules are associated with the mineralization process. Under compression, negative charges on the collagen surface become uncovered and entice calcium cations, which are followed by phosphate ions (Noris-Suárez et al., 2007; Ferreira et al., 2009).

Non-collagenous proteins, present in much smaller quantities, are also paramount for normal bone function and properties. Some of these proteins are shortly introduced: osteopontin, fibronectin, osteonectin and bone sialoprotein.

Osteopontin (OPN) is a non-collagenous secreted glycoprotein, present in bone matrix, where it binds both to cell surface and to hydroxyapatite. It is mainly produced by proliferating pre-osteoblasts, osteoblasts and osteocytes, but also by fibroblasts, osteoclasts and macrophages (Ashizawa et al., 1996; Perrien et al., 2002). OPN intervenes in cell migration, adhesion, and survival in many cell types. OPN production is known to be increased in association with mechanical loading (Harter et al., 1995; Perrien et al., 2002), and its deficiency significantly diminishes bone fracture toughness and causes anomalous mineral distribution (Fisher et al., 2001; Thurner et al., 2010).

Fibronectin mediates a large number of cellular interactions with the ECM, also playing an important part in cell adhesion, migration, growth and differentiation. It is vital for vertebrate development and is mainly synthesized by osteoblast precursors and mature bone cells, but can also be produced at distant sites (such as the liver), and enter systemic circulation. Some studies suggested that only circulating fibronectin exerts effects on the bone matrix (Young, 2003; Bentmann et al., 2010). Fibronectin binds to collagen and may act as an extracellular scaffold that binds and facilitates interactions of BMP1 with substrates that include procollagen and biglycan (Huang et al., 2009). Fibronectin may also be vital for MSC differentiation into osteoblastic lineage (Linsley et al., 2013).

Osteonectin or SPARC (secreted protein acidic and rich in cysteine) is one of the most abundant non-collagenous protein present in bone matrix. It has a strong affinity to collagen and mineral content; osteonectin knockout mice suffer from osteopenia in consequence of low bone turn-over, and osteoblasts and osteoclasts defective function. Changes in osteonectin encoding gene have also been linked to idiopathic osteoporosis and osteogenesis imperfecta (Rosset & Bradshaw, 2016).

Thrombospondin-2 is another matricellular protein that also exerts its effects on osteoblast proliferation and function, being involved in MSCs adhesion and migration; it has also influence on angiogenesis and tumour growth (Delany et al., 2000; Delany & Hankenson, 2009).

Bone sialoprotein (BSP) is a highly glycosylated and sulphated phosphoprotein that is found almost exclusively in mineralized connective tissues (Ganss et al., 1999). BSP knockout mice present reduced amounts of cortical bone and higher trabecular bone mass with very low turn-over. BSP defective mice maintain unloading bone response, as opposite to OPN knockout mice (Malaval et al., 2008).

Proteoglycan (PG) encoding genes are expressed both in skeletal and non-skeletal tissues but with stronger expression in bone, joints and liver; in bone PG encoding PrG4 gene expression is under PTH control (Novince et al., 2012); structure and localization is varied and PG perform a large number of biological functions. PGs help structuring the bone tissue by regulating collagen secretion and fibril organization. PGs also modulate cytokines and growth factors biological activity in bone (Lamoureux et al., 2007).

2.5 Bone cell population

Mature bone comprises three main types of cells: osteoblasts, osteocytes and osteoclasts.

2.5.1 Osteoblasts

Osteoblasts derive from MSCs, sharing a common background with chondrocytes, myoblasts and fibroblasts. Osteoblasts differentiate under the influence of a variety of hormones and cytokines and the local mechanical environment (Nakamura, 2007). These cells, when active, are characteristically round, with specific features consistent with their secretory role (Fig. 4).

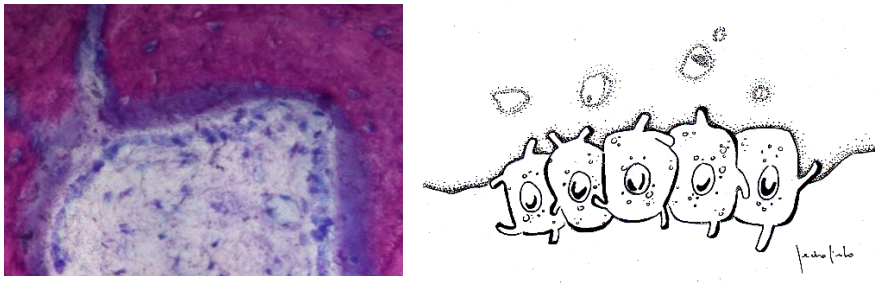

Fig. 4 Osteoblasts are round cells that when actively deposing matrix on bone surfaces show prominent Golgi complexes (on the left, microphotograph, undecalcified bone section, Giemsa Eosin, magnification 100x). When quiescent, osteoblasts appear as flat bone lining cells.

These cells present very evident Golgi complexes and endoplasmic reticulum (with multiple vesicles and vacuoles) especially ostensive during matrix secretion and early stages of mineralization (Palumbo, 1986).

Osteoblasts can also remain on inactive bone surfaces as flat bone lining cells, with scarce cell organelles evident. Increased levels of expression of pro-collagen, osteopontin and osteocalcin are present during osteoblast maturation process; bone sialoprotein seems to be more strongly expressed at intermediate phases of differentiation (Bellows et al., 1999; Bellows & Herschel, 2001). Osteoblast differentiation is impaired when gap junctions are inhibited, suggesting communication to neighbouring cells is essential for differentiation (Schiller et al., 2001). Osteoblasts produce non-mineralized matrix – osteoid – that becomes gradually mineralized, wherein they become trapped and some differentiate into osteocytes. Osteoblast differentiation is influenced by $1,25(OH)_2D_3$ and mechanical stimuli, amongst other factors (van der Meijden et al., 2016).

2.5.2 Osteocytes

Osteocytes are the most abundant cells of bone by far, comprising more than 90% of the osteoblast lineage and contributing to both bone formation and resorption (van Bezooijen et al., 2004; Bonewald et al., 2007). They are fully differentiated osteoblasts embedded in mineralized matrix, sitting in the osteocytic lacunae.

Lacunae are located between adjacent lamellae and are interconnected to surrounding lacunae by a canalicular system (Fig. 5). Osteocytes' long cell processes lay within the canaliculi. The extremities of the dendritic processes connect osteocytes amongst themselves, also establishing contact with osteoblasts and bone lining cells (Carter & Beaupré, 2001; Knothe Tate et al., 2004; Jiang et al., 2007). The resulting functional syncytium shares a common environment (Knothe Tate, 2003).

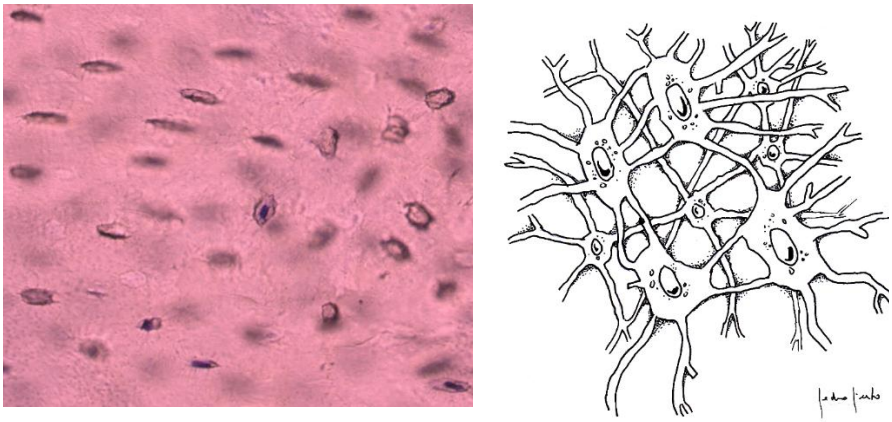

Fig. 5 Microphotograph of undecalcified bone section of sheep vertebra, Giemsa-Eosin, on the left, showing osteocytes (Giemsa-Eosin, 24x magnification; slide digitalized using Nanozoomer SQ, Hamamatsu Photonics, Portugal). Some of the canaliculi where cell processes run are evident. The image on the right illustrates the resulting three-dimensional syncytium.

Osteocytes have no matrix secretion functions; however, they are responsible for sensing changes in the bone structure and commanding bone remodelling.

Pre-osteoblasts and osteoblasts are less responsive to fluid shear stress than osteocytes. Mechanosensitivity seems to increase during differentiation although it is now known that osteoblasts are able to modulate response to mechanical stimulate in function of its intensity (Sommerfeldt et al., 2001; Kringelbach et al., 2015). Osteocyte functions include maintaining bone matrix and mechanosensing (Burger & Klein-Nulend, 1999; Mullender et al., 2004). Sensation of electrical signals may be one of the functions of osteocytes, and electrical signals mediated by osteocytes may regulate the cell behaviour in bone tissue (Huang et al., 2008). The same mechanical stimulus may cause a different response in osteocytes according to their cell body shape (van Oers et al., 2015).
Osteocytes early response to mechanical loading results in vesicular ATP release by exocytosis, tuned according to the magnitude of the stimulus (Kringelbach et al., 2015).

Osteocytes also respond to mechanical stimuli by producing various messengers' molecules such as nitric oxide and prostaglandins, in particular prostaglandin E_2

(PGE_2) (Klein-Nulend et al., 1998; Cherian et al., 2003; Mullender et al., 2004). This response is dependent on function of stretch-activated calcium channels (Rawlinson et al., 1996). PGE_2 has anabolic effects, stimulating osteoblast activity and new bone formation (Jee et al., 1990). Nitric oxide inhibits bone resorption, by suppressing osteoclast formation and increasing the expression of osteoprotegerin (Kasten et al., 1994; Fan et al., 2004).

The life span of osteocytes is highly variable but is probably associated with the rate of bone remodelling, depending on mechanical and environmental factors such as hormones; osteocytes apoptosis may be inhibited or induced by a variety of physiological, pathological conditions and by biological effectors such as hormones, without being necessarily accompanied by an increase in osteoclastogenesis (Tomkinson et al., 1997; Lee et al., 2004; Plotkin et al., 2005; Hirose et al., 2007; Jika et al., 2013).
Osteocyte density is intimately related to bone architecture and thus to its mechanical behaviour (Metz et al., 2003). Young osteocytes are polarized toward the mineralization front, just like osteoblasts are, with the nucleus remaining in close to vessels (Palumbo, 1986). As lamellar bone matures, the osteocytes tend to spread their processes perpendicularly to the longitudinal axis of trabeculae and long bones and appear as flattened cells. In immature bone, plump osteocytes with randomly distributed processes predominate (Hirose et al., 2007).

2.5.3 Osteoclasts

Osteoclasts are multinucleated cells, of the same lineage as macrophages and monocytes (Fig. 6).

Like macrophages, they have the ability to merge and form multinucleated cells, and to phagocytise (Rubin & Greenfield, 2005). The cell precursor may differentiate into either an osteoclast or a macrophage, and the differentiation path depends on the precursor cell being exposed to a receptor activator of several ligands (Receptor Activator of Nuclear factor κB Ligand - RANKL, osteoprotegerin (OPG) and osteoclast differentiation factor - ODF) or to colony-stimulating factors related to immune system (Nakagawa et al., 1998; Asagiri & Takayanagi, 2007; Takayanagi, 2008).

The osteoclast presents distinctive functional features:

- osteoclasts are able to attach firmly to the bone surface, isolating the area under the cell membrane from its surroundings; the membrane domain responsible for the isolation of the resorption site is called sealing zone (Marchisio et al., 1984; Väänänen & Horton, 1995);
- osteoclasts acidify the mineral matrix by the action of protons pumps at the ruffled border membrane, a resorbing organelle; the lowering of the pH causes the dissolution of the hydroxyapatite crystals (Baron et al., 1985; Blair et al., 1989; Rousselle & Heymann, 2002);
- osteoclasts are capable of synthetizing and secreting enzymes such as tartrate-resistant acid phosphatase (TRAP) and cathepsins in a directional manner; the proteases secreted by osteoclasts cleave the organic matrix;

through the combined action of lysosome enzymes, matrix metalloproteinases and the pH reduction, bone is resorbed (Littlewood-Evans et al., 1997; Vääräniemi et al., 2004);

- osteoclasts can phagocytise the resultant organic debris and minerals, removing them from the resorption lacunae, through a transcytosis process (Salo et al., 1997; Yamaki et al., 2005).

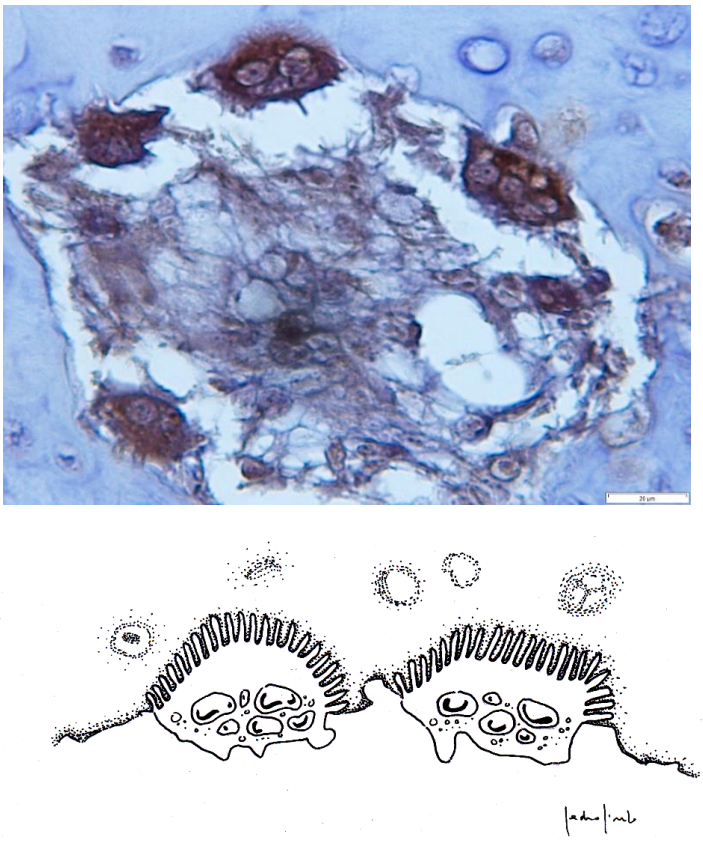

Fig. 6 On top, microphotograph of TRAP positive osteoclasts in cutting cone; on bottom, a schematic detail of the ruffled border membrane in direct contact with bone. This is the resorbing organelle; along its enlarged ruffled contact surface, proton pumps lower the local pH, dissolving hydroxyapatite.

The bone resorption process begins with differentiation and recruitment of osteoclast precursors, which merge and originate matured multinucleated bone-resorbing osteoclasts. To initiate resorption the osteoclast attaches to the bone matrix via the interaction of integrins with matrix proteins, like osteopontin and bone sialoprotein, previously laid down by osteoblasts (Väänänen & Horton, 1995). However, bone resorption is only attainable if appropriate matrix mineralization exists (Chambers & Fuller, 1985).

2.6 Bone remodelling and cell interplay

The dynamic process of bone resorption and formation occurs on both cortical and trabecular bone, and arises in response to mechanical loading, calcium serum levels and a wide array of paracrine and endocrine factors.

The bone remodelling process depends on the coordinate actions of osteoblasts, osteoclasts, osteocytes and osteoblast-derived bone lining cells, along with other cells, such as macrophages and immune cells, in what is known as the "Basic Multicellular Unit" (BMU) or "Bone Remodelling Unit" (BRU). In the BMU, the amount of bone destructed by osteoclasts is equal to the amount produced by osteoblasts. The balance between osteoblastic and osteoclastic activity is known as coupling. Osteoclasts can resorb bone in the absence of osteoblasts and bone is formed in the absence of osteoclasts, signifying that osteoclasts and osteoblasts within the BMU may function under the control of other cell types (Corral et al., 1998; Kong et al., 1999). This scenario is reinforced by the fact that cells from the osteoblast lineage express receptors for cytokines and other local secreted factors that stimulate osteoclast formation (Suda et al., 1999). The BMU may be inhibited by old age, drugs, endocrine, metabolic or inflammatory diseases.

Independently from the triggering stimulus, osteoclast formation depends on RANKL. Osteoblasts express membrane-bond RANKL and this regulatory molecule interacts with a receptor (receptor activator of nuclear factor-κB - RANK), expressed on the surface of osteoclast precursors. The RANK activation by RANKL is essential for fusion of the osteoclast precursor cells and osteoclast formation (Miyamoto & Suda, 2003). Whilst some studies suggest down-regulation of the RANKL expression by osteoblasts under mechanical stimulation, others describe up-regulation of RANKL expression under similar mechanical conditions (Fan et al., 2006; Kreja et al., 2008).

RANKL-bond (that is reported to increase) and soluble RANKL (reported to decrease) are differentially secreted by osteoblasts in response to different mechanical stimuli regimens (Kim & Lee, 2006). Human osteoblasts subjected to strains varying from 0.8 to 3.2% respond to higher strain with increased expression of osteocalcin, type I collagen and Cbfa1/Runx2, and to lower strain magnitudes with an increase of alkaline phosphatase activity (Zhu et al., 2008).

Cells belonging to the osteoblast-cell lineage also produce OPG. OPG is soluble and blocks the interaction between RANKL and RANK (it acts as a decoy receptor for RANKL), thus inhibiting osteoclast formation. Osteoblasts, in addition, secrete macrophage colony stimulating factor-1 (M-CSF-1); this factor promotes osteoclast precursor proliferation and expression of RANK by these same precursor cells (Arai et al., 1999; Romas et al., 2002), demonstrating how intimate is the interplay of these different cell types.

Osteoblast-like cells cultures mechanically stimulated may respond by a decrease in the production of OPG, without change in the RANKL production, with consequent increase in the ratio of RANKL/OPG. In an *in vivo* scenario, this would translate into increased bone remodelling. However, subjecting osteoclast-like cells

to the same mechanical stimuli regimen, decreased TRAP and with one-minute stimulation at 0.3 Hz frequencies, a decrease in cell fusion and resorption activity was observed (Kadow-Romacker et al., 2009).

RANKL expression by osteoblast-lineage cells is enhanced when microdamage within the bone matrix occurs. Microdamage may occur in pathological conditions or under physiological bone loading. The existence of microcracks is sensed by osteocytes, and may induce osteocyte apoptosis, as suggested by several studies; osteocyte apoptosis may also be induced by disuse and is closely correlated with higher bone remodelling levels (Mori & Burr, 1993; Bentolila et al., 1998; Verborgt et al., 2002; Noble et al., 2003; Mann et al., 2006; Martin, 2007, Jika et al., 2013).

Pulsating fluid flow (PFF)-treated osteocyte cultures condition the culture medium, inhibiting osteoclast formation and decreasing *in vitro* bone resorption. These effects have not been detected in the medium from PFF-treated fibroblast cultures (Tan et al., 2007).

Consequently, osteocytes regulate osteoclastogenesis and osteoclast activity, through soluble factors and messenger molecules. In osteocytes subjected to PFF, nitric oxide is involved in the up and down regulation of at least two apoptosis-related genes (Bcl-2 and caspase-3, with antiapoptotic protective and pro-apoptotic functions, respectively) (Tan et al., 2008). Nitric oxide (NO) is a second messenger molecule produced in response to mechanical stimulation of osteoblasts and osteocytes, and other cell types such as endothelial cells, with a large variety of biological functions (Smalt et al., 1997; Zaman et al., 1999; Rössig et al., 2000; van'T Hof, 2001).

Other pathways are relevant for osteoblasts, osteocytes and osteoclasts interweaved regulation, such as the Notch signalling pathway. In osteocytes, the Notch receptors activation induces OPG and Wnt signalling, decreasing cancellous bone remodelling and inducing cortical bone formation (Canalis et al., 2013).

2.7 Bone mechanotransduction

Bone mechanotransduction, essential in health and disease states, is not fully understood, despite the many advances. The transduction elements include ECM, cell-cell adhesions, cell-ECM adhesions, membrane components, specialized surface processes, nuclear structures and cytoskeleton filaments.

2.7.1 The membrane elements, ECM-cell and cell-cell adhesions

Cell membrane-associated mechanotransduction mechanisms depend on the integrity of the phospholipid bilayer. Mechanotransduction pathways are disrupted if membrane cholesterol is depleted, inhibiting the response to hydrostatic and fluid shear stress (Ferraro et al., 2004; Xing et al, 2011). Cytoskeleton actin polymerization and assembly is influenced by membrane cholesterol levels (Klausen et al., 2006; Qi et al., 2009). More recently, it has been proposed that actin polymerization during synaptic vesicle recycling is influenced by vesicular

cholesterol, but not plasma membrane cholesterol, as shown by a study wherein the inhibition of actin polymerization by the extraction of vesicular cholesterol resulted in the dispersal of synaptic vesicle proteins (Dason et al., 2014). But even with an intact membrane, if integrin binding is impaired, actin cytoskeleton will not reorganize in response to shear stress (Radel & Rizzo, 2005).

The integrins are a superfamily of cell adhesion receptors that bind to ECM ligands, cell-surface ligands, and soluble ligands. Integrins are heterodimers of non-covalently associated 18α and 8β subunits, in mammals, that can combine to generate 24 different receptors with different binding properties and different tissue distribution (Hynes et al., 2002; Barczyk et al. 2010). These subunits possess an extracellular portion with several domains, able to bind to large multi-adhesive ECM molecules, which in turn bind to other ECM molecules, growth factors, cytokines and matrix-degrading proteases (Barczyk et al., 2010). Integrins were first acknowledged as bridging the ECM and the cell cytoskeleton, including the actin cytoskeleton but also the intermediate filament network, essentially vimentin and laminin (Nievers et al., 1999). Recruitment of vimentin has been shown to depend on integrin β3 subunits, further pointing out the relationship between the various cytoskeletal elements and integrins (Bhattacharya et al., 2009). The cytoplasmatic portions of integrin β subunit are able to bind to talin, which can also directly bind to vinculin and actin filaments (Cram & Schwarzbauer, 2004). On the other hand, integrin α4 subunit binds to paxillin (Brown et al., 1996), a protein that integrates focal adhesions.

Integrins allow communication between structures within and out of the cell, in a bi-directional way. The inside-out signalling brings the integrin extracellular domains into the active conformation. In the outside-in pathway, receptor clustering and redistribution of cytoskeletal and signalling molecules occurs into focal adhesions at the sites of cell-ECM contact (Cram & Schwarzbauer, 2004; Geiger et al., 2009). Recently, it has been demonstrated that the connective tissue growth factor (CTGF), which is a matrix protein, enhances osteoblast adhesion (via $\alpha_v\beta_1$ integrin) and cell proliferation, by inducing cytoskeletal reorganization and Rac1 activation (Hendesi et al., 2015). Another study suggested that another matrix protein – osteoactivin – also plays a role in the regulation of osteoblast differentiation and function, by stimulating alkaline phosphatase (ALP) activity, osteocalcin production, nodule formation, and matrix mineralization (Moussa et al., 2015). Finally, α5β1 integrin interacts with its high affinity ligand CRRETAWAC, enhancing the Wnt/β-catenin signalling mechanism to promote osteoblast differentiation independently of cell adhesion (Saidak et al., 2015).

Initial adhesions to substrates are characterized by small dot-like or punctuate areas at the edges of lamellipodia, usually known as focal complexes. The mature elongated form of cell-matrix adhesion, referred to as focal adhesions or focal contacts, is associated with bundles of actin and myosin (stress fibres). There is a specialized form of focal contact, in which integrin binds to fibronectin fibrils and tensin but with low levels of tyrosine kinases (Katz et al., 2000; El-Hoss et al., 2014). Most focal adhesions contain several types of signalling molecules like

tyrosine phosphatases and tyrosine kinases and adaptor proteins (Parsons, 1996; Yamada & Geiger, 1997; Geiger et al., 2009; Teo et al., 2013).

Force application to bound integrins activates the GTPase Rho, causing myosin II contraction, making the cell apply tension to the substrate; another one of the Rho targets, when active, ensures by itself the development of focal contacts (Riveline et al., 2001).

Cell adhesion and mechanical stimulation depend on integrin mediation (Carvalho et al., 1998). Forces applied to integrin receptors cause local adhesion proteins to be recruited and the cell adapts by making the integrin-cytoskeleton linkages more rigid (Riveline et al., 2001). Different signalling pathways are triggered by sensed stress through integrin receptors. Sequential expression of integrin ligands (osteopontin, fibronectin and bone sialoprotein) in response to mechanical stimulation of osteoblasts has been described (Carvalho et al., 2002). Bonds between integrin and ligands becomes stronger in the presence of cell tension (Friedland et al., 2009).

Osteocytes are highly specialized in their interaction with ECM; osteocyte cell bodies express β1 integrins while cell processes express β3 integrins, the latter in a punctuate distribution similar to matrix attachment sites but involving far fewer integrins, being essential for mechanically induced bone formation (Phillips et al., 2008; McNamara et al., 2009; Litzenberger et al., 2009 Litzenberger et al., 2010). Thi et al. identified the cell processes as the mechanosensory organs in osteocytes (Thi et al., 2013). Recently, it has been demonstrated that integrin αvβ3 is essential for the maintenance of osteocyte cell processes and also for mechanosensation and mechanotransduction by osteocytes (Haugh et al., 2015). These conclusions are supported by another study, wherein cortical osteocytes from knockout mice were depleted of β1 integrin, but the unloading of the hindlimb did not reduce cortical bone size and strength, in contrast to wild type mice (Phillips et al., 2008). Another study showed that ERK1/2 activation by strain prevented osteocyte apoptosis, however it required the integrin/cytoskeleton/Src/ERK signalling pathway activation (Plotkin et al., 2005).

Apart from integrin, other membrane proteins are responsible for conduction of mechanical stimuli. Cadherins, which connect to the cytoskeleton, mediate force-induced calcium influx (Gillespie & Walker, 2001; Kazmierczak et al., 2007), and participate also in the Wnt/β-catenin pathway, potentially interfering in osteoblastogenesis and bone formation (Marie et al., 2013). In osteoblasts, mechanical load applied to β1-integrin subunit results in calcium influx (Pommerenke et al., 2002), independently from gap junctions (Saunders et al., 2001). Also in osteoblasts, it has been suggested that GPI-anchored proteins may play an important role in osteoblastic mechanosensing, by demonstrating that the overexpression of GPI-PLD, an enzyme that can specifically cleave GPI-anchored proteins from cell membranes, inhibits flow-induced intracellular calcium mobilization and ERK1/2 activation in MC3T3-E1cells (Xing et al., 2011). Ephrins (ligands) and Ephs (receptors) contribute to cell-cell interactions between osteoclasts and osteoblasts, helping to regulate bone resorption and formation, and

appear to be necessary for hMSC differentiation (Tamma & Zallone, 2012; Matsuo & Otaki, 2012). Lastly, another family of proteins – galectins –, are also involved in regulating osteogenesis; for example, Gal-3, which is expressed both by osteocytes and osteoblasts, plays a significant role as a modulator of major signalling pathways, such as Wnt signalling, MAPK pathway, and PI3K/AKT pathway (Nakajima et al., 2016); Gal-8 induces RANKL expression by osteoblasts and osteocytes, osteoclastogenesis and bone mass reduction in mice (Vinik et al., 2015); and Gal-9 induces osteoblast differentiation through the CD44/Smad signalling pathway in the absence of bone morphogenetic proteins (BMPs) (Tanikawa et al., 2010).

Gap junctions are transmembrane channels that connect the cytoplasm of neighbouring cells. Small metabolites, ions and signalling molecules like calcium and cAMP pass through these channels, since molecular weight must be lower than 1 kDa (Flagg-Newton et al., 1979; Steinberg et al., 1994). Gap junctions are essential for bone mechanosensation and thus for bone remodelling, since in osteoblastic cells fluid flow induces PGE2 production, dependent on intact gap junctions; if these are disturbed, PGE2 production does not occur (Saunders et al., 2001; Saunders et al., 2003). Mice lacking Cx43 gap junctions in osteoblasts and/or osteocytes exhibit increased osteocyte apoptosis, endocortical resorption, and periosteal bone formation (Bivi et al., 2012).

2.7.2 Primary cilia

In different cell types, different structures ensure recognition of mechanical stimuli; kidney epithelial cells possess a sole microvillar projection on their apical surface (primary cilia). The same kind of structure was described in osteoblasts and osteoblast-like cells (Myers et al., 2007; Delaine-Smith et al., 2014). Primary cilia originate in the centrosome and project from the surface of bone cells; its deflection during flow indicates that they have the potential to sense fluid flow. These cilia deflect upon application of 0.03 Pa steady fluid flow and recoil after cessation of flow (Xiao et al., 2006; Malone et al., 2007).

In bone, primary cilia translate fluid flow into cellular responses, independently of Ca^{2+} flux and stretch-activated ion channels (Malone et al., 2007). Moreover, recently it has been demonstrated *in vitro* that, apart from mediating the up-regulation of specific osteogenic genes, primary cilia are also important mediators of oscillatory fluid flow-induced extracellular calcium deposition, thereby playing an essential role in load-induced mineral matrix deposition (Delaine-Smith et al., 2014). Finally, two *in vivo* studies using knockout mice of Kif3a, which results in defective primary cilia, showed that primary cilia are essential for the ability of pre-osteoblasts to sense strain-related mechanical stimuli at a healing bone-implant interface and induce differentiation into bone-forming osteoblasts (Leucht et al., 2013) and MSCs to sense mechanical signals and enhance osteogenic lineage commitment *in vivo* (Chen & Hoey et al., 2016).

Shear stresses resulting from fluid flow cause calcium influx through mechanosensitive channels (Nauli et al., 2003; Praetorius et al., 2003). Calcium

influx occurs is osteoblasts in response to oscillatory fluid flow (Saunders et al., 2001).

Finally, concerning osteocytes, there are still many conflicting information regarding *in vivo* expression of cilia. Their role as mechanosensors depends on the type and number of cells with cilia, and on the local mechanical environment. The low incidence of primary cilia in osteocytes (about 4%) may indicate that cilia function as mechanosensors on a selected number of cells or that cilia function in concert with other mechanosensing mechanisms (Coughlin et al., 2015).

2.7.3 The cytoskeleton

Specific transmembrane receptors couple the cell cytoskeleton network to the ECM. Integrins connect to the cytoskeleton through focal adhesions that contain actin-associated proteins such as talin, vinculin, paxillin and zyxin. Both paxillin and zyxin belong to a group of LIM domain proteins, which have been suggested as mechanoresponders responsible for regulate stress fibres assembly, repair, and remodelling in response to changing forces (Smith et al., 2014). The transfer of forces across the network of microfilaments, microtubules and cell adhesions allows that focused stresses applied to the surface membrane affect distant cellular sites such as the mitochondria and nucleus, or the plasma membrane on the opposite side of the cell. The transmission of strain towards the ECM stimulates structural changes at a higher organization level, making it stronger (Wang et al., 1993; Wang & Ingber, 1994).

The cell deformation in consequence of an applied stress does not correspond to the predicted behaviour of an isotropic viscoelastic material; the interior of the cell, and thus the cytoskeleton, is anisotropic. The complex network of microtubules and microfilaments and the way this network spreads and is connected to the point of applied force, may result in structures away from the load application point to be further displaced than closer ones; displacements towards the origin of the compressive stimulus are also possible. Behaving in an anisotropic way, cells are able to respond to an external force according to its magnitude and direction (Hu et al., 2003; del Álamo et al., 2008; Silberberg et al., 2008). An intact cytoskeleton is necessary for the rendering of applied forces into mitochondria movements. Since mitochondria are semi-autonomous organelles, highly dynamic, the distress caused by mechanical stimulus exerts biological effects on their function (Silberberg et al., 2008), both in health and disease (Koike et al., 2015).

Nonetheless, there is evidence that mechanical properties of the ECM affect the behaviour of cells from osteoblastic lineage, with mature focal adhesions and a more organized actin cytoskeleton associated with more rigid substrates, suggesting that controlling substrate compliance enables control over differentiation (Khatiwala et al., 2006) and that this influence on differentiation is independent from protein tethering and substrate porosity (Wen et al., 2014).

Other factors are determinant for cell fate. A recent *in vitro* study showed similar patterns in cell growth, differentiation, and gene expression in human osteoblasts

and endothelial cells, when implanted in two different ceramic scaffolds – beta tricalciumphosphate and calcium-deficient hydroxyapatite –, with different chemical and physical characteristics, which suggested that the interaction between different cell types and scaffold materials is crucial for growth, differentiation, and long-term outcomes of tissue-engineered constructs (Ritz et al., 2016). Moreover, biomaterial surface modification with chitosan enhances osteoblast mechanical response and induces favourable structural organization for the implant integration (Moutzouri & Athanassiou, 2014). Lately, it has also been highlighted the importance of surface roughness of the biomaterials in osteogenic differentiation, and demonstrated the contribution of specific integrin subunits in mediating cell response to different materials (Olivares-Navarrete et al., 2015); additionally, the application of synthetic integrin-binding peptidomimetic ligands (αvβ3- or α5β1-selective) to a titanium graft enhanced cell adhesion, proliferation, differentiation and ALP expression in *in vitro* osteoblast-like cells, resulting in a higher mineralization on the surfaces coated with the ligands (Fraioli et al., 2015).

The biochemical nature of the substrate, its rigidity and spatial organization are recognized by cells through signalling from molecular complexes that are integrin-based.

In most anchorage-dependent cells, cell spreading on ECM is required for cell progression and growth; increasing cytoskeletal tension results in cell flattening, a rise in actin bundling and bucking of microtubules. Spread cells are able to transfer most of the load to the ECM.

The cell shape is influenced by how the cytoskeleton organizes its elements and it is determinant for cell function. For example, osteocyte morphology and alignment differ in two types of bone, fibula and calvaria, probably due to different mechanical loading patterns, which influence cytoskeletal structure and thus cell shape (Vatsa et al., 2008). Also, osteocyte and lacunae morphology may vary in pathological bone conditions, and these morphological variations may be an adaptation to the differences in matrix properties and thus, different bone strain levels under similar stimulus (van Hove et al., 2009). Osteocyte morphology is characterized by long dendritic-like processes, cell shape also assumed by osteoblast MC3T3 cells cultured in 3D; however, differences in cytoskeleton elements in the processes of these two cell types may indicate differences in function; microtubules are predominant on osteoblasts' processes while actin ensures integrity of osteocytes' cytoplasmatic projections (Murshid et al., 2007). In agreement with section 2.7.1, osteocyte sensitivity to mechanical load applied to the microparticles varies between those attached to the cell bodies and those to the processes: a much smaller displacement of the second ones is needed to cause an intracellular calcium influx that rapidly propagates to the cell body; if local stimulus is applied to the cell body, the reaction is slower and a higher displacement is needed to elicit the calcium transient (Adachi et al., 2009).

Osteoblasts, osteoid-osteocytes and mature osteocytes have different mechanical properties. The elastic modulus is higher on the cell peripheral area than in the nuclear region; as bone cells mature, the elastic modulus decreases, both in the

peripheral and nuclear regions. These differences in elastic modulus probably depend on the amount of actin filaments, as it has been shown in other cell types. Furthermore, focal adhesion area is smaller in mature osteocytes, when comparing to osteoblasts. If peptides containing RGD sequence are added to culture medium, both the focal adhesion area and the elastic modulus of osteoblasts decreases whilst osteocytes remain unaffected (Sugawara et al., 2008).

2.8 Mechanotransduction mechanisms

Although there is emergent gathered knowledge on mechanotransduction mechanisms in distinct cells and tissues, the multitude of cellular structures, messenger substances, environmental factors and organ levels of organization, makes it extremely complex to understand how responses are composed at cellular, organ and living organism levels.

2.8.1 Strain, frequency and loading duration

Strain magnitude, frequency and loading duration influence bone remodelling. Wolff defined the mathematical equations that allowed prediction of trabeculae orientation and thickness (Prendergast & Huiskes, 1995). Turner enunciated three essential rules critical for bone remodelling:

1. Dynamic loading determines remodelling;
2. Short periods of loading quickly trigger a response; prolonging loading times any further diminishes the magnitude of bone cell response;
3. Bone cells have memory and accommodate to routine loading, diminishing the amplitude of the answer triggered by a same repeated stimulus.

In *in vivo* studies, increasing loading frequency decreased the threshold for osteogenesis and increased strain-related bone deposition (Hsieh & Turner, 2001). Cortical bone adaptation is nonlinear when it comes to frequency response; the changes in geometry are more significant with increasing load frequency, with a plateau for frequencies beyond 10 Hz (Warden & Turner, 2004). Bone formation also depends on strain magnitude (Mosley et al., 1997), along with the number of loading cycles at low frequencies (Cullen et al., 2001). The skeletal adaptation is also conditioned by strain distribution. Unusual strain distribution will quickly trigger an osteogenic response, as suggested by the extensive periosteal and endosteal bone proliferation described by Rubin & Lanyon (1984) in a study conducted in poultry. Rest periods between loading cycles also intensify osteogenic response (Srinivasan et al., 2007) and maximize cell response (Pereira & Shefelbine, 2014).

Other mechanisms apart from direct deformation of cells, are involved in bone cells mechanical stimulation. Peak strains may be considerable high in long bones during strenuous exercise, but strains as low as 0.15% are enough to ensure osteoblast

recruitment *in vivo* (Rubin & Lanyon, 1984). Due to bone's architectural complexity, it is impractical to measure with precision the separate actual deformation of a cell.

Bone is a porous structure and the canalicular system within it is filled with fluid. The fluid flows within the canalicular system wherein the osteocytes extend their cell processes, and it is displaced by loading. Simulation of load levels as the ones described as inducing significant osteogenesis, has produced higher shear stresses due to fluid flow in the canaliculi, reinforcing osteocyte processes as the main mechanosensing organ in mature bone cells (Verbruggen et al., 2014).

Fluid also carries electrically charged particles. When bone is deformed, a thin layer of fluid with particles with opposite charge to that of the matrix and bone cells is formed (Gross & Williams, 1982); when a non-uniform mechanical load is applied to the bone structure, the freely moving ions in the fluid move away from the matrix.

The fluid flow phenomenon thus resulting is common to other biological tissues, but not only. The fact that fluid flow changes interfacial chemistry has been acknowledged; for example, the flow of fresh water along the surfaces disturbs the equilibrium of dissolved ions, changing the surface charge and the molecular orientation of the water at the interface (Waychunas, 2014). Likewise, in bone, the displacement of the electrically charged fluid creates an electrical field aligned with the fluid flow. This causes an electrical potential and the phenomenon is known as strain generated bone streaming potential (Gross & Williams, 1982; Frijns et al., 2005; Hong et al., 2008). The density of matrix fixed charges influences the magnitude of the generated streaming potential (Iatridis et al., 2003), so the mechanosensory ability along bone may vary and ultimately, influence dynamic stiffness.

2.8.2 Bone piezoelectricity

Fukada and Yasuda first described bone piezoelectrical properties, in the 50's. In dry bone samples submitted to compressive load, an electrical potential was generated, a phenomenon explicated by the direct piezoelectric effect (Fukada & Yasuda, 1957). In connective tissues, such as bone, skin, tendon and dentine, the dipole moments are probably related to the collagen fibres, composed by strongly polar protein molecules aligned (Fukada & Yasuda, 1964; Elmessiery, 1981; Halperin et al., 2004). The proper architecture of bone, with neatly aligned lamellae, contributes for potentials' generation along bone structure (Elmessiery, 1981).

The polarization generated per unit of mechanical stress, that is, the bone piezoelectric constants, changes with moisture content, maturation state (immature bone has lower piezoelectric constants than mature bone) and architectural organization (altered areas, such as the ones with bone neoplasia osteosarcoma, show lower values) (Marino & Becker, 1974). Piezoelectric constants are higher in dentin when moisture contents increase and behave in an anisotropic fashion; tubule orientation strongly effects piezoelectricity (Wang et al., 2007). Initially, it was also argued whether or not wet bone behaved as a piezoelectric material; it is now

accepted that certainly it does (Fukada & Yasuda, 1957; Marino & Becker, 1974; Reinish & Nowick, 1975).

Bone piezoelectrical properties have been related to bone remodelling processes, and to streaming potential mechanisms (Ramtani, 2008; Ahn & Grodzinsky, 2009). Due to its potential impact on therapeutic approaches to bone remodelling and healing, more and more research is being conducted.

The use of a piezoelectric substrate and the piezoelectric converse effect were tested *in vitro* and *in vivo* with promising results, mechanically stimulating osteoblastic cells and bone, suggesting the potential for clinical application (Frias et al, 2010; Reis et al, 2012). The development of new synthetic scaffolds, like for instance hydroxyapatite/ barium titanate, with high piezoelectric coefficients that could enhance bone remodelling, is a new emergent field for the bone tissue engineering industry (Zhang et al., 2014).

Acknowledgements This work has been partially supported by the European Commission under the 7th Framework Programme through the project RESTORATION, grant agreement CP-TP 280575-2. The support from Medtronic Spine LLC Company, Portugal in supplying surgical material is gratefully acknowledged. The support from Hamamatsu Photonics in supplying the Nanozoomer SQ is also gratefully acknowledged. The authors would also like to thank Mr. Pedro Félix Pinto for the artwork included in this chapter.

3. References

1. Abe E, Marians RC, Yu W et al (2003) TSH is a negative regulator of skeletal remodelling. Cell 115:151–62.
2. Abu EO, Bord S, Horner A et al (1997) The expression of thyroid hormone receptors in human bone. Bone 21:137-142.
3. Adachi T, Aonuma Y, Tanaka M et al (2009) Calcium response in single osteocytes to locally applied mechanical stimulus: Differences in cell process and cell body. J Biomech 42:1989-1995.
4. ADHR Consortium (2000) Autosomal dominant hypophosphataemic rickets is associated with mutations in FGF23. Nat Genet 26: 345–348.
5. Ahn AC & Grodzinsky AJ (2009) Relevance of collagen piezoelectricity to "Wolff's Law": A critical review. Med Eng Phys 31:733-741.
6. Anava S, Greenbaum A, Ben Jacob E et al (2009) The Regulative Role of Neurite Mechanical Tension in Network Development. Biophys J 96:1661-1670.
7. Arai F, Miyamoto T, Ohneda O et al (1999) Commitment and differentiation of osteoclast precursor cells by the sequential expression of c-Fms and receptor activator of nuclear factor κb (RANK) receptors. J Exp Med 190:1741-1754.
8. Arnett, T (2003) Regulation of bone cell function by acid–base balance Proc Nutr Soc 62:511-520.

9. Asagiri M & Takayanagi H (2007) The molecular understanding of osteoclast differentiation. Bone 40:251-264.
10. Ashizawa N, Graf K, Do YS et al (1996) Osteopontin is produced by rat cardiac fibroblasts and mediates A (II)-induced DNA synthesis and collagen gel contraction. J Clin Invest 98:2218-2227.
11. Barczyk M, Carracedo S & Gullberg D (2010) Integrins. Cell Tissue Res 339:269-80.
12. Baron R, Neff L, Louvard D & Courtoy PJ (1985) Cell-mediated extracellular acidification and bone resorption: evidence for a low pH in resorbing lacunae and localization of a 100-kD lysosomal membrane protein at the osteoclast ruffled border. J Cell Biol 101:2210-2222.
13. Bassett JD & Williams GR (2016) Role of thyroid hormones in skeletal development and bone maintenance. Endocr Rev, 37:135-187.
14. Baylink DJ, Finkelman RD & Mohan S (1993) Growth factors to stimulate bone formation. J Bone Miner Res 8:S565-S572.
15. Beederman M, Lamplot JD, Nan G et al (2013) BMP signaling in mesenchymal stem cell differentiation and bone formation. J Biomed Sci Eng 6: 32–52.
16. Belanger LF (1969) Osteocytic osteolysis. Calcif Tissue Res 4:1–12.
17. Bellows CG & Heersche JNM (2001) The frequency of common progenitors for adipocytes and osteoblasts and of committed and restricted adipocyte and osteoblast progenitors in fetal rat calvaria cell populations. J Bone Miner Res 16:1983-1993.
18. Bellows CG, Reimers SM & Heersche JNM (1999) Expression of mRNAs for type-I collagen, bone sialoprotein, osteocalcin, and osteopontin at different stages of osteoblastic differentiation and their regulation by 1,25 dihydroxyvitamin D_3. Cell Tissue Res 297:249-259.
19. Ben-Dov IZ, Galitzer H, Lavi-Moshayoff V et al (2007) The parathyroid is a target organ for FGF23 in rats. J Clin Invest 117:4003-4008.
20. Bentmann A, Kawelke N, Moss D et al (2010) Circulating fibronectin affects bone matrix, whereas osteoblast fibronectin modulates osteoblast function. J Bone Miner Res 25:706-715.
21. Bentolila V, Boyce TM, Fyhrie DP et al (1998) Intracortical remodelling in adult rat long bones after fatigue loading. Bone 23:275-281.
22. Bhattacharya R, Gonzalez AM, DeBiase PJ et al (2009) Recruitment of vimentin to the cell surface by β3 integrin and plectin mediates adhesion strength. J Cell Sci 122:1390-1400.
23. Bivi N, Condon KW & Allen MR (2012) Cell autonomous requirement of connexin 43 for osteocyte survival: consequences for endocortical resorption and periosteal bone formation. J Bone Miner Res 27:374-389.
24. Blair HC, Teitelbaum SL, Ghiselli R & Gluck S (1989) Osteoclastic bone resorption by a polarized vacuolar proton pump. Science 245:855-857.
25. Bodian DL, Chan T-F, Poon A et al (2009) Mutation and polymorphism spectrum in osteogenesis imperfecta type II: implications for genotype-phenotype relationships. Hum Mol Gen 18:463-471.

26. Boissy P, Saltel F, Bouniol C et al (2002) Transcriptional activity of nuclei in multinucleated osteoclasts and its modulation by calcitonin. Endocrinology 143:1913-1921.
27. Bonewald LF (2007) Osteocyte messages from a bony tomb. Cell Metab. 5:410–411.
28. Bray D (1979) Mechanical tension produced by nerve cells in tissue culture. J Cell Sci 37: 391-410.
29. Brighton CT, Sennett BJ, Farmer JC et al (1992) The inositol phosphate pathway as a mediator in the proliferative response of rat calvarial bone cells to cyclical biaxial mechanical strain. J Orthop Res 10:385-393.
30. Britto JM, Fenton AJ, Holloway WR et al (1994) Osteoblasts mediate thyroid hormone stimulation of osteoclastic bone resorption. Endocrinology 134:169–176.
31. Brown MC, Perrotta JA & Turner CE (1996) Identification of LIM3 as the principal determinant of paxillin focal adhesion localization and characterization of a novel motif on paxillin directing vinculin and focal adhesion kinase binding. J Cell Biol 135:1109-1123.
32. Burger EH & Klein-Nulend J (1999) Mechanotransduction in bone—role of the lacuno-canalicular network. FASEB J 13:101-112.
33. Burr DB, Milgrom C, Fyhrie D et al (1996) *In vivo* measurement of human tibial strains during vigorous activity. Bone 18:405-410.
34. Bushinsky DA & Krieger NS (2015) Acid–base balance and bone health. In Nutrition and bone health (pp. 335-357). Springer New York.
35. Calvi LM, Adams GB, Weibrecht KW et al (2003) Osteoblastic cells regulate the haematopoietic stem cell niche. Nature 425:841-846.
36. Canalis E, Adams DJ, Boskey A et al (2013) Notch signaling in osteocytes differentially regulates cancellous and cortical bone remodelling. J Biol Chem 288:25614-25625.
37. Carbonare LD, Valenti MT, Bertoldo F, et al (2005) Bone microarchitecture evaluated by histomorphometry. Micron 36, 609-616.
38. Carreira AC, Lojudice FH, Halcsik E et al (2014) Bone morphogenetic proteins facts, challenges, and future perspectives. J Dent Res 93:335-45.
39. Carter DR & Beaupré GS (2001) Skeletal tissue histomorphology and mechanics. Skeletal function and form. Cambridge, United Kingdom.
40. Cartwright JHE, Piro O & Tuval I (2004) Fluid-dynamical basis of the embryonic development of left-right asymmetry in vertebrates. Proc Natl Acad Sci U S A 101**:**7234-7239.
41. Carvalho RS, Schaffer JL & Gerstenfeld LC (1998) Osteoblasts induce osteopontin expression in response to attachment on fibronectin: Demonstration of a common role for integrin receptors in the signal transduction processes of cell attachment and mechanical stimulation. J Cell Biochem 70:376-390.
42. Carvalho RS, Bumann A, Schaffer JL & Gerstenfeld LC (2002) Predominant integrin ligands expressed by osteoblasts show preferential regulation in response to both cell adhesion and mechanical perturbation. J Cell Biochem 84:497-508.

43. Chambers TJ & Fuller K (1985) Bone cells predispose bone surfaces to resorption by exposure of mineral to osteoclastic contact. J Cell Sci 76:155-165.
44. Chen JC, Hoey DA, Chua M et al (2016) Mechanical signals promote osteogenic fate through a primary cilia-mediated mechanism. FASEB J 30:1504-1511.
45. Chen JH, Liu C, You L & Simmons CA (2010) Boning up on Wolff's Law: mechanical regulation of the cells that make and maintain bone. J Biomech 43:108-118.
46. Cheng H, Jiang W, Phillips FM et al (2003) Osteogenic activity of the fourteen types of human bone morphogenetic proteins (BMPs). J Bone Joint Surg Am 85:1544-1552.
47. Cherian PP, Cheng B, Gu S et al (2003) Effects of mechanical strain on the function of gap junctions in osteocytes are mediated through the prostaglandin EP2 receptor. J Biol Chem 278:43146-43156.
48. Clarke B (2008) Normal bone anatomy and physiology. Clin J Am Soc Nephrol 3:S131-S139.
49. Collignon J, Varlet I & Robertson EJ (1996) Relationship between asymmetric nodal expression and the direction of embryonic turning. Nature 381:155-158.
50. Compston JE (2001) Sex steroids and bone. Physiol Rev 81:419-447.
51. Corral DA, Amling M, Priemel M et al (1998) Dissociation between bone resorption and bone formation in osteopenic transgenic mice. Proc Natl Acad Sci U S A 95:13835-13840.
52. Coughlin TR, Voisin M, Schaffler MB et al (2015) Primary cilia exist in a small fraction of cells in trabecular bone and marrow. Calcif Tissue Int 96:65-72.
53. Cram EJ & Schwarzbauer JE (2004) The talin wags the dog: new insights into integrin activation. Trends Cell Biol 14:55-57.
54. Cullen DM, Smith RT & Akhter MP (2001) Bone-loading response varies with strain magnitude and cycle number. J Appl Physiol 91:1971-1976.
55. Currey JD (2003) The many adaptations of bone. J Biomech 36:1487-1495.
56. Dason JS, Smith AJ, Marin L & Charlton MP (2014) Cholesterol and F-actin are required for clustering of recycling synaptic vesicle proteins in the presynaptic plasma membrane. J Physiol 592:621-633.
57. de Vries WN, Evsikov AV, Haak BE et al (2004) Maternal β-catenin and E-cadherin in mouse development. Development 131:4435-4445.
58. del Álamo JC, Norwich GN, Y-shuan JL et al (2008) Anisotropic rheology and directional mechanotransduction in vascular endothelial cells. Proc Natl Acad Sci U S A 105:15411-15416.
59. Delaine-Smith RM, Sittichokechaiwut A & Reilly GC (2014) Primary cilia respond to fluid shear stress and mediate flow-induced calcium deposition in osteoblasts. FASEB J 28:430-439.
60. Delany AM, Amling M, Priemel M et al (2000) Osteopenia and decreased bone formation in osteonectin-deficient mice. J Clin Invest 105:915-923.

61. Delany AM & Hankenson KD (2009) Thrombospondin-2 and SPARC/osteonectin are critical regulators of bone remodelling. J Cell Commun Signal, 3:227-238.
62. Dennerll TJ, Lamoureux P, Buxbaum RE & Heidemann SR (1989) The cytomechanics of axonal elongation and retraction. J Cell Biol 109:3073-3083.
63. Ding W, Li J, Singh J et al (2015) miR-30e targets IGF2-regulated osteogenesis in bone marrow-derived mesenchymal stem cells, aortic smooth muscle cells, and ApoE−/− mice. Cardiovasc Res, cvv030.
64. Doi S, Zou Y, Togao O et al (2011) Klotho inhibits transforming growth factor-β1 (TGF-β1) signaling and suppresses renal fibrosis and cancer metastasis in mice. J Biol Chem 286:8655-8665.
65. Draper CR, Edel MJ, Dick IM et al (1997) Phytoegens reduce bone loss and bone resorption in oophorectomized rats. J Nut 127:1795-1799.
66. Ducy P, Amling M, Takeda S et al (2000). Leptin inhibits bone formation through a hypothalamic relay: a central control of bone mass. Cell 100:197–207.
67. Duncan RL & Turner CH (1995) Mechanotransduction and the functional response of bone to mechanical strain. Calcif Tissue Int 57:344-358.
68. El Hadidy M, Ghonaim M, El Gawad S & El Atta MA (2011) Impact of severity, duration, and etiology of hyperthyroidism on bone turnover markers and bone mineral density in men. BMC Endocr Disord 11.1:1.
69. El-Hoss J, Arabian A, Dedhar S & St-Arnaud R (2014) Inactivation of the integrin-linked kinase (ILK) in osteoblasts increases mineralization. Gene, 533, 246-252.
70. Elefteriou F, Takeda S, Ebihara K et al (2004) Serum leptin level is a regulator of bone mass. Proc Natl Acad Sci U S A 101:3258-3263.
71. Elmessiery MA (1981) Physical basis for piezoelectricity of bone matrix. IEE Proc A 128:336-346.
72. Emerton KB, Hu B, Woo AA et al (2010) Osteocyte apoptosis and control of bone resorption following ovariectomy in mice. Bone 46:577-583.
73. Faloni APS, Sasso-Cerri E, Katchburian E & Cerri PS (2007) Decrease in the number and apoptosis of alveolar bone osteoclasts in estrogen-treated rats. J Periodont Res 42:193–201.
74. Faloni APDS, Sasso-Cerri E, Rocha FRG et al (2012) Structural and functional changes in the alveolar bone osteoclasts of estrogen-treated rats. J Anat 220:77-85.
75. Fan X, Roy E, Zhu L et al (2004) Nitric oxide regulates receptor activator of nuclear factor κB ligand and osteoprotegerin expression in bone marrow stromal cells. Endocrinology 145:751-759.
76. Fan X, Rahnert JA, Murphy TC et al (2006) Response to mechanical strain in an immortalized pre-osteoblast cell is dependent on ERK1/2. J Cell Physiol 207:454-460.
77. Feng JQ, Ward LM, Liu S et al (2006) Loss of DMP1 causes rickets and osteomalacia and identifies a role for osteocytes in mineral metabolism. Nat Genet 38:1310-1315.

78. Ferraro JT, Daneshmand M, Bizios R & Rizzo V (2004) Depletion of plasma membrane cholesterol dampens hydrostatic pressure and shear stress-induced mechanotransduction pathways in osteoblast cultures. Am J Physiol - Cell Physiol 286:831-839.
79. Ferreira AM, González G, González-Paz RJ et al (2009) Bone collagen role in piezoelectric mediated remineralization. Acta Microsc 18:278-286.
80. Ferron M, Hinoi E, Karsenty G & Ducy P (2008) Osteocalcin differentially regulates β cell and adipocyte gene expression and affects the development of metabolic diseases in wild-type mice. Proc Natl Acad Sci U S A 105:5266-5270.
81. Ferron M, Wei J, Yoshizawa T et al (2010) Insulin signaling in osteoblasts integrates bone remodelling and energy metabolism. Cell 142:296-308.
82. Fisher LW, Torchia DA, Fohr B et al (2001) Flexible structures of SIBLING proteins, bone sialoprotein, and osteopontin. Biochem Biophys Res Commun 280:460-465.
83. Flagg-Newton J, Simpson I & Loewenstein WR (1979) Permeability of the cell-to-cell membrane channels in mammalian cell junctions. Science 205:404-407.
84. Fowlkes JL, Bunn RC, Liu L et al (2008) Runt-related transcription factor 2 (RUNX2) and RUNX2-related osteogenic genes are down-regulated throughout osteogenesis in type 1 diabetes mellitus. Endocrinology 149: 1697 –704.
85. Fraioli R, Rechenmacher F, Neubauer S et al (2015) Mimicking bone extracellular matrix: Integrin-binding peptidomimetics enhance osteoblast-like cells adhesion, proliferation, and differentiation on titanium. Colloids Surfaces B 128:191-200.
86. Franceschi RT, Wang D, Krebsbach PH & Rutherford RB (2000) Gene therapy for bone formation: *in vitro* and *in vivo* osteogenic activity of adenovirus expressing BMP-7. Ann Arbor 1001:48109-1078.
87. Frias C, Reis J, e Silva FC, Potes J, Simões J & Marques AT (2010) Polymeric piezoelectric actuator substrate for osteoblast mechanical stimulation. J Biomech 43:1061-1066.
88. Frijns A, Huyghe J & Wijlaars M (2005) Measurements of deformations and electrical potentials in a charged porous medium. In IUTAM Symposium on Physicochemical and Electromechanical Interactions in Porous Media, pp. 133-139.
89. Fukada E & Yasuda I (1957) On the piezoelectric effect of bone. J Phys Soc Jpn 12:1158-1162.
90. Fukada E & Yasuda I (1964) Piezoelectric effects in collagen. Jpn. J. Appl. Phys 3:117-121.
91. Fukumoto S & Martin TJ (2009) Bone as an endocrine organ. Trends Endocrinol Metab 20:230-236.
92. Fukumoto S & Yamashita T (2007) FGF23 is a hormone-regulating phosphate metabolism–unique biological characteristics of FGF23. Bone 40:1190–1195.

93. Fulzele K, Riddle RC, DiGirolamo DJ et al (2010) Insulin receptor signaling in osteoblasts regulates postnatal bone acquisition and body composition. Cell 142: 309 – 19.
94. Ganss B, Kim RH & Sodek J (1999) Bone sialoprotein. Crit Rev Oral Biol Med 10:79-98.
95. Geiger B, Spatz JP & Bershadsky AD (2009) Environmental sensing through focal adhesions. Nature Rev Mol Cell Biol 10:21-33.
96. Gillespie PG & Walker RG (2001) Molecular basis of mechanosensory transduction. Nature 413:194-202.
97. Green J & Kleeman CR (1991) The role of bone in the regulation of systemic acid-base balance. Kidney Int 39:9-26.
98. Gross D & Williams WS (1982) Streaming potential and the electromechanical response of physiologically-moist bone. J Biomech 15:277-295.
99. Guevarra MS, Yeh JK, Castro Magana M & Aloia JF (2010) Synergistic effect of parathyroid hormone and growth hormone on trabecular and cortical bone formation in hypophysectomized rats. Hormone Res Paediatr 73: 248–257.
100. Hadjidakis DJ & Androulakis II (2006) Bone remodelling. Ann N Y Acad Sci 1092:385-96.
101. Halperin C, Mutchnik S, Agronin A et al (2004). Piezoelectric effect in human bones studied in nanometer scale. Nano Letters 4:1253-1256.
102. Hamrick MW, Ferrari SL (2008) Leptin and the sympathetic connection of fat to bone. Osteoporos Int J Establ Result Coop Eur Found Osteoporos Natl Osteoporos Found U S A 19:905–12.
103. Harada SI & Rodan GA (2003) Control of osteoblast function and regulation of bone mass. Nature 423:349-355.
104. Harter LV, Hruska KA & Duncan RL (1995) Human osteoblast-like cells respond to mechanical strain with increased bone matrix protein production independent of hormonal regulation. Endocrinology 136:528-535.
105. Harvey RD, McHardy KC, Reid IW et al (1991) Measurement of bone collagen degradation in hyperthyroidism and during thyroxine replacement therapy using pyridinium cross-links as specific urinary markers. J Clin Endocrinol Metab 72:1189–94.
106. Haugh MG, Vaughan TJ & McNamara LM (2015) The role of integrin α V β 3 in osteocyte mechanotransduction. J Mech Behav Biomed Mater 42:67-75.
107. Haussler MR, Whitfield GK, Haussler CA et al (1998) The nuclear vitamin D receptor: biological and molecular regulatory properties revealed. J Bone Miner Res 13:325-349.
108. Haussler MR, Whitfield GK, Kaneko I et al (2012). The role of vitamin D in the FGF23, klotho, and phosphate bone-kidney endocrine axis. Rev Endocr Metab Disord 13:57-69.

109. Heinonen A, Oja P, Kannus P et al (1995) Bone mineral density in female athletes representing sports with different loading characteristics of the skeleton. Bone 17:197-203.
110. Hendesi H, Barbe MF, Safadi FF et al (2015) Integrin mediated adhesion of osteoblasts to connective tissue growth factor (CTGF/CCN2) induces cytoskeleton reorganization and cell differentiation. PloS One 10.
111. Hirose S, Li M, Kojima T et al (2007) A histological assessment on the distribution of the osteocytic lacunar canalicular system using silver staining. J Bone Miner Metab 25:374-382.
112. Holloway WR, Collier FM, Aitken CJ et al (2002) Leptin inhibits osteoclast generation. J Bone Miner Res 17:200-209.
113. Hong J, Ko S, Khang G & Mun M (2008) Intraosseous pressure and strain generated potential of cylindrical bone samples in the drained uniaxial condition for various loading rates. J Mater Sci Mater Med 19:2589-2594.
114. Hsieh Y-F & Turner CH (2001) Effects of loading frequency on mechanically induced bone formation. J Bone Miner Res 16:918-924.
115. Hu S, Chen J, Fabry B et al (2003) Intracellular stress tomography reveals stress focusing and structural anisotropy in cytoskeleton of living cells. Am J Physiol 285:1082-1090.
116. Huang CP, Chen XM & Chen ZQ (2008) Osteocyte: The impresario in the electrical stimulation for bone fracture healing. Med Hypotheses 70:287-290.
117. Huang E, Zhu G, Jiang W et al (2012) Growth hormone synergizes with BMP9 in osteogenic differentiation by activating the JAK/STAT/IGF1 pathway in murine multilineage cells. J Bone Miner Res 27:1566-1575.
118. Huang G, Zhang Y, Kim B et al (2009) Fibronectin binds and enhances the activity of bone morphogenetic protein 1. J Biol Chem 284:25879-25888.
119. Hughes DE, Dai A, Tiffee JC et al (1996) Estrogen promotes apoptosis of murine osteoclasts mediated by TGF-β. Nature Med 2:1132–1136.
120. Hynes RO (2002) Integrins: bidirectional, allosteric signaling machines. Cell 110:673-687.
121. Iatridis J, Laible J & Krag M (2003) Influence of fixed charge density magnitude and distribution on the intervertebral disc: applications of a poroelastic and chemical electric (PEACE) model. J Biomech Eng 125:12-24.
122. Ingber DE (1997) Tensegrity: The Architectural Basis of Cellular Mechanotransduction. Annu Rev Physiol 59:575-599.
123. Ingber DE (2006) Mechanical control of tissue morphogenesis during embryological development. Dev Biol 50:255-266.
124. Isaksson OG, Jansson JO & Gause IA (1982) Growth hormone stimulates longitudinal bone growth directly. Science 216:1237-1239.
125. Jee WSS, Mori S, Li XJ & Chan S (1990) Prostaglandin E2 enhances cortical bone mass and activates intracortical bone remodelling in intact and ovariectomized female rats. Bone 11, 253-266.
126. Jilka RL, Noble B & Weinstein RS (2013) Osteocyte apoptosis. Bone, 54: 264-271.

127. Kadow-Romacker A, Hoffmann JE, Duda G et al (2009) Effect of mechanical stimulation on osteoblast- and osteoclast-like cells *in vitro*. Cells Tissues Organs 190:61-68.
128. Kang, Q, Sun, MH, Cheng H et al (2004) Characterization of the distinct orthotopic bone-forming activity of 14 BMPs using recombinant adenovirus-mediated gene delivery. Gene Ther 11:1312-1320.
129. Kang Q, Song WX, Luo Q et al (2009) A comprehensive analysis of the dual roles of BMPs in regulating adipogenic and osteogenic differentiation of mesenchymal progenitor cells. Stem Cells Dev 18:545-559.
130. Karsenty G, Kronenberg HM & Settembre C (2009) Genetic control of bone formation. Annu Rev Cell Dev Biol 25:629-648.
131. Kasten TP, Collin-Osdoby P, Patel N et al (1994) Potentiation of osteoclast bone-resorption activity by inhibition of nitric oxide synthase. Proc Natl Acad Sci U S A 91:3569-3573.
132. Katz B-Z, Zamir E, Bershadsky A et al (2000) Physical state of the extracellular matrix regulates the structure and molecular composition of cell-matrix adhesions. Mol Biol Cell 11:1047-1060.
133. Kazmierczak P, Sakaguchi H, Tokita J et al (2007) Cadherin 23 and protocadherin 15 interact to form tip-link filaments in sensory hair cells. Nature 449:87-91.
134. Khatiwala CB, Peyton SR & Putnam AJ (2006) Intrinsic mechanical properties of the extracellular matrix affect the behavior of pre-osteoblastic MC3T3-E1 cells. Am J Physiol Cell Physiol 290:1640-1650.
135. Khosla S, Oursler MJ & Monroe DG (2012) Estrogen and the skeleton. Trends Endocrinol Metab 23:576-581.
136. Kim DW, Lee HJ, Karmin JA et al (2006) Mechanical loading differentially regulates membrane-bound and soluble RANKL availability in MC3T3-E1 cells. Ann N Y Acad Sci 1068:568-572.
137. Kindblom JM, Ohlsson C, Ljunggren Ö et al (2009) Plasma osteocalcin is inversely related to fat mass and plasma glucose in elderly Swedish men. J Bone Miner Res 24:785–791.
138. Klausen TK, Hougaard C, Hoffmann EK & Pedersen SF (2006) Cholesterol modulates the volume-regulated anion current in Ehrlich-Lettre ascites cells via effects on Rho and F-actin. Am J Physiol Cell Physiol 291:757-771.
139. Klein-Nulend J, Helfrich MH, Sterck JGH et al (1998) Nitric oxide response to shear stress by human bone cell cultures is endothelial nitric oxide synthase dependent. Biochem Biophys Res Commun 250:108-114.
140. Knothe Tate ML (2003) Whither flows the fluid in bone? An osteocyte's perspective. J Biomech 36:1409-1424.
141. Knothe Tate ML, Adamson JR, Tami AE & Bauer TW (2004) The osteocyte. Int J Biochem Cell Biol 36:1-8.
142. Kong Y-Y, Feige U, Sarosi I et al (1999) Activated T cells regulate bone loss and joint destruction in adjuvant arthritis through osteoprotegerin ligand. Nature 402:304-309.

143. Kobayashi T, Lyons KM, McMahon AP & Kronenberg HM (2005) BMP signaling stimulates cellular differentiation at multiple steps during cartilage development. Proc Natl Acad Sci U S A 102:18023-18027.
144. Koike M, Nojiri H, OzawaY et al (2015) Mechanical overloading causes mitochondrial superoxide and SOD2 imbalance in chondrocytes resulting in cartilage degeneration. Sci Rep, 5. doi:10.1038/srep11722.
145. Kousteni S, Chen JR, Bellido T et al (2002) Reversal of bone loss in mice by nongenotropic signaling of sex steroids. Science 298:843-846.
146. Krajisnik T, Bjorklund P, Marsell R et al (2007) Fibroblast growth factor-23 regulates parathyroid hormone and 1alpha-hydroxylase expression in cultured bovine parathyroid cells. J Endocrinol 195:125–131.
147. Kreja L, Liedert A, Hasni S, Claes L & Ignatius A (2008) Intermittent mechanical strain increases RANKL expression in human osteoblasts. J Biomech 41:S462-S462.
148. Kringelbach TM, Aslan D, Novak I et al (2015) Fine-tuned ATP signals are acute mediators in osteocyte mechanotransduction. Cell Signal 27:2401-2409.
149. Krings A, Rahman S, Huang S et al (2012) Bone marrow fat has brown adipose tissue characteristics, which are attenuated with aging and diabetes. Bone 50:546-552.
150. Kurosu H, Ogawa Y, Miyoshi M et al. (2006) Regulation of fibroblast growth factor-23 signaling by klotho. J Biol Chem 281:6120–6123.
151. Kuzma M, Kuzmova Z, Zelinkova Z et al (2014) Impact of the growth hormone replacement on bone status in growth hormone deficient adults. Growth Horm IGF Res 24:22–28.
152. Lamoureux F, Baud'huin M, Duplomb L et al (2007) Proteoglycans: key partners in bone cell biology. BioEssays 29: 758-771.
153. le Noble F, Klein C, Tintu A et al (2008) Neural guidance molecules, tip cells, and mechanical factors in vascular development. Cardiovasc Res 78:232-241.
154. Lee KC, Jessop H, Suswillo R et al (2004) The adaptive response of bone to mechanical loading in female transgenic mice is deficient in the absence of oestrogen receptor-alpha and -beta. J Endocrinol 182:193-201.
155. Lee NK & Karsenty G (2008) Reciprocal regulation of bone and energy metabolism. Trends Endocrinol Metab 19:161-166.
156. Leucht P, Monica SD, Temiyasathit S et al (2013) Primary cilia act as mechanosensors during bone healing around an implant. Med Eng Phys 35:392-402.
157. Li RD, Deng ZL, Hu N et al (2012) Biphasic effects of TGFβ1 on BMP9-induced osteogenic differentiation of mesenchymal stem cells. BMB Rep 45:509-514.
158. Liel Y, Shany S, Smirnoff P & Schwartz B (1999) Estrogen increases 1, 25-dihydroxyvitamin D receptors expression and bioresponse in the rat duodenal mucosa 1. Endocrinology 140:280-285.

159. Lin GL & Hankenson KD (2011) Integration of BMP, Wnt, and notch signaling pathways in osteoblast differentiation. J Cell Biochem 112:3491–3501.
160. Littlewood-Evans A, Kokubo T, Ishibashi O et al (1997) Localization of cathepsin K in human osteoclasts by in situ hybridization and immunohistochemistry. Bone 20:81-86.
161. Litzenberger JB, Tang WJ, Castillo AB & Jacobs CR (2009) Deletion of β1 integrins from cortical osteocytes reduces load-induced bone formation. Cell Mol Bioeng 2:416-424.
162. Litzenberger JB, Kim JB, Tummala P & Jacobs CR (2010) β1 integrins mediate mechanosensitive signaling pathways in osteocytes. Calcif Tissue Int 86:325-332.
163. Liu H, Fergusson MM, Castilho RM et al (2007) Augmented Wnt signaling in a mammalian model of accelerated aging. Science 317:803-806.
164. López I, Rodríguez-Ortiz ME, Almadén Y et al (2011). Direct and indirect effects of parathyroid hormone on circulating levels of fibroblast growth factor 23 *in vivo*. Kidney Int 80:475-482.
165. López I, Pineda C, Raya AI et al (2016) Leptin directly stimulates parathyroid hormone secretion. Endocrine Abstracts 41:GP144.
166. Lupu F, Terwilliger JD, Lee K et al (2001) Dev. Biol. 229:141–162.
167. Lyles KW, Halsey DL, Friedman NE & Lobaugh B (1988) Correlations of serum concentrations of 1,25-dihydroxyvitamin D, phosphorus, and parathyroid hormone in tumoral calcinosis. J Clin Endocrinol Metab 67:88–92.
168. Malaval L, Wade-Guéye NM, Boudiffa M et al (2008) Bone sialoprotein plays a functional role in bone formation and osteoclastogenesis. J Exp Med 205:1145-1153.
169. Malone AMD, Anderson CT, Tummala P et al (2007) Primary cilia mediate mechanosensing in bone cells by a calcium-independent mechanism. Proc Natl Acad Sci U S A. 104:13325-13330.
170. Mann V, Huber C, Kogianni G et al (2006) The influence of mechanical stimulation on osteocyte apoptosis and bone viability in human trabecular bone. J Musculoskelet Neuronal Interact 6, 408-417.
171. Mantzoros CS, Magkos F, Brinkoetter M et al (2011). Leptin in human physiology and pathophysiology. Am J Physiol Endocrinol Metab 301:E567-E584.
172. Maor G, Rochwerger M, Segev Y & Phillip M (2002) Leptin acts as a growth factor on the chondrocytes of skeletal growth centres. J Bone Miner Res 17:1034-1043.
173. Marchisio PC, Cirillo D, Naldini L et al (1984) Cell-substratum interaction of cultured avian osteoclasts is mediated by specific adhesion structures. J Cell Biol 99:1696-1705.
174. Marino AA & Becker RO (1974) Piezoelectricity in bone as a function of age. Calcif Tissue Int 14:327-331.

175. Martin RB (2007) Targeted bone remodelling involves BMU steering as well as activation. Bone 40:1574-1580.
176. Masuyama R, Stockmans I, Torrekens S et al (2006). Vitamin D receptor in chondrocytes promotes osteoclastogenesis and regulates FGF23 production in osteoblasts. J Clin Invest 116:3150-3159.
177. Matsuo K & Otaki N (2012) Bone cell interactions through Eph/ephrin: bone modeling, remodelling and associated diseases. Cell Adh Migr 6:148-156.
178. Matthews BD, Overby DR, Mannix R & Ingber DE (2006) Cellular adaptation to mechanical stress: role of integrins, Rho, cytoskeletal tension and mechanosensitive ion channels. Journal Cell Sci 119:508-518.
179. McGrath J, Somlo S, Makova S et al (2003) Two Populations of Node Monocilia Initiate Left-Right Asymmetry in the Mouse. Cell 114:61-73.
180. McNamara LM, Majeska RJ, Weinbaum S et al (2009) Attachment of osteocyte cell processes to the bone matrix. Anat Rec 292:355-363.
181. Metz LN, Martin RB & Turner AS (2003) Histomorphometric analysis of the effects of osteocyte density on osteonal morphology and remodelling. Bone 33:753-759.
182. Meyer U & Wiesmann HP (2006) Bone and cartilage. In Bone and Cartilage Engineering, 1st edn, ed. Schröder G, pp. 7-46 Springer-Verlag, Berlin.
183. Mitchison TJ & Cramer LP (1996) Actin-based cell motility and cell locomotion. Cell 84:371-379.
184. Miyamoto T & Suda T (2003) Differentiation and function of osteoclasts. Keio J Med 52:1-7.
185. Mohan S & Baylink DJ (1991) Bone growth factors. Clin Orthop Relat Res 263:30-48.
186. Mori S & Burr DB (1993) Increased intracortical remodelling following fatigue damage. Bone 14:103-109.
187. Mosley JR, March BM, Lynch J & Lanyon LE (1997) Strain magnitude related changes in whole bone architecture in growing rats. Bone 20:191-198.
188. Moussa FM, Hisijara IA, Sondag GR et al (2014) Osteoactivin promotes osteoblast adhesion through HSPG and αvβ1 integrin. J Cell biochem 115:1243-1253.
189. Moutzouri AG & Athanassiou GM (2014) Insights into the alteration of osteoblast mechanical properties upon adhesion on chitosan. BioMed Res Int 2014.
190. Mullender M, El Haj AJ, Yang Y et al (2004) Mechanotransduction of bone cells *in vitro*: mechanobiology of bone tissue. Med Biol Eng Comput 42:14-21.
191. Murayama A, Takeyama K, Kitanaka S et al (1998) The promoter of the human 25-hydroxyvitamin D3 1 alpha-hydroxylase gene confers positive and negative responsiveness to PTH, calcitonin, and $1\alpha,25(OH)_2D_3$. Biochem Biophys Res Commun 249:11–16.

192. Murshid SA, Kamioka H, Ishihara Y et al (2007) Actin and microtubule cytoskeletons of the processes of 3D-cultured MC3T3-E1 cells and osteocytes. J Bone Miner Metab 25:259-259.
193. Myers KA, Rattner JB, Shrive NG & Hart DA (2007) Osteoblast-like cells and fluid flow: Cytoskeleton-dependent shear sensitivity. Biochem Biophys Res Commun 364:214-219.
194. Nakagawa N, Kinosaki M, Yamaguchi K et al (1998). RANK is the essential signaling receptor for osteoclast differentiation factor in osteoclastogenesis. Biochem Biophys Res Commun 253:395-400.
195. Nakajima K, Kho DH, Yanagawa T et al (2016) Galectin-3 in bone tumor microenvironment: a beacon for individual skeletal metastasis management. Cancer Metastasis Rev 1-14.
196. Nakamura H (2007) Morphology, function, and differentiation of bone cells. Journal of Hard Tissue Biology 16:15-22.
197. Nakamura T, Mine N, Nakaguchi E et al (2006) Generation of Robust Left-Right Asymmetry in the Mouse Embryo Requires a Self-Enhancement and Lateral-Inhibition System. Dev Cell 11:495-504.
198. Nauli SM, Alenghat FJ, Luo Y et al (2003). Polycystins 1 and 2 mediate mechanosensation in the primary cilium of kidney cells. Nature Genet 33:129-137.
199. Nievers MG, Schaapveld RQJ & Sonnenberg A (1999) Biology and function of hemidesmosomes. Matrix Biol 18:5-17.
200. Noble BS, Peet N, Stevens HY et al (2003) Mechanical loading: biphasic osteocyte survival and targeting of osteoclasts for bone destruction in rat cortical bone. Am J Physiol 284:934-943.
201. Noris-Suárez K, Lira-Olivares J, Ferreira AM et al (2007) *In vitro* deposition of hydroxyapatite on cortical bone collagen stimulated by deformation-induced piezoelectricity. Biomacromolecules 8:941-948.
202. Novince CM, Michalski MN, Koh AJ, Sinder BP, Entezami P, Eber MR, Pettway GJ, Rosol TJ, Wronski TJ, Kozloff KM & McCauley LK (2012). Proteoglycan 4: a dynamic regulator of skeletogenesis and parathyroid hormone skeletal anabolism. J Bone Miner Res 27: 11-25.
203. Ohlsson C, Bengtsson BA, Isaksson OG et al (1998) Growth Hormone and Bone. Endocrine Rev 19:55-79.
204. Okada Y, Nonaka S, Tanaka Y et al (1999) Abnormal Nodal Flow Precedes Situs Inversus in iv and inv mice. Mol Cell 4:459-468.
205. Olivares-Navarrete R, Rodil SE, Hyzy SL et al (2015) Role of integrin subunits in mesenchymal stem cell differentiation and osteoblast maturation on graphitic carbon-coated microstructured surfaces. Biomaterials 51:69-79.
206. Oster GF, Murray JD & Harris AK (1983) Mechanical aspects of mesenchymal morphogenesis. J Embryol Exp Morphol 78:83-125.
207. Oury F, Sumara G, Sumara O et al (2011) Endocrine regulation of male fertility by the skeleton. Cell 144:796-809.
208. Palumbo C (1986) A three-dimensional ultrastructural study of osteoid-osteocytes in the tibia of chick embryos. Cell Tissue Res 246: 125-131.

209. Parsons JT (1996) Integrin-mediated signalling: regulation by protein tyrosine kinases and small GTP-binding proteins. Curr Opin Cell Biol 8:146-152.
210. Patwari P & Lee RT (2008) Mechanical Control of Tissue Morphogenesis. Circ Res 103:234-243.
211. Pereira AF & Shefelbine SJ (2014) The influence of load repetition in bone mechanotransduction using poroelastic finite-element models: the impact of permeability. Biomechan model mechanobiol 13:215-225.
212. Perrien DS, Brown EC, Aronson J et al (2002) Immunohistochemical study of osteopontin expression during distraction osteogenesis in the rat. J Histochem Cytochem 50:567-574.
213. Phillips JA, Almeida EA, Hill EL et al (2008) Role for β1 integrins in cortical osteocytes during acute musculoskeletal disuse. Matrix Biol, 27:609-618.
214. Pienkowski D & Pollack SR (1983) The origin of stress-generated potentials in fluid-saturated bone. J Orthop Res 1:30-41.
215. Pittas AG, Harris SS, Eliades M et al (2009) Association between serum osteocalcin and markers of metabolic phenotype. J Clin Endocrinol Metab 94:827–832.
216. Plotkin LI, Mathov I, Aguirre JI et al (2005) Mechanical stimulation prevents osteocyte apoptosis: requirement of integrins, Src kinases, and ERKs. Am J Physiol 289:633-643.
217. Pommerenke H, Schmidt C, Durr F et al (2002) The mode of mechanical integrin stressing controls intracellular signaling in osteoblasts. J Bone Miner Res 17:603-611.
218. Praetorius HA, Frokiaer J, Nielsen S & Spring KR (2003) Bending the primary cilium opens Ca^{2+}-sensitive intermediate-conductance K^{+} channels in MDCK Cells. J Membr Biol 191:193-200.
219. Prendergast PJ & Huiskes R (1995) The biomechanics of Wolff's law: recent advances. Ir J Med Sci 164:152-154.
220. Prince RL (1994) Counterpoint: estrogen effects on calcitropic hormones and calcium homeostasis. Endocr rev 15:301-309.
221. Qi M, Liu Y, Freeman MR & Solomon KR (2009) Cholesterol-regulated stress fibre formation. J Cell Biochem 106:1031-1040.
222. Quarles LD (2012) Role of FGF23 in vitamin D and phosphate metabolism: implications in chronic kidney disease. Exp Cell Res 318:1040-1048.
223. Radel C & Rizzo V (2005) Integrin mechanotransduction stimulates caveolin-1 phosphorylation and recruitment of Csk to mediate actin reorganization. Am J Physiol 288:936-945.
224. Rahman MS, Akhtar N, Jamil HM et al (2015) TGF-/BMP signaling and other molecular events: regulation of osteoblastogenesis and bone formation. Bone Res 3.
225. Ramtani S (2008) Electro-mechanics of bone remodelling. Int J Eng Sci 46:1173-1182.

226. Rawlinson SCF, Pitsillides AA & Lanyon LE (1996) Involvement of different ion channels in osteoblasts' and osteocytes' early responses to mechanical strain. Bone 19:609-614.
227. Reid IR, Ames R, Evans MC et al (1992) Determinants of total body and regional bone mineral density in normal postmenopausal women--a key role for fat mass. J Clin Endocrinol Metab 75:45-51.
228. Reinish GB & Nowick AS (1975) Piezoelectric properties of bone as functions of moisture content. Nature 253:626-627.
229. Reis J, Frias C, Canto e Castro C, Botelho ML, Marques AT, Simões JA, Capela e Silva F & Potes J (2012) A new piezoelectric actuator induces bone formation *in vivo*: a preliminary study. BioMed Res Int.
230. Rho J-Y, Kuhn-Spearing L & Zioupos P (1998) Mechanical properties and the hierarchical structure of bone. Med Eng Phys 20:92-102.
231. Rhee Y, Bivi N, Farrow E et al (2011) Parathyroid hormone receptor signaling in osteocytes increases the expression of fibroblast growth factor-23 *in vitro* and *in vivo*. Bone, 49:636-643.
232. Ribot C, Tremollieres F, Pouilles JM et al (1987) Obesity and postmenopausal bone loss: the influence of obesity on vertebral density and bone turnover in postmenopausal women. Bone 8:327-331.
233. Riggs BL, Khosla S & Melton LJ (1998) A unitary model for involutional osteoporosis: estrogen deficiency causes both type I and type II osteoporosis in postmenopausal women and contributes to bone loss in aging men. J Bone Miner Res 13:763-773.
234. Ritz U, Götz H, Baranowski A et al (2016) Influence of different calcium phosphate ceramics on growth and differentiation of cells in osteoblast–endothelial co-cultures. J Biomed Mater Res B: Appl Biomater doi: 10.1002/jbm.b.33728.
235. Riveline D, Zamir E, Balaban NQ et al (2001) Focal contacts as mechanosensors: externally applied local mechanical force induces growth of focal contacts by an mDia1-dependent and ROCK-independent mechanism. J Cell Biol 153:1175-1185.
236. Robinson LJ, Yaroslavskiy BB, Griswold RD et al (2009) Estrogen inhibits RANKL-stimulated osteoclastic differentiation of human monocytes through estrogen and RANKL-regulated interaction of estrogen receptor-α with BCAR1 and Traf6. Exp Cell Res 315: 1287-1301.
237. Rodan GA & Martin TJ (2000) Therapeutic approaches to bone diseases. Science 289:1508-1514.
238. Rodriguez-Ortiz ME, Lopez I, Muñoz-Castañeda JR et al (2012) Calcium deficiency reduces circulating levels of FGF23. J Am Soc Nephrol 23:1190-1197.
239. Roelofs-Iverson RA, Mulder DW, Elveback LR et al (1984) ALS and heavy metals: a pilot case-control study. Neurology 34:393-393.
240. Romas E, Sims NA, Hards DK et al (2002) Osteoprotegerin reduces osteoclast numbers and prevents bone erosion in collagen-induced arthritis. Am J Pathol 161:1419-1427.

241. Rosen CJ, Ackert-Bicknell C, Rodriguez JP & Pino AM (2009) Marrow fat and the bone microenvironment: developmental, functional, and pathological implications. Crit Rev Eukaryot Gene Expr 19(2).
242. Rössig L, Haendeler J, Hermann C et al (2000) Nitric oxide down-regulates MKP-3 mRNA levels. J Biol Chem 275:25502-25507.
243. Rousselle AV & Heymann D (2002) Osteoclastic acidification pathways during bone resorption. Bone 30:533-540.
244. Rosset EM & Bradshaw AD (2016) SPARC/osteonectin in mineralized tissue. Matrix Biol 52:78-87.
245. Rubin CT & Lanyon LE (1984) Regulation of bone formation by applied dynamic loads. J Bone Joint Surg 66:397-402.
246. Rubin J & Greenfield EM (2005) Osteoclast: origin and differentiation. In Bone Resorption ed. Farach-Carson MC, Bronner F & Rubin J, pp. 1-23. Springer-Verlag, London.
247. Saidak Z, Le Henaff C, Azzi S et al (2015) Wnt/β-catenin signaling mediates osteoblast differentiation triggered by peptide-induced α5β1 integrin priming in mesenchymal skeletal cells. J Biol Chem 290:6903-6912.
248. Saini RK, Kaneko I, Jurutka PW et al (2013) 1, 25-dihydroxyvitamin d3 regulation of fibroblast growth factor-23 expression in bone cells: Evidence for primary and secondary mechanisms modulated by leptin and interleukin-6. Calcif Tissue Int 92:339-353.
249. Salo J, Lehenkari P, Mulari M et al (1997) Removal of osteoclast bone resorption products by transcytosis. Science 276:270-273.
250. Saunders MM, You J, Trosko JE et al (2001) Gap junctions and fluid flow response in MC3T3-E1 cells. Am J Physiol - Cell Physiol 281:1917-1925.
251. Saunders MM, You J, Zhou Z et al (2003) Fluid flow-induced prostaglandin E2 response of osteoblastic ROS 17/2.8 cells is gap junction-mediated and independent of cytosolic calcium. Bone 32:350-356.
252. Schiller PC, D'Ippolito G, Balkan W et al (2001) Gap-junctional communication is required for the maturation process of osteoblastic cells in culture. Bone 28:362-369.
253. Schmidt A, Brixius K & Bloch W (2007) Endothelial precursor cell migration during vasculogenesis. Circ Res 101:125-136.
254. Sharma B, Singh S & Siddiqi NJ (2014) Biomedical implications of heavy metals induced imbalances in redox systems. BioMed Research Int, 2014.
255. Shi Y, Yadav VK, Suda N et al (2008) Dissociation of the neuronal regulation of bone mass and energy metabolism by leptin *in vivo*. Proc Natl Acad Sci U S A 105:20529–20533.
256. Shimada T, Mizutani S, Muto T et al (2001) Cloning and characterization of FGF23 as a causative factor of tumor-induced osteomalacia. Proc Natl Acad Sci U S A 98:6500–6505.
257. Shimada T, Hasegawa H, Yamazaki Y et al (2004) FGF-23 is a potent regulator of vitamin D metabolism and phosphate homeostasis. J Bone Miner Res 19:429–435.

258. Silberberg YR, Pelling AE, Yakubov GE et al (2008) Mitochondrial displacements in response to nanomechanical forces. J Mol Recognit 21:30-36.
259. Small J, Anderson K & Rottner K (1996) Actin and the coordination of protrusion, attachment and retraction in cell crawling. Biosci Rep 16:351-368.
260. Smalt R, Mitchell FT, Howard RL & Chambers TJ (1997) Induction of NO and prostaglandin E2 in osteoblasts by wall-shear stress but not mechanical strain. Am J Physiol273:751-758.
261. Smith MA, Hoffman LM & Beckerle MC (2014) LIM proteins in actin cytoskeleton mechanoresponse. Trends Cell Biol 24:575-583.
262. Sommerfeldt D & Rubin C (2001) Biology of bone and how it orchestrates the form and function of the skeleton. Eur Spine J 10:S86-S95.
263. Souza Faloni AP, Sasso-Cerri E, Rocha FRG et al (2012) Structural and functional changes in the alveolar bone osteoclasts of estrogen-treated rats. J Anat 220:77–85.
264. Srinivasan S, Ausk BJ, Poliachik SL et al (2007) Rest-inserted loading rapidly amplifies the response of bone to small increases in strain and load cycles. J Appl Physiol 102:1945-1952.
265. Steinberg TH, Civitelli R, Geist ST et al (1994) Connexin43 and connexin45 form gap junctions with different molecular permeabilities in osteoblastic cells. EMBO J 13:744-750.
266. Suda T, Takahashi N, Udagawa N et al (1999) Modulation of osteoclast differentiation and function by the new members of the tumor necrosis factor receptor and ligand families. Endocr Rev 20:345-357.
267. Suchacki KJ, Cawthorn WP & Rosen CJ (2016) Bone marrow adipose tissue: formation, function and regulation. Curr Opin Pharmacol 28:50-56.
268. Sugawara Y, Ando R, Kamioka H et al (2008) The alteration of a mechanical property of bone cells during the process of changing from osteoblasts to osteocytes. Bone 43:19-24.
269. Sun L, Vukicevic S, Baliram R et al (2008) Intermittent recombinant TSH injections prevent ovariectomy-induced bone loss. Proc Natl Acad Sci U S A 105:4289–4294.
270. Takayanagi H (2008) Regulation of osteoclastogenesis and osteoimmunology. Bone 42:S40-S40.
271. Takeichi M (1988). The cadherins: cell-cell adhesion molecules controlling animal morphogenesis. Development 102:639-655.
272. Tamma R & Zallone A (2012) Osteoblast and osteoclast crosstalks: from OAF to Ephrin. Inflamm Allergy-Drug Targets 11:196-200.
273. Tan SD, de Vries TJ, Kuijpers-Jagtman AM et al (2007) Osteocytes subjected to fluid flow inhibit osteoclast formation and bone resorption. Bone 41:745-751.
274. Tan SD, Bakker AD, Semeins CM et al (2008) Inhibition of osteocyte apoptosis by fluid flow is mediated by nitric oxide. Biochem Biophys Res Commun 369:1150-1154.

275. Tanikawa R, Tanikawa T, Hirashima M et al (2010) Galectin-9 induces osteoblast differentiation through the CD44/Smad signaling pathway. Biochem Biophys Res Commun 394:317-322.
276. ten Bolscher M, Netelenbos JC, Barto R & van Buuren LM (1999) Estrogen regulation of intestinal calcium absorption in the intact and ovariectomized adult rat. J Bone Miner Res, 14:1197-1202.
277. Teo BKK, Wong ST, Lim CK et al (2013) Nanotopography modulates mechanotransduction of stem cells and induces differentiation through focal adhesion kinase. ACS Nano 7:4785-4798.
278. Teti A & Zallone A (2009) Do osteocytes contribute to bone mineral homeostasis? Osteocytic osteolysis revisited. Bone 44:11-16.
279. Thi MM, Suadicani SO, Schaffler MB, Weinbaum S & Spray DC (2013) Mechanosensory responses of osteocytes to physiological forces occur along processes and not cell body and require αVβ3 integrin. Proc Natl Acad Sci U S A 110: 21012-21017.
280. Thurner PJ, Chen CG, Ionova-Martin S et al (2010) Osteopontin deficiency increases bone fragility but preserves bone mass. Bone 46:1564-1573.
281. Tomkinson A, Reeve J, Shaw RW & Noble BS (1997) The death of osteocytes via apoptosis accompanies estrogen withdrawal in human bone. J Clin Endocrinol Metab 82:3128-3135.
282. Tsuji K, Maeda T, Kawane T et al (2010) Leptin stimulates fibroblast growth factor 23 expression in bone and suppresses renal 1α25-dihydroxyvitamin D_3 synthesis in leptin-deficient ob/ob mice. J Bone Miner Res 25:1711-1723.
283. Turner CH (1998) Three rules for bone adaptation to mechanical stimuli. Bone 23:399-407.
284. Turner CH (2006) Bone strength: current concepts. Ann N Y Acad Sci 1068:429-446.
285. Turner RT, Riggs BL & Spelsberg TC (1994) Skeletal Effects of Estrogen*. Endocr Rev 15:275-300.
286. Urakawa I, Yamazaki Y, Shimada T et al (2006) Klotho converts canonical FGF receptor into a specific receptor for FGF23. Nature 444:770–774.
287. Urist MR (1965) Bone: formation by autoinduction. Science 150:893–899.
288. Väänänen HK & Horton M (1995) The osteoclast clear zone is a specialized cell-extracellular matrix adhesion structure. J Cell Sci 108:2729-2732.
289. Väänänen HK (2005) Mechanism of osteoclast mediated bone resorption-rationale for the design of new therapeutics. Adv Drug Deliv Rev 57:959–971.
290. Vääräniemi J, Halleen JM, Kaarlonen K et al (2004) Intracellular machinery for matrix degradation in bone-resorbing osteoclasts. J Bone Miner Res 19:1432-1440.
291. Van Bezooijen RL, Roelen BA, Visser A et al (2004) Sclerostin is an osteocyte-expressed negative regulator of bone formation, but not a classical BMP antagonist. J Exp Med 199:805–814.

292. Van De Graaff K (2001) Skeletal system: introduction and the axial skeleton. In Human Anatomy, 6th edn, ed. Lange M, Tibbetts K & Queck K, pp. 131-171. McGraw-Hill College, Boston.
293. van der Meijden K, Bakker AD, van Essen HW et al (2016) Mechanical loading and the synthesis of 1, 25 (OH) 2 D in primary human osteoblasts. J Steroid Biochem Mol Biol 156:32-39.
294. Van Hove RP, Nolte PA, Vatsa A et al (2009) Osteocyte morphology in human tibiae of different bone pathologies with different bone mineral density—Is there a role for mechanosensing? Bone 45:321-329.
295. Vanderschueren D, Vandenput L, Boonen S et al (2004) Androgens and bone. Endocr Rev 25:389-425.
296. van'T Hof RJ & Ralston SH (2001) Nitric oxide and bone. Immunology 103:255-261.
297. Vatsa A, Breuls RG, Semeins CM et al (2008) Osteocyte morphology in fibula and calvaria—is there a role for mechanosensing? Bone 43:452-458.
298. Verborgt O, Tatton NA, Majeska RJ & Schaffler MB (2002) Spatial distribution of Bax and Bcl-2 in osteocytes after bone fatigue: complementary roles in bone remodelling regulation? J Bone Miner Res 17:907-914.
299. Verbruggen SW, Vaughan TJ & McNamara LM (2014) Fluid flow in the osteocyte mechanical environment: a fluid–structure interaction approach. Biomechan model mechanobiol 13: 85-97.
300. Vinik Y, Shatz-Azoulay H, Vivanti A et al (2015) The mammalian lectin galectin-8 induces RANKL expression, osteoclastogenesis, and bone mass reduction in mice. Elife 4:e05914.
301. Waychunas GA (2014) Disrupting dissolving ions at surfaces with fluid flow. Science 344:1094-1095.
302. Wang N, Butler JP & Ingber DE (1993) Mechanotransduction across the cell surface and through the cytoskeleton. Science 260:1124-1127.
303. Wang N & Ingber DE (1994) Control of cytoskeletal mechanics by extracellular matrix, cell shape, and mechanical tension. Biophys J 66:2181-2189.
304. Wang T, Feng Z, Song Y & Chen X (2007) Piezoelectric properties of human dentin and some influencing factors. Dent Mater 23:450-453.
305. Warden SJ & Turner CH (2004) Mechanotransduction in the cortical bone is most efficient at loading frequencies of 5-10 Hz. Bone 34:261-270.
306. Waring AC, Harrison S, Fink HA et al (2013) A prospective study of thyroid function, bone loss, and fractures in older men: The MrOS study. J Bone Miner Res 28:472-479.
307. Weiner S, Traub W & Wagner HD (1999) Lamellar bone: structure-function relations. J Struct Biol 126:241-255.
308. Wen JH, Vincent LG, Fuhrmann A et al (2014) Interplay of matrix stiffness and protein tethering in stem cell differentiation. Nat Mater 13:979-987.
309. Wiren KM & Marcus R (2010) Fundamentals of Osteoporosis.

310. Xiao Z, Zhang S, Mahlios J et al (2006) Cilia-like structures and polycystin-1 in osteoblasts/osteocytes and associated abnormalities in skeletogenesis and Runx2 expression. J Biol Chem 281:30884-30895.
311. Xing Y, Gu Y, Xu LC et al (2011) Effects of membrane cholesterol depletion and GPI-anchored protein reduction on osteoblastic mechanotransduction. J Cell Physiol 226:2350-2359.
312. Yamada KM & Geiger B (1997) Molecular interactions in cell adhesion complexes. Curr Opin Cell Biol 9:76-85.
313. Yamaki M, Nakamura H, Takahashi N et al (2005). Transcytosis of calcium from bone by osteoclast-like cells evidenced by direct visualization of calcium in cells. Arch Biochem Biophys 440:10-17.
314. Yamashita T, Yoshioka M & Itoh N (2000) Identification of a novel fibroblast growth factor, FGF-23, preferentially expressed in the ventrolateral thalamic nucleus of the brain. Biochem Biophys Res Commun 277:494–498.
315. Young MF (2003) Bone matrix proteins: their function, regulation, and relationship to osteoporosis. Osteoporos Int 14:35-42.
316. Zallone A, Teti A, Primavera MV & Pace G (1983) Mature osteocytes behaviour in a repletion period: the occurrence of osteoplastic activity. Basic Appl Histochem 27:191-204.
317. Zaman G, Pitsillides AA, Rawlinson SCF et al (1999) Mechanical strain stimulates nitric oxide production by rapid activation of endothelial nitric oxide synthase in osteocytes. J Bone Miner Res 14:1123-1131.
318. Zhang M, Xuan S, Bouxsein ML et al (2002) Osteoblast-specific knockout of the insulin-like growth factor (IGF) receptor gene reveals an essential role of IGF signaling in bone matrix mineralization. J Biol Chem 277:44005-44012.
319. Zhang W, Shen X, Wan C et al (2012) Effects of insulin and insulin-like growth factor 1 on osteoblast proliferation and differentiation: differential signalling via Akt and ERK. Cell Biochem Funct 30:297-302.
320. Zhang Y, Chen L, Zeng J et al (2014) Aligned porous barium titanate/hydroxyapatite composites with high piezoelectric coefficients for bone tissue engineering. Mater Sci Eng: C 39:143-149.
321. Zhu J, Zhang X, Wang C et al (2008) Different magnitudes of tensile strain induce human osteoblasts differentiation associated with the activation of ERK1/2 phosphorylation. Int J Mol Sci 9:2322-2332.

Chapter 3

Analgesia em Modelo Animal Superior para Ortopedia

Abstract published in the Proceedings Book of the 6th Portuguese Congress on Biomechanics, February 2015, ISSN: 2333-4959.

ANALGESIA EM MODELO ANIMAL SUPERIOR PARA ORTOPEDIA

Maria Teresa Oliveira[1], José Caeiro Potes[2], Maria Cristina Queiroga[3], João Carlos Fragoso[4], José Lopes de Castro[5], Alfredo Franco Pereira[6] e Joana da Costa Reis[7]

[1] DMV, ECT, ICAAM, Universidade de Évora, Portugal; teresoliveira@uevora.pt

[2] DMV, ECT, ICAAM, Universidade de Évora, Portugal; jacpotes@uevora.pt

[3] DMV, ECT, ICAAM, Universidade de Évora, Portugal; crique@uevora.pt

[4] DMV, ECT, Universidade de Évora, Portugal; jfragoso@uevora.pt

[5] DZOO, ECT, ICAAM, Universidade de Évora, Portugal; jcastro@uevora.pt

[6] DZOO, ECT, ICAAM, Universidade de Évora, Portugal; apereira@uevora.pt

[7] DMV, ECT, Universidade de Évora, Portugal; CICECO, Universidade de Aveiro, Portugal; jmfcr@uevora.pt

PALAVRAS CHAVE: Modelos Animais, Ortopedia, Ovino, Analgesia, Biomateriais.

RESUMO: *O teste de novos biomateriais para aplicações clínicas em ortopedia, ou noutras áreas da medicina, em modelos animais vivos e sencientes, em prol do benefício humano, deve ser objecto de planeamento cuidado e ponderado, dado o conflito ético que se coloca. Compete-nos, enquanto investigadores, garantir que as condições de vida, saúde e bem-estar são asseguradas. O uso de ovinos como modelo superior pré-clínico, para investigação em Ortopedia, tem-se evidenciado devido às suas características translacionais para a espécie humana. Neste estudo retrospectivo deu-se ênfase ao plano anestésico/ analgésico instituído em três tipos de técnicas cirúrgicas ortopédicas, realizadas em ovinos. Os animais intervencionados foram adquiridos com 2 meses de antecedência em relação às cirurgias e mantidos em rebanho, com condições adequadas de abrigo, alimentação e maneio. As técnicas cirúrgicas inovadoras foram treinadas previamente em peças anatómicas adquiridas no matadouro. Todas as cirurgias e anestesias foram realizadas por médicos veterinários devidamente qualificados. Durante os períodos pós-operatórios os animais foram mantidos no Hospital Veterinário, sob vigilância e tratamento, após o que regressaram ao pasto. Considera-se que os protocolos anestésico e analgésico instituídos foram suficientes para eliminar a dor ortopédica/ neuropática causada pelas técnicas cirúrgicas referidas.*

1 INTRODUÇÃO

O teste de novos biomateriais para aplicações clínicas em ortopedia, ou noutras áreas da medicina, em modelos animais vivos e sencientes, em prol do benefício humano, deve ser objecto de planeamento cuidado e ponderação, dado o conflito ético que se coloca. Existem diversas correntes de pensamento na comunidade científica internacional, quer a favor quer contra a utilização de animais. Por exemplo, o "Medical Research Modernization Comittee" considera que a experimentação animal é movida principalmente por interesses económicos. Mais, afirma que perante as diferenças anatómicas, fisiológicas e patológicas entre humanos e não humanos, a experimentação animal não deve ser considerada um método válido para

investigação médica [1]. Contudo, inúmeras evidências mostram que a experimentação animal é, inevitavelmente, uma via importante para o avanço da ciência, por permitir a observação de processos *in vivo* que, de outra forma, não teriam condições de ser avaliados [2].

Actualmente a sociedade encontra-se sensibilizada para a questão do bem-estar animal, encontrando-se esta temática bem documentada e legislada (Directiva 2010/63/EU, Decreto-Lei nº 113/2013, de 7 de Agosto) [3], [4]. Como tal, também a utilização de animais em investigação é abrangida por regras e leis que têm de ser cumpridas. Assim, qualquer projecto que passe pela utilização de modelos animais, desde o ratinho de laboratório ao cão, deverá ser aprovado por um órgão institucional (Comissão de ética), responsável pelo bem-estar dos animais e, posteriormente, submetido à Direcção Geral do Alimentação e Veterinária (DGAV), enquanto autoridade sanitária e veterinária, para obtenção das respectivas autorizações legais. Só deverão ser submetidos projectos com modelos animais se não existirem alternativas "não animais" viáveis. Todos os projectos deverão garantir métodos susceptíveis de proporcionar resultados satisfatórios provocando o mínimo de dor, sofrimento ou angústia ao animal, sendo fixado limites máximos a partir dos quais os animais não podem ser submetidos a mais procedimentos científicos. Todos os procedimentos que causem dor severa, sofrimento ou angústia, susceptíveis de serem prolongados e sem possibilidade de serem aliviados não estão autorizados. Os procedimentos devem ser realizados, quando possível, sob anestesia geral ou local, analgesia ou outro método de contenção adequado, para assegurar que a dor, o sofrimento e a angústia são reduzidos ao mínimo. A morte, como limite crítico de um procedimento, deve ser evitada, e quando necessária deverá ser indolor. O decreto-lei supracitado prevê, ainda, a realização de inspecções periódicas aos criadores, fornecedores e utilizadores, que deverão assegurar condições condignas de alojamento e enriquecimento ambiental, capacidade de avaliação da dor, da angústia e do sofrimento infligidos e devido acompanhamento médico-veterinário dos animais.

A legislação em vigência rege-se assaz pelo princípio dos 3R's, de modo a minimizar o uso de animais em investigação científica: "replacement" (substituição), "reduction" (redução) e "refinement" (refinamento) [5]. Sempre que possível, o uso de animais deve ser **substituído** e/ou precedido por modelos computacionais, estudos *in vitro*, estudos em tecidos animais obtidos em matadouros ou tecidos humanos doados, estudos em invertebrados, entre outros. O número de animais deverá ser **reduzido**, entre outros, através do uso de testes piloto e da determinação do *Power* das análises e de delineamento experimental apropriado, utilizando animais com características similares de modo a diminuir a variabilidade dos grupos, do desenvolvimento preferencial de estudos *ex vivo*, da utilização de técnicas não invasivas de diagnóstico, como é o caso dos fluorocromos, ecografia e radiografia, que permitem a recolha de informação do mesmo animal em tempos distintos e, quando viável, da colaboração entre investigadores, que poderão retirar dados de um mesmo animal, e também da reutilização de animais para projectos distintos, em condições excepcionais previstas pela legislação portuguesa. Deverá haver um **refinamento** da metodologia, de modo a minimizar a dor, o sofrimento e a angústia inevitavelmente infligidos, ou em arranjos de enriquecimento ambiental que possibilitem o desenvolvimento dos comportamentos intrínsecos à espécie. Neste ponto é importante referir a experiência e o conhecimento técnico-científico do investigador, de forma a minimizar o impacto negativo sobre o animal. Quando as

características e exigências dos projectos forem impeditivas do tratamento de dor e desconforto, devem-se considerar o estabelecimento de limites humanamente aceitáveis (*humane endpoints*), que em última análise levarão à eutanásia do animal. É ainda de extrema importância todo um conjunto de condições de maneio prestadas aos animais, em conformidade com a legislação vigente e a espécie seleccionada, do alojamento à alimentação e cuidados higiossanitários, que deverão ser instituídos desde a recepção dos animais até ao términus do projecto. O manuseamento deverá ser efectuado com base no maneio racional que envolvem procedimentos que reduzam a angústia e a reactividade. Deve ter-se em consideração a necessidade dos animais serem recebidos em instalações adequadas com alguma antecedência em relação ao período das cirurgias (no mínimo três a quatro semanas) [6], [7], uma vez que o transporte, alojamento e maneios distintivos e diferentes níveis de actividade indubitavelmente causarão ansiedade nos animais e de forma a minimizar a angústia nos animais intervencionados e a influência alterada sobre a actividade de remodelação óssea, causada pela deslocação, alojamento e maneio distintivos em relação ao rebanho de origem [6], [7]. Ademais, durante este período, os animais deverão ser vigiados para detecção prévia de qualquer problema existente e, se necessário, serem substituídos.

É no âmbito do refinamento da metodologia que se encaixa o plano analgésico e anestésico, encontrando-se inclusive esta questão contemplada na legislação. A analgesia é tanto mais efectiva quanto mais cedo for iniciada (no período pré-operatório), uma vez que a dor pós-operatória, resultante dos danos teciduais infligidos pelo cirurgião, podem originar sensibilização e desinibição central e periférica. Recomenda-se a utilização de um plano multimodal, que iniba todos os mecanismos responsáveis pela produção de dor [8], [9]. Este deverá ser iniciado no período pré-operatório, através da administração de fármacos da família dos α2- agonistas, opiáceos e anti-inflamatórios não esteróides (AINE's), e prolongar-se até ao fim do período pós-operatório, em consonância com a avaliação clínica. Nos ovinos uma das tarefas mais difícil no controlo da dor é o reconhecimento da mesma, pois são animais extremamente estóicos, que não demonstram facilmente sinais de desconforto [8], [9]. Deve-se ter em atenção desvios, por vezes subtis, de comportamento, de apetite e de hábitos de defecação e micção, e outros sinais de dor, como odontoprise, alterações na locomoção, que darão informação acerca do estado nociceptivo do animal. Os α2-agonistas (ex.: xilazina, detomidina e medetomidina) são primordialmente utilizados pelo seu efeito sedativo; têm também um ligeiro efeito analgésico visceral (de curta duração) e podem potenciar a acção de outros analgésicos opiáceos. Como principais efeitos secundários refere-se a hipotensão. São reversíveis (por exemplo, com atipamezole ou ioimbina), no entanto é preciso ter em atenção que a analgesia produzida por estes fármacos será também revertida. Os opiáceos são analgésicos potentes, mas de curta duração; induzem algum grau de sedação, depressão respiratória, diminuição da motilidade gastro-intestinal e do apetite. Em ovinos apresentam eficácia variável contra estímulos nocivos [8], [9]. Entre os mais utilizados temos a morfina, buprenorfina, o butorfanol e, mais recentemente, o fentanilo. O uso do fentanilo transdérmico vislumbra-se como uma alternativa em casos de dor severa prolongada uma vez que a duração da analgesia é de 72 horas após uma aplicação única [10]. Os AINE's reduzem a inflamação secundária ao trauma, apresentando indirectamente algum efeito analgésico. Têm várias vantagens em relação aos α2- agonistas e aos opiáceos, tal

como não causarem sedação e depressão cardiovascular e terem uma acção mais prolongada no tempo. Não são analgésicos potentes, sendo eficazes contra dor ligeira a moderada. O seu uso não deve ser muito prolongado no tempo uma vez que podem levar a ulcerações do tracto gastrintestinal e nefrotoxicidades. Existem mais fármacos passíveis de providenciar analgesia, como é o caso de alguns anestésicos locais, como a lidocaína, que apresentam efeitos analgésicos sistémicos comprovados, entre outros [9]. Em conclusão, recomendam-se terapias analgésicas multimodais, de modo a potenciar a acção dos fármacos das diferentes famílias, com recurso a doses inferiores, minimizando assim os seus efeitos secundários. Neste estudo retrospectivo dar-se-á ênfase ao plano analgésico instituído em três tipos de técnicas cirúrgicas ortopédicas, realizadas neste modelo animal superior, o ovino.

O uso de ovinos como modelo superior pré-clínico para investigação biomédica tem-se evidenciado devido às suas características translacionais para a espécie humana, à sua disponibilidade, baixo custo, facilidade de alojamento e maneio e boa homogeneidade, quando seleccionados para a idade, raça e género. Ademais é considerado um bom modelo para investigação ortopédica devido às suas semelhanças anatómicas, quando comparado com o modelo humano, relativamente ao tamanho, peso, estrutura óssea, processo de remodelação óssea e comportamento biomecânico do osso, permitindo o uso de alguns dos mesmos materiais prostéticos [11].

Por último, fala-se ainda de um quarto "R" – a **responsabilidade.** A responsabilidade do uso dos animais é de todos aqueles que se encontram ligados ao projecto. Logo, compete aos investigadores procurar a redução, substituição e refinamento no projecto que integramos, garantir que as condições de vida, saúde e bem-estar dos animais são asseguradas no período total em que decorre a experiência e estabelecer limites de sofrimento humanamente aceitáveis a partir dos quais a experiência cessa.

2 EXPERIMENTAL

Foram realizadas, no âmbito de projectos distintos, três técnicas cirúrgicas: a) hemi-artroplastia coxofemoral, b) vertebroplastia percutânea e c) artrotomia/ artroplastia medial do joelho. Todos os projectos foram desenvolvidos de acordo com as directrizes da FELASA e foram submetidos à aprovação da Comissão de Ética do Hospital Veterinário da Universidade de Évora (HVUE) e da DGAV. Com dois meses de antecedência adquiriram-se ovelhas fêmeas adultas, de raça Merina, que foram mantidas em rebanho, numa cerca de pastagem natural exclusiva para o grupo, onde constava um abrigo com 40 m^2. Os animais foram alimentados com feno de erva *ad libitum* e suplementados bidiariamente com concentrado comercial (calculado para 1,2% de peso vivo). O maneio efectuado teve como objectivo a redução da reactividade, utilizando-se técnicas de reforço positivo sempre que foram necessárias verificações higiossanitárias nos animais. Todas as técnicas cirúrgicas inovadoras foram treinadas previamente em peças anatómicas adquiridas no matadouro e, no caso da vertebroplastia, seleccionadas de forma a serem minimamente invasivas, com acesso percutâneo e recurso à imagiologia, através do uso do fluoroscópio (figura 1).

Fig. 1 Vertebroplastia percutânea com fluoroscopia.

Antes da cirurgia, com o objectivo de minimizar os riscos de pneumonia por aspiração, os animais foram sujeitos a um jejum de 24 horas, numa boxe do HVUE, onde se juntaram os animais em grupos de dois. O plano anestésico utilizado incluiu pré-medicação com atropina subcutânea (0,05 mg/kg), xilazina intramuscular (0,1 mg/kg), butorfanol intravenoso (0,01 mg/kg) e carprofeno subcutâneo (2 mg/kg); a indução da anestesia realizou-se com tiopental sódico a 5% intravenoso (5-10 mg/kg) e a manutenção com isofluorano volátil a 1-2,5% em ventilação espontânea. Todos animais foram intubados orogastricamente para prevenir a ocorrência de pneumonias por aspiração e timpanismo ruminal. A anestesia foi vigiada por um médico veterinário qualificado, com apoio de um monitor anestésico que avalia a frequência respiratória, a actividade eléctrica cardíaca (ECG), a pressão arterial não invasiva, a pulsoximetria e a capnografia (figura 2).

Fig. 2 Vertebroplastia em ovino com monitorização anestésica adequada.

Os animais intervencionados ao joelho foram, imediatamente após a cirurgia, submetidos a um exame radiológico. Após a recuperação anestésica os animais foram recolhidos, em grupo, numa boxe, onde ficaram alojados durante o período pós-operatório (10 dias), sob vigilância do médico veterinário. A medicação analgésica pós-operatória instituída foi efectuada por meio de butorfanol intramuscular (0,15 mg/kg, de 12 em 12 horas, durante 3 dias), carprofeno subcutâneo (2 mg/kg, uma vez por dia, durante 7 dias) e antibioterapia, para prevenção de infecções, com amoxicilina/ácido clavulânico subcutâneos (15 mg/kg, uma vez por dia, durante 7 dias). Após a cirurgia foi administrado a cada animal, por via subcutânea, um fluorocromo (calceína verde, 15 mg/kg). Terminado o período pós-operatório as ovelhas regressaram para o rebanho (figura 3). No final do período de implantação, a eutanásia é efectuada com pentobarbital sódico concentrado endovenoso, que será antecedida pela administração subcutânea de outro fluorocromo (alizarina complexona, 25 mg/kg).

Fig. 3 Ovinos intervencionados em pasto.

3 DISCUSSÃO

A minimização da dor e do desconforto dos animais foi alcançada quer através da terapêutica médica instituída (analgesia e anestesia), quer através das outras medidas preventivas tomadas, referentes ao alojamento e maneio.

Durante todo o trabalho foi dedicada extrema atenção ao maneio dos animais intervencionados. O planeamento temporal do projecto assumiu um papel fulcral, tendo sido tomada em consideração a necessidade dos animais serem recebidos com alguma antecedência em relação ao período das cirurgias (dois meses), de forma a minimizar a ansiedade nos animais e permitir a detecção prévia de animais doentes ou, por outro motivo, incapazes de serem sujeitos ao procedimento cirúrgico. Durante o período em que decorreu o projecto os animais foram sujeitos a vigilância bidiária por técnicos qualificados para a espécie seleccionada, e assim vocacionados para a detecção precoce

de problemas, o que se considera uma importante mais-valia para o sucesso do seu tratamento e maneio.

Relativamente ao refinamento das técnicas cirúrgicas, o treino prévio *ex vivo* foi absolutamente relevante, visto que permitiu o aperfeiçoamento de técnicas inovadoras, de modo a minimizar as lesões, e consequentemente dor, infligidas ao animal. É ainda de referir a importância dos meios complementares de diagnóstico, como é o caso do fluorocoscópio e da radiografia, que permitiram, por um lado a utilização de técnicas minimamente invasivas (no caso da vertebroplastia percutânea) e por outro a avaliação, em pontos temporais distintos, do processo cirúrgico desenvolvido. Ainda no seguimento deste propósito, considera-se também relevante a administração de fluorocromos, que irão permitir a datação histológica das alterações ósseas ocorridas. O protocolo analgésico utilizado verificou-se suficiente, tendo sido verificado o retorno ao nível de actividade normal, ao fim do período pós-operatório, em todas as ovelhas. Contudo, não inviabiliza a utilização de outros fármacos mais potentes, tais como o fentanilo e a flunixina meglumina, em casos de dor mais severa, de acordo com a avaliação clínica.

4 CONCLUSÕES

O protocolo analgésico instituído foi suficiente para eliminar a dor ortopédica/ neuropática causada pelas técnicas cirúrgicas referidas, pelo que se afigura uma alternativa viável para este tipo de procedimentos.

Não foi nosso propósito neste artigo avaliar tão-somente a acção dos fármacos usados, mas antes sensibilizar os investigadores para uma ciência mais altruísta, responsável e ética.

AGRADECIMENTOS

Este trabalho foi suportado pela Comissão Europeia, ao abrigo do Sétimo Programa-Quadro, através do projecto Restoration, ao abrigo da acção "SME-targeted Collaborative project", grant agreement NMP.2011.2.1-1.

REFERÊNCIAS

[1] C. Anderegg, "A critical look at animal experimentation", Medical Research Modernization Committee, 2002.

[2] E.F. Paul, J. Paul (eds.), "Why Animal Experimentation Matters: The Use of Animals in Medical Research", Transaction Publishers, 2001.

[3] Directiva 2010/63/EU, Diário Oficial da União Europeia, L276/33-79, 2010, ISSN 1725-2601.

[4] Decreto-Lei nº 113/2013, de 7 de Agosto. Diário da República, 1.ª série — N.º 151. Ministério da Agricultura, do mar, do ambiente e do ordenamento do território, Lisboa.

[5] W. M. S. Russell, R.L. Burch, "The principles of humane experimental technique", Methuen & Co. Ltd, London, 1959.

[6] J.A. Auer, *et al.*, "Refining animal models in fracture research: seeking consensus in optimising both animal welfare and scientific validity for appropriate biomedical use", BMC musculoskeletal disorders, Vol. 8, nº 1, 72, 2007.

[7] S.M. van Gaalen, *et al.*, "Use of fluorochrome labels in in vivo bone tissue engineering research", Tissue Engineering Part B: Reviews, Vol. 16, 209-217, 2010.

[8] I. Lizarraga, J.P. Chambers. "Use of analgesic drugs for pain management in sheep", New Zealand veterinary journal, Vol. 60, 87-94, 2012.

[9] A.D. Galatos, "Anesthesia and analgesia in sheep and goats", Veterinary Clinics of North America: Food Animal Practice, Vol. 27, 47-59, 2011.

[10] B.D. Ahern, L.R. Soma, J.A. Rudy *et al.*, "Pharmacokinetics of fentanyl administered transdermally and intravenously in sheep", Am. J. Vet. Res., Vol. 71, nº10, 1127–1132, 2010.

[11] J.C. Potes, J. Reis, F. Capela e Silva, C. Relvas, A.S. Cabrita, J.A. Simões, "The Sheep as an Animal Model in Orthopaedic Research", Experimental Pathology and Health Sciences, Vol. 2, 29-32, 2008.

Chapter 4

Ex vivo Model for Percutaneous Vertebroplasty

Published in Key Engineering Materials, 2015, Volume 631: 408-413

Key Engineering Materials Vol. 631 (2015) pp 408-413
Online available since 2014/Nov/17 at www.scientific.net

doi:10.4028/www.scientific.net/KEM.631.408

Submitted: 01.07.2014
Revised: 30.07.2014
Accepted: 07.08.2014

EX VIVO MODEL FOR PERCUTANEOUS VERTEBROPLASTY

OLIVEIRA MT[1, 2, 7, a *], LUCENA S[1, 2, 7, b], POTES J[1, 2, c], QUEIROGA MC[1, 2, d], REHMAN S[3, e], DALGARNO K[4, f], RAMOS A[5, g], REIS JC[1, 6, h]

[1]Veterinary Medicine Department, School of Science and Technology, University of Évora, Apartado 94, 7002-554 Évora, Portugal

[2]Institute of Mediterranean Agricultural and Environmental Sciences (ICAAM), University of Évora, Apartado 94, 7002-554 Évora, Portugal

[3]JRI Orthopaedics, Sheffield, United Kingdom

[4]School of Mechanical and Systems Engineering, Newcastle University, United Kingdom

[5]Biomechanics Research Group, TEMA, University of Aveiro, Portugal

[6]Centre in Research for Ceramics & Composite Materials (CICECO), University of Aveiro, Portugal

[7] Both authors contributed equally to this work

[a]toliveir@uevora.pt, [b]slucena@uevora.pt, [c]jacpotes@uevora.pt, [d]crique@uevora.pt, [e]sarrawat.rehman@jri-ltd.co.uk, [f]kenny.dalgarno@newcastle.ac.uk, [g]a.ramos@ua.pt, [h]jmfcr@uevora.pt

* corresponding author

Keywords: percutaneous vertebroplasty, animal model, ovine, biomaterial, microCT.

Abstract. The testing of novel biomaterials for percutaneous vertebroplasty depends on suitable animal models. The aim of this study was to develop *ex vivo* a reproducible and feasible model of percutaneous vertebroplasty for ulterior application *in vivo*. A large animal model was used (Merino sheep) due to its translational properties. Vertebroplasty was performed under tactile and fluoroscopic control through a bilateral modified parapedicular access in lumbar vertebrae. Care was taken in order to avoid disruption of the vertebral foramen. The average defect volume was 1234±240 mm^3 which ensures practical defects to test novel injectable biomaterials. Six vertebrae were injected with a commercial cement (Cerament®, Bone Support, Sweden) and adequate defect filling was observed in all vertebrae. All vertebrae were assessed by microCT, prior to and post defect creation, and after biomaterial injection. All vertebrae were mechanical tested and no mechanical failure was observed under loads higher than the physiological ones. Ultimately, this model is considered suitable for pre-clinical *in vivo* studies, mimicking clinical application.

Introduction. Percutaneous vertebroplasty (PVP) and kyphoplasty (KP) are minimally invasive techniques used for effective vertebral augmentation in humans when conservative treatment for vertebral compression fractures is not possible and/ or sufficient. Their purpose is to augment and stabilize the defective vertebral body by injecting percutaneously a material that will fill the bone defect. This will allow to achieve immediate pain relief and function [1–3]. In PVP small entry points for needle placement are made through the soft tissues (skin and muscles) to access the vertebrae, under fluoroscopic guidance, as an alternative to the conventional "open" approach techniques wherein an incision along the soft tissues is made.

To test biomaterials for PVP, the availability of a feasible animal model close to the human conditions is vital. Sheep is considered a suitable model for biomedical research due to its availability, low animal cost, easy handling and housing, and good homogeneity, when selected for age, breed, and sex [4]. Moreover, due to its anatomical similarities when compared to human bones, regarding weight, size, bone structure, bone remodelling process and biomechanical behaviour [7–9], it is also considered a good model for orthopaedic research, as these enables the use of the same prosthetic devices [4,8].

Up to date a small number of PVP studies were performed in animals, as most of the procedures were executed under "open" techniques wherein an incision through the skin and muscles is made; for example, Zhu *et al*. (2011) developed a sheep vertebral model with bone defect through a lateral open approach with different diameter drills; the vertebral model bone defect was replicable and effective for assessing injectable biomaterials [8]. Regarding minimal invasive techniques, a recent study by Benneker *et al*. (2012), using PVP advocated that the transition between the transverse process and the pedicle is the ideal entry point, aiming towards the cranial- and caudal hemivertebra respectively, through a para- to transpedicular approach; however cement leakage into the vertebral foramen was observed in 19 of the 33 vertebrae studied [4]. Galovich *et al.* (2011) developed another sheep PVP model for biocements testing in which a lateral approach to the vertebral body was performed; nevertheless created bone defects were small, thus this model wasn't considered suitable for biomechanical analysis of biocements [5].

Considering the limitations of the models described so far, not safe enough for the animal and bone defect volume too small to allow a satisfactory product assessment, this study aimed at developing *ex vivo* a reproducible and feasible model of percutaneous vertebroplasty, for ulterior application *in vivo*. A large animal model was used (Merino sheep), due to its translational properties [7,8], and important features were taken into account. Although considered a suitable model, differences between sheep and human vertebrae exist, such as the hourglass-shape of vertebral bodies, the sagitally oriented pedicles, the size of the transverse processes, the different orientation of the facet joints, and ultimately the hard cortical bone and high bone mineral density of sheep lumbar vertebrae [9], which make surgical approach complex and somewhat different of that advocated for humans [4]. Thus, bilateral modified parapedicular approach was developed to create two interconnected defects in the cranial hemivertebrae, with average defect volumes sufficient to ensure practical defects in which novel injectable biomaterials may be tested, concerning both their biological and biomechanical responses.

For this study a commercial biphasic cement (Cerament®, Bone Support, Sweden), 60% calcium sulphate: 40% hydroxyapatite, was chosen for its known qualities as a bone substitute [10] and microCT was used to allow easily visualization of: vertebrae distinctive anatomic features; vertebral body defects; and bone cement. The following parameters were evaluated: (1) vertebral body height (VBH), (2) bone mineral density (BMD), (3) volume of interest of each bone defect (VOI) and (4) vertebrae stiffness. Cortical disruption, injected cement volume, bone cement radiopacity, and cement leakage (into the vertebral foramen/ nutritional foramen) were also assessed.

Experimental. Eighteen vertebral segments (L4-L6) were excised from 6 skeletally mature Merino sheep and divided into 3 groups: group A (n=6) – intact vertebrae; group B (n=6) – vertebrae with defect; group C (n=6) – vertebrae injected with cement.

Soft tissue was detached; spinous and transverse processes were removed using a bone saw, in order to fit into the microCT chamber. Vertebrae were conserved in the freeze at -18°C.

All vertebrae underwent microCT scanning when intact. MicroCT examination was done using a CT scanner (Skyscan 1174, Kontich, Belgium). The vertebrae were posed in air in a rotation stage fixed by commercial play-dough, with their longitudinal axis matching the system rotational axis. Scans were performed with 50 kVp, 800 µA, 1 mm aluminium filter, the pixel size was 62.08, exposure time 2200 ms, rotation step 0.8º, full rotation over 360º, 2 average frames per image. Each vertebra went through two consecutive automated scans (oversize scan), over approximately 110 min, to assure the imaging of the whole vertebral body, comprising 906 cross-sections. The cross-section images were reconstructed using N-Recon software (Skyscan, Kontich, Belgium). The following parameters were evaluated in the analyzing software (CTAn, Skyscan, Kontich, Belgium): vertebral body height (VBH), endplates area and trabecular bone mineral density (BMD). Uniform threshold method was applied.

After scanning the intact vertebrae, vertebral body defects were made in groups B and C. All defects were created under tactile control and fluoroscopic guidance (Digital C-Arm ZEN 2090 Pro, Genoray, Co., Ltd., Korea). Vertebrae were fixed in a radiolucent table in supine position and two

defects were made bilaterally in each cranial hemivertebra, through a parapedicular approach. For this purpose, an osteo introducer system (Medtronic Spine LLC, Portugal) was used. The access was made between the pedicles and transverse processes of each vertebra. Thus a 3.5 mm-blunt osteo introducer stylet inside a 4 mm-cannula was positioned to manually access the dorsolateral cortex of the vertebral bodies. Then the blunt osteo introducer stylet was removed and a 3.35 mm-manual drill was advanced inside the cannula, with an orientation of 30-50º regarding a transverse plane, and 0º-30º regarding the frontal plane, towards the centre of the cranial hemivertebra. Bone debris were removed from the defects. All vertebrae underwent scanning again under the same procedure described above. In CTAn a volume of interest (VOI) was defined for each bone defect and its area was calculated; it was also evaluated the disruption of cortical bone (ventral vertebral body's cortical bone and ventral vertebral foramen's cortical bone). Vertebrae were conserved at -18ºC.

In group B vertebrae the defects remained empty. Vertebrae with defect from group C were then injected with 60% calcium sulphate: 40% hydroxyapatite commercial cement (Cerament®, Bone Support, Sweden). For the vertebroplasty procedure all vertebrae were fixed in a radiolucent table and injected under fluoroscopic guidance. Biomaterial injection was performed using a bone filler system device (Medtronic Spine LLC, Portugal). Cerament® was prepared at room temperature accordingly to the manufacturer instructions. Regard was taken towards handleability, injectability and radiopacity. Cerament® is easy to handle, with 8-10 minutes setting time, good injectability and high radiopacity, conferred by an iodate positive contrast (iohexol), when comparing to the bone's radiopacity.

All injected vertebrae underwent scanning again under the same procedure described for group A. In CTAn a volume of interest was defined limiting the injected cement and the VOI area was calculated. Cement leakage to vertebral and nutritional foramina was also assessed.

After vertebroplasty all vertebrae (including intact group) were mechanical tested under axial compression. In order to do so vertebrae were embedded in two parallel flat plates of polymethyl methacrylate resin (PMMA, Vertex Cold Cure), one for each top. The tests were conducted using a Shimadzu Autograph AG-50 kNG. The load was applied over a ventral point of the vertebral bodies relative to 25% of their heights with a crossing velocity of 2 mm/s for all vertebrae.

Results data from microCT analysis, *i.e.* vertebral body height, bone mineral density and volume of interest of each bone defect, and stiffness assessment, according to mechanical compression tests, from the three groups were treated using SPSS. One way ANOVA analysis was performed. Normality was verified using the Kolmogorov-Smirnov test, homogeneity of variance was verified with resource to Brown-Forsythe test and means compared using Tukey.

Results and Discussion.

Interconnected bone defects were created bilaterally in each cranial hemivertebra, through a modified parapedicular approach, with an access point placed between the pedicles and transverse processes of each vertebra (figure 1). Some limitations of the ovine model are anatomical differences between ovine and human vertebrae, such as the orientation angle of the lumbar facet joints and pedicles (less than 30° to the frontal plane, compared to over 60° in humans) and the relative short and sagitally oriented pedicles. In order to diminish the risk of pedicle's fracture and vertebral foramina's disruption verified in the transpedicular approach, a parapedicular approach was chosen.

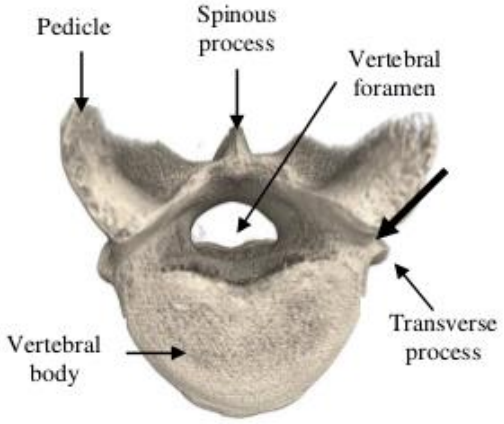

Fig. 1: 3D partial reconstructed L4 showing major anatomical landmarks and PVP access point, with the advocated access angle (large arrow).

The transpedicular approach was used by Benneker and co-workers (2012), with a resulting cement leakage into the vertebral foramen in 19 of the 33 vertebrae studied. Moreover, transpedicular approach only permits a limited access angle, which would result in smaller and not connected defects.

The relatively high trabecular bone density and the hard cortical bone of ovine lumbar vertebrae were other of the difficulties verified on the defects creation. The wide lumbar vertebrae nutritional foramina were a surgical limitation (figure 2). Precaution must be taken to maintain vertebral and nutritional foramina intact so that neurologic complications, and ultimately death, do not occur. In L6 vertebrae, problems arose due to short vertebral bodies, leading to smaller defects, in order to prevent vertebral foramina disruption. The resulting interconnected bone defect is reproducible (figure 3); minor cement leakage into the vertebral foramen was observed in 2 out of 6 vertebrae.

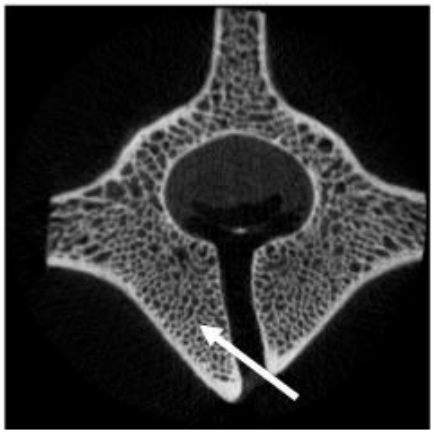

Fig. 2: Scan image of a ovine lumbar vertebra showing the wide nutritional foramen (white arrow).

Fig. 3: 3D partial reconstructed L4 showing the interconnected defect (white arrow).

The mean total VBH (n=18) was 37.52 ± 1.83 mm; the mean total BMD (n=18) was 0.371 ± 0.039 gcm^{-3}; and the mean total defect VOI (n=12) was 1234.51 ± 251.23 mm^3. Individual group results are shown in table 1.

Table 1. Descriptive statistics analysis for vertebrae groups (n=18)

Vertebrae Groups	N	VBH [mm]	BMD [gcm^{-3}]	Defect VOI [mm^3]
A – intact vertebrae	6	38.13 ± 2.01	0.397 ± 0.010	-
B – vertebrae with defect	6	37.19 ± 2.03	0.359 ± 0.056	1160,99 ± 168,26
C – vertebrae with cement	6	37.23 ± 1.61	0.358 ± 0.029	1308,03 ± 312,36

MicroCT provided important information for the development and refinement of the surgical procedure, allowing adaptation to the distinctive anatomic characteristics of ovine vertebrae. Scans and 3D reconstructed images were useful to decide the entry point and to correct the angle orientation for the access to the vertebral body, allowing to perform defects without disrupting cortical bone and vertebral and nutritional foramina. MicroCT analysis also enabled to acknowledge that in 25% of the vertebrae a small disruption of the vertebral foramen occurred (figure 4). This fact, followed by an eventual leakage, may decrease with further training. The usage of slightly smaller instrumentation, as the ones used for PVP of thoracic vertebrae, could also be beneficial.

The presence of iohexol in Cerament®'s constitution contributes to its high radiopacity which is convenient as it enables visualization of the cement whilst injected. However, iohexol also generates artefacts in the microCT images that prevent the correct evaluation of the injected cement in the bone defect, so as to calculate the volume of injected cement and to evaluate its possible leakage to the vertebral formanen. Artefacts were not eliminated due to Skyscan 1174's limitations (figure 5).

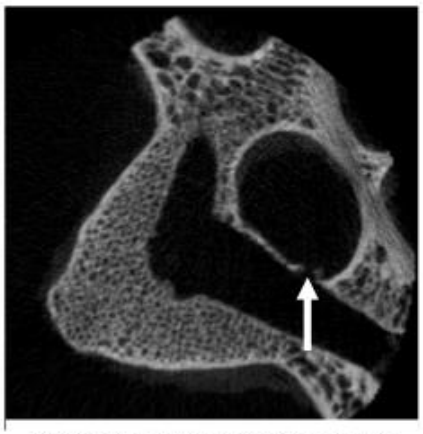

Fig. 4: MicroCT scan image of a L4 showing the disrupted vertebral foramen (white arrow).

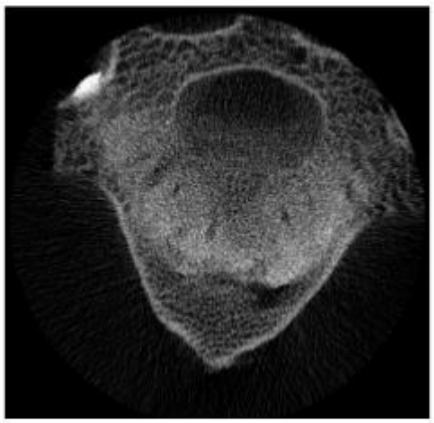

Fig. 5: MicroCT scan image of a L4 showing the artefact caused by Cerament®.

Regarding mechanical compression tests, fracture and failure were observed in the PMMA plates but not on the vertebrae, so it was not possible to determine the compressive strength of vertebrae from any of the groups. However, vertebrae stiffness was determined for all groups. For one of the vertebrae of group A (intact vertebrae), it was not possible to recover the data, so for this group, results are presented for n=5 (Figure 6). Two very important conclusions are drawn from these results: 1) all vertebrae withstood compressive loads much higher than the expected peak compressive loads under physiological conditions (reported as 1.3 kN); and 2) the developed model is reproducible and safe under much higher loads than the physiological ones. No statistical significant differences were found in stiffness of the different groups.

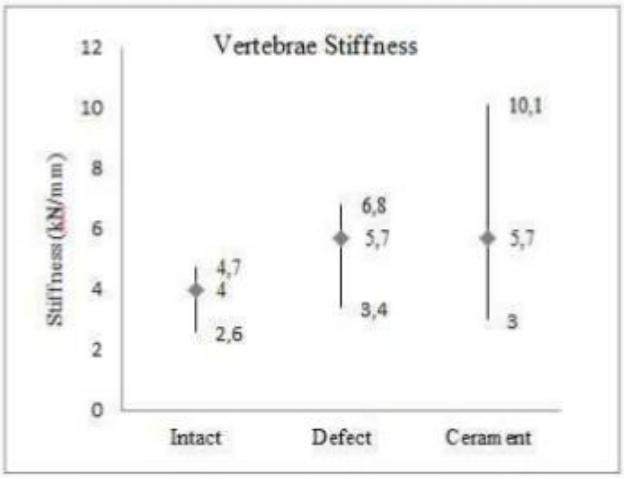

Fig. 6: Stiffness of vertebrae (groups A-C).

This paper presents an *ex vivo* ovine model for PVP testing which allowed to evaluate some specific features of ovine vertebrae that will enable a much safer approach for the *in vivo* PVP procedure. The designed defect is innovative regarding both the parapedicular approach and the interconnected bone defects created bilaterally in each cranial hemivertebra, which allows a higher volume of cement to be injected with lower risk of cement leakage.

Conclusions. This experimental model developed e*x vivo* was reproducible, and safe under physiological loads. The model is considered to be suitable for pre-clinical *in vivo* studies, mimicking clinical applications.

Acknowledgements. This work has been supported by the European Commission under the 7th Framework Programme through the project Restoration, under the action "Collaborative project targeted to SMEs", grant agreement NMP.2011.2.1-1.

The support from Medtronic Spine LLC Company, Portugal is gratefully acknowledged for supplying surgical material.

References.

[1] S. Masala, R. Mastrangeli, M.C. Petrella, F. Massari, A. Ursone, G. Simonetti, Percutaneous vertebroplasty in 1,253 levels: results and long-term effectiveness in a single centre, Eur. Radiol. 19 (2009) 165–171.

[2] W.C.G. Peh, P.L. Munk, F. Rashid, L.A. Gilula, Percutaneous Vertebral Augmentation: Vertebroplasty, Kyphoplasty and Skyphoplasty, Radiol. Clin. North. Am. 46 (2008) 611–635.

[3] M.H.J. Voormolen, W.P.T.M. Mali, P.N.M. Lohle, H. Fransen, L.E.H. Lampmann, Y. van der Graaf, *et al*., Percutaneous Vertebroplasty Compared with Optimal Pain Medication Treatment: Short-Term Clinical Outcome of Patients with Subacute or Chronic Painful Osteoporotic Vertebral Compression Fractures. The VERTOS Study, Am. J. Neuroradiol. 28 (2007) 555–560.

[4] L.M. Benneker, A. Gisep, J. Krebs, A. Boger, P.F. Heini, V. Boner, Development of an in vivo experimental model for percutaneous vertebroplasty in sheep, Vet. Comp. Orthop. Traumatol.: V.C.O.T. 25 (2012) 173–177.

[5] L.A. Galovich, A. Perez-Higueras, J.R. Altonaga, J.M. Gonzalo Orden, M.L. Marinoso Barba, M.T. Carrascal Morillo, Biomechanical, histological and histomorphometric analyses of calcium phosphate cement compared to PMMA for vertebral augmentation in a validated animal model, Eur. Spine. J. 20 (2011) 376–382.

[6] X.S. Zhu, Z.M. Zhang, H.Q. Mao, D.C. Geng, J. Zou, G.L. Wang, *et al*., A novel sheep vertebral bone defect model for injectable bioactive vertebral augmentation materials, J. Mater. Sci. Mater. Med. 22 (2011) 159–164.

[7] M. Alini, S.M. Eisenstein, K. Ito, C. Little, A.A. Kettler, K. Masuda, *et al*., Are animal models useful for studying human disc disorders/degeneration?, Eur. Spine. J. 17 (2008) 2–19.

[8] J.C. Potes, J. Reis, F. Capela e Silva, C. Relvas, A.S. Cabrita, J.A. Simões, The Sheep as an Animal Model in Orthopaedic Research (2008), Available from: http://hdl.handle.net/10174/1548.

[9] H-J. Wilke, A. Kettler, K.H. Wenger, L.E. Claes, Anatomy of the sheep spine and its comparison to the human spine, Anat. Rec. 247 (1997) 542–555.

[10] S. Marcia, C. Boi, M. Dragani, S. Marini, M. Marras, E. Piras, *et al*., Effectiveness of a bone substitute (CERAMENT^{TM}) as an alternative to PMMA in percutaneous vertebroplasty: 1-year follow-up on clinical outcome, Eur. Spine. J. 21 (2012) 112–118.

Bioceramics Volume 26
10.4028/www.scientific.net/KEM.631

***Ex Vivo* Model for Percutaneous Vertebroplasty**
10.4028/www.scientific.net/KEM.631.408

DOI References
[2] W.C.G. Peh, P.L. Munk, F. Rashid, L.A. Gilula, Percutaneous Vertebral Augmentation: Vertebroplasty, Kyphoplasty and Skyphoplasty, Radiol. Clin. North. Am. 46 (2008) 611-635.
http://dx.doi.org/10.1016/j.rcl.2008.05.005
[6] X.S. Zhu, Z.M. Zhang, H.Q. Mao, D.C. Geng, J. Zou, G.L. Wang, et al., A novel sheep vertebral bone defect model for injectable bioactive vertebral augmentation materials, J. Mater. Sci. Mater. Med. 22 (2011) 159-164.
http://dx.doi.org/10.1007/s10856-010-4191-5
[7] M. Alini, S.M. Eisenstein, K. Ito, C. Little, A.A. Kettler, K. Masuda, et al., Are animal models useful for studying human disc disorders/degeneration?, Eur. Spine. J. 17 (2008) 2-19.
http://dx.doi.org/10.1007/s00586-007-0414-y
[9] H-J. Wilke, A. Kettler, K.H. Wenger, L.E. Claes, Anatomy of the sheep spine and its comparison to the human spine, Anat. Rec. 247 (1997) 542-555.
http://dx.doi.org/10.1002/(SICI)1097-0185(199704)247:4<542::AID-AR13>3.0.CO;2-P

Chapter 5

Percutaneous vertebroplasty: a new animal model

Published in The Spine Journal,
October 2016, Volume 16(10): 1253-1262.

ELSEVIER

CrossMark

The Spine Journal 16 (2016) 1253–1262

THE SPINE JOURNAL

Basic Science

Percutaneous vertebroplasty: a new animal model

Maria Teresa Oliveira, DVM[a,*], José Potes, PhD, DVM[a], Maria Cristina Queiroga, PhD, DVM[a], José L. Castro, PhD[b], Alfredo F. Pereira, PhD, BS[b], Sarrawat Rehman, PhD, BEng, CEng MIMechE[c], Kenneth Dalgarno, PhD[d], António Ramos, PhD[e], Chiara Vitale-Brovarone, PhD[f,g], Joana C. Reis, PhD, MsC, DVM[h,i]

[a]*Departamento de Medicina Veterinária (DMV), Escola de Ciências e Tecnologia (ECT), Instituto de Ciências Agrárias e Ambientais Mediterrânicas (ICAAM), University of Évora, Apartado 94, 7002-554 Évora, Portugal*

[b]*Departamento de Zootecnia, Escola de Ciências e Tecnologia, Instituto de Ciências Agrárias e Ambientais Mediterrânicas, Apartado 94, 7002-554 Évora, Portugal*

[c]*JRI Orthopaedics Limited, 18 Churchill Way, Sheffield, S35 2PY, UK*

[d]*School of Mechanical and Systems Engineering, Newcastle University, Stephenson Building, Claremont Rd, Newcastle upon Tyne, NE1 7RU, UK*

[e]*Biomechanics Research Group, Centre for Mechanical Technology and Automation (TEMA), Department of Mechanical Engineering of the University of Aveiro, Campus Universitário de Santiago, 3810-193, Aveiro, Portugal*

[f]*Politecnico di Torino, Corso Duca degli Abruzzi, 24-10129, Torino, Italy*

[g]*Consorzio per la Ricerca e l'Educazione Permanente (Corep), Sede legale Via Ventimiglia, 115-10126, Torino, Italy*

[h]*Departamento de Medicina Veterinária (DMV), Escola de Ciências e Tecnologia (ECT), Apartado 94, 7002-554 Évora, Portugal*

[i]*Complexo de Laboratórios Tecnológicos (CICECO), Campus Universitário de Santiago, 3810-193 Aveiro, Portugal*

Received 3 January 2016; revised 25 May 2016; accepted 21 June 2016

Abstract

BACKGROUND CONTEXT: Percutaneous vertebroplasty (PVP) is a minimally invasive surgical procedure and is frequently performed in humans who need surgical treatment of vertebral fractures. PVP involves cement injection into the vertebral body, thereby providing rapid and significant pain relief.

PURPOSE: The testing of novel biomaterials depends on suitable animal models. The aim of this study was to develop a reproducible and safe model of PVP in sheep.

STUDY DESIGN: This study used ex vivo and in vivo large animal model study (Merino sheep).

METHODS: Ex vivo vertebroplasty was performed through a bilateral modified parapedicular access in 24 ovine lumbar hemivertebrae, divided into four groups (n=6). Cerament (Bone Support, Lund, Sweden) was the control material. In the experimental group, a novel composite was tested—SpineGhost—which consisted of an alpha-calcium sulfate matrix enriched with micrometric particles of mesoporous bioactive glass. All vertebrae were assessed by micro-computed tomography (micro-CT) and underwent mechanical testing.

For the in vivo study, 16 sheep were randomly allocated into control and experimental groups (n=8), and underwent PVP using the same bone cements. All vertebrae were assessed postmortem by micro-CT, histology, and reverse transcription-polymerase chain reaction (rt-PCR).

FDA device/drug status: Not applicable.

Author disclosures: ***MTO:*** Grant: European Commission (G, Paid directly to institution/employer), pertaining to the submitted work. ***JP:*** Grant: European Commission (G, Paid directly to institution/employer), pertaining to the submitted work. ***MCQ:*** Grant: European Commission (G, Paid directly to institution/employer), pertaining to the submitted work. ***JLC:*** Grant: European Commission (G, Paid directly to institution/employer), pertaining to the submitted work. ***AFP:*** Grant: European Commission (G, Paid directly to institution/employer), pertaining to the submitted work. ***SR:*** Grants: European Commission (F, Paid directly to institution/employer), pertaining to the submitted work, Innovate UK (G, Paid directly to institution/employer), European Commission (F, Paid directly to institution/employer), outside the submitted work. ***KD:*** Grants: European Commission (G, Paid directly to institution/employer), pertaining to the submitted work, DePuy International (F, Paid directly to institution/employer), Glass Technology Services Ltd (D, Paid directly to institution/employer), QuantuMDx Group Ltd (D, Paid directly to institution/employer), Alcyomics Ltd (D, Paid directly to institution/employer), outside the submitted work. ***AR:*** Nothing to disclose. ***CVB:*** Grant: European Commission (F, Paid directly to institution/employer), pertaining to the submitted work. ***JCR:*** Grant: European Commission (G, Paid directly to institution/employer), pertaining to the submitted work.

The disclosure key can be found on the Table of Contents and at www.TheSpineJournalOnline.com.

* Corresponding author. Departamento de Medicina Veterinária, Escola de Ciências e Tecnologia, Instituto de Ciências Agrárias e Ambientais Mediterrânicas, Universidade de Évora, Apartado 94, 7002-554 Évora, Portugal. Tel.: +351 266760859.

E-mail address: teresoliveira@uevora.pt (M.T. Oliveira)

http://dx.doi.org/10.1016/j.spinee.2016.06.011

This work has been supported by the European Commission under the 7th Framework Programme for collaborative projects (600,000–650,000 USD).

RESULTS: In the ex vivo model, the average defect volume was 1,275.46±219.29 mm^3. Adequate defect filling with cement was observed. No mechanical failure was observed under loads which were higher than physiological. In the in vivo study, cardiorespiratory distress was observed in two animals, and one sheep presented mild neurologic deficits in the hind limbs before recovering.

CONCLUSIONS: The model of PVP is considered suitable for preclinical in vivo studies, mimicking clinical application. All sheep recovered and completed a 6-month implantation period. There was no evidence of cement leakage into the vertebral foramen in the postmortem examination.

Keywords: Animals models; Biomaterials; Micro-CT; Ovine; Parapedicular access; Percutaneous vertebroplasty

Introduction

Percutaneous vertebroplasty (PVP) is a minimally invasive technique of vertebral augmentation for compression fractures. Its aim is to augment and stabilize the defective vertebral body by percutaneously injecting a material that will fill the bone defect, thus achieving immediate pain relief and functional recovery [1–5].

Sheep are considered a suitable model for biomedical research because of availability, low cost, easy handling and housing, and good homogeneity (when selected for age, breed, and sex) [6]. Moreover, because of the anatomical similarities to human bones (regarding weight, size, structure, remodeling process, and biomechanical behavior) [7–9], sheep are considered a good model for orthopedic research [6,8].

To date only a small number of PVP studies have been performed in animals. Most were executed using "open surgery" techniques, wherein an incision through the skin and muscles is made to expose the vertebrae [10–12]. Studies using minimally invasive techniques, including the ones with a modified parapedicular approach, encountered varied issues, including cement leakage into the vertebral foramen [6], incomplete defect filling, or lack of information on postoperative evolution [13,14].

Our study aimed to develop ex vivo a reproducible and feasible model of PVP, and its use in vivo. A large animal model was used based on Merino sheep because of its potential to support preclinical translation [7–9]. Consideration of the differences between sheep and human vertebrae [6] resulted in the development of a modified approach, enabling the creation of large enough defects as to ensure testing of novel biomaterials without neurologic or biomechanical compromise [15].

Material and methods

Ex vivo model development

Animal model

From 8 skeletally mature Merino sheep, 24 vertebral segments (L4–L6) were excised, collected from cadavers from different sources, with no further information on their background. The segments were randomly distributed (n=6) into four groups: A, intact vertebrae; B, vertebrae with defects; C, vertebrae with defects injected with a well-known biphasic commercial cement, Cerament; and D, vertebrae with defects injected with a novel composite—Spine-Ghost—which consists of an alpha-calcium sulfate matrix enriched with micrometric particles of mesoporous bioactive glass [16]. Soft tissue was extracted, and using a bone saw, the spinous and transverse processes were removed to fit the vertebrae into the micro-computed tomography (micro-CT) chamber while preserving the vertebral arch. Vertebrae were stored at −18°C.

Micro-CT assessment

All vertebrae underwent initial micro-CT scanning (Skyscan 1174, Kontich, Belgium) while still intact. The vertebrae were posed in a rotation stage fixed by commercial play-dough, with their longitudinal axis matching the system's rotational axis. Scans were performed with 50-kVp, 800-μA, and a 1-mm aluminum filter. The pixel size was 62.08, exposure time 2,200 ms, rotation step 0.8°, full rotation over 360°, with 2 average frames per image. Each vertebra went through two consecutive automated scans (oversize scan), over approximately 110 minutes, to assure the imaging of the whole vertebral body, comprising 906 cross sections. The cross-section images were reconstructed using N-Recon software (Skyscan, Kontich, Belgium). The following parameters were evaluated in the analyzing software (CTAn, Skyscan, Kontich, Belgium): vertebral body height (VBH), end plates area, and trabecular bone mineral density (BMD). A uniform threshold method was applied.

Bone defect creation

In all vertebrae from Groups B, C, and D, vertebral body defects were created, in the order B-C-D, under visual and tactile control and fluoroscopic guidance (Digital C-Arm ZEN 2090 Pro, Genoray, Co, Ltd, Gyeonggi-Do, Korea). With the vertebrae fixed on a radiolucent table, in their ventral position, an osteo introducer system (Medtronic Spine LLC, Lisboa, Portugal) was used to create two interconnected defects (one in each side of the cranial hemivertebra). A 3.5-mm blunt stylet was positioned through a 4-mm cannula to manually access the dorsolateral cortex of the vertebral bodies—between the pedicles and transverse processes of each vertebra in a parapedicular approach. The stylet was then removed and

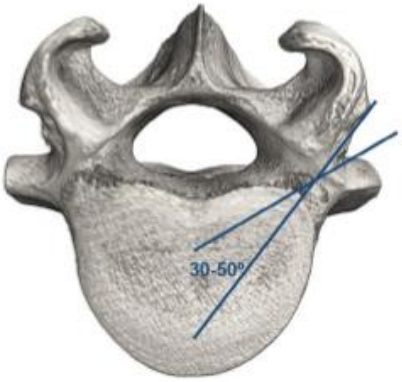

Fig. 1. Three-dimensional (3D) partially reconstructed L4 showing the instruments' orientation regarding a transverse plane.

a 3.35-mm manual drill was advanced toward the center of the cranial hemivertebra—orientation: 30–50° regarding a transverse plane (Fig. 1); 0°–30° regarding a frontal plane (Fig. 2), creating a V-shaped defect of two intersecting cylinders. Bone debris were removed from the defects.

Cement injection

Group B vertebrae defects remained empty. Vertebrae defects from Groups C and D were injected with their corresponding cement. During the vertebroplasty procedure, all vertebrae were fixed on a radiolucent table and injected under fluoroscopic guidance. Biomaterial injection was performed using a bone filler system device (Medtronic Spine LLC, Portugal). Cerament and Spine Ghost were prepared at room temperature, according to the manufacturers' instructions. Regard was taken toward handleability, injectability, and radiopacity.

All these vertebrae underwent rescanning using the same procedure as outlined above for initial scanning. In CTAn a volume of interest (VOI) was defined for each bone defect and its area was calculated. Cement distribution and integrity of the anatomical structures were assessed. Vertebrae were stored at −18°C, with vertebrae from every group undergoing the same number of freezing and thawing cycles.

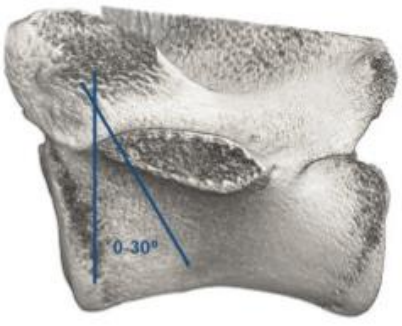

Fig. 2. Three-dimensional (3D) partially reconstructed L4 showing the instruments' orientation regarding a frontal plane.

Mechanical testing

After vertebroplasty all vertebrae were mechanically tested under axial compression to assess stiffness and fracture strength. End caps for the vertebrae were made using polymethylmethacrylate resin (Vertex Cold Cure, Vertex Dental, Soesterberg, The Netherlands), with care taken to try to keep the two outer flat surfaces parallel. The tests were conducted using a Shimadzu Autograph AG-50 kNG (Shimadzu Corporation, Kyoto, Japan). The load was applied over a ventral point of the vertebral bodies relative to 25% of their heights with a crosshead speed of 2 mm/s.

Statistical analysis

Results from the micro-CT analysis (VBH, BMD, and VOI of each bone defect) and stiffness assessment were analyzed using SPSS Statistics for Windows, Version 22.0 (IBM Corp., Armonk, NY, USA). One-way analysis of variance was performed. Normality was verified using the Kolmogorov-Smirnov test, homogeneity of variance was verified with resource to Brown-Forsythe test, and means were compared using Tukey.

In vivo model application

Animal model

Animal handling and surgical procedures were conducted according to European Community guidelines for the care and use of laboratory animals (Directive 2010/63/UE) and after obtaining approval from the national competent authorities [17–19]. Sixteen skeletally mature female Merino sheep with an average body weight of 56.8±5.3 kg underwent PVP, divided into two groups: Group E (n=8), a control group injected with Cerament; and Group F (n=8), an experimental group injected with a novel biphasic cement, SpineGhost. Before surgery the animals fasted for 24 hours.

Anesthetic protocol

The animals were premedicated with atropine (0.05 mg/kg subcutaneous), xilazine (0.1 mg/kg intramuscular), butorphanol (0.01 mg/kg intravenous), and carprofen (2 mg/kg subcutaneous); induction was achieved with thiopental sodium 5% (5–10 mg/kg intravenous) and maintenance with isoflurane 1%–2% under spontaneous ventilation. After premedication the sheep were inducted and positioned in ventral decubitus with the hind limbs retracted caudally and fixed to the surgery radiolucent table (Fig. 3). The surgical field was prepared with povidone-iodine solution and alcohol at 70° and the anesthetic monitoring equipment was connected to the animal (Fig. 4). Anesthetic monitoring included cardiac electric activity; respiratory rate; partial CO_2 concentration in expired air; partial blood O_2 concentration and noninvasive arterial blood pressure. Orogastric intubation was performed.

Fig. 3. Anesthetized sheep, with the surgical location (over the lumbar vertebrae) already clipped and sheep's position supported with foam wedges.

Surgery

L4 was identified under tactile and fluoroscopic guidance (Digital C-Arm ZEN 2090 Pro, Genoray, Co, Ltd, Korea) and 2.5-mm surgical osteo introducer stylet (Kyphon, Express, Osteo Introducer System, size 2, Medtronic Spine LLC, Portugal) was positioned inside a 3-mm cannula approximately 2–3 cm apart from the spine midline in a 45° angle regarding a transverse plane. At this point, the surgical instrumentation was introduced, crossing the skin and muscles, until the vertebra was reached. As advocated in the ex vivo study, the access point into the vertebral body was the space between the pedicle and the cranial side of the transverse process.

After penetrating the cortical bone of the vertebral body, the osteo introducer stylet was replaced by a 2.5-mm precision manual drill which advanced 1–2 cm until reaching the cranial hemivertebra's midline (orientation: 30°–50° regarding a transverse plane; 0°–30° regarding the frontal plane). The same procedure was performed contralaterally, and care

Fig. 4. Anesthetic monitor providing data from the sheep.

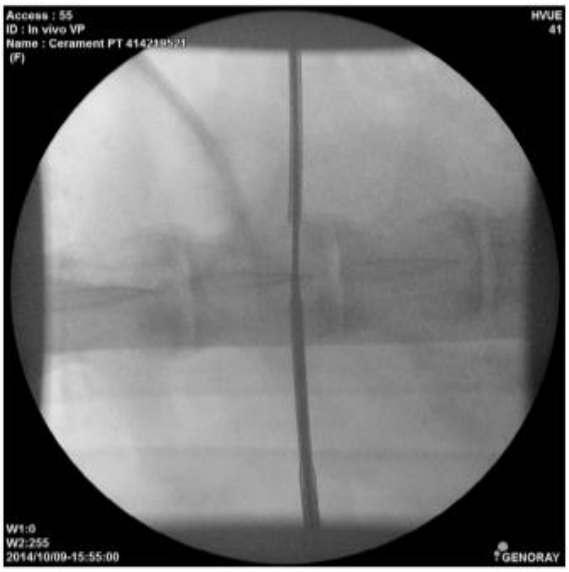

Fig. 5. C-Arm image showing an L4 with an interconnected defect, in a dorsoventral projection.

was taken to interconnect both defects and extend them as much as possible, again creating a V-shaped defect (Fig. 5).

Biomaterial injection

Cerament and Spine-Ghost were prepared at room temperature, according to the manufacturers' instructions. The osteo introducer system was replaced by a nozzle (Kyphon Express Bone Biopsy Device size 2, Medtronic Spine LLC, Portugal), and sterile cement was injected into the defect, under fluoroscopic guidance, using a bone-filler system device (Medtronic Spine LLC, Portugal). The mean time of injection was 1 minute (as shown in the animation Online Resource 1), and the injected volume was approximately 1.2 mL (Fig. 6).

Post-surgery

After injection all sheep remained anesthetized for 2 hours, assuring immobilization to allow the curing process of the cement. Upon recovery, sheep were moved into a pen, inside the Veterinary Hospital of the University of Évora, and treated with amoxicillin and clavulanate acid (15 mg/kg, once a day, subcutaneous), carprofen (2 mg/kg, once a day, subcutaneous), and butorphanol (0.15 mg/kg, twice a day, intramuscular), for 7 days. Fifteen days postsurgery, a fluorochrome (calcein green, 15 mg/kg) was subcutaneously injected, and sheep were released into the pasture. Another fluorochrome (alizarin complexone 25 mg/kg) was subcutaneously injected 2 weeks before sacrifice. After 6 months of implantation time, the animals were sacrificed by pentobarbiturate intravenous injection. Biological response and material integration were assessed by micro-CT, histologic studies, and reverse transcription-polymerase chain reaction.

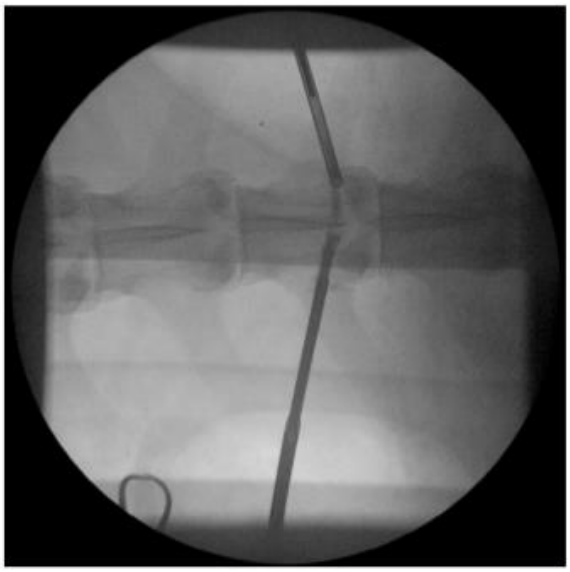

Fig. 6. C-Arm image showing Cerament filling the interconnected defects (in vivo study), in a dorsoventral projection.

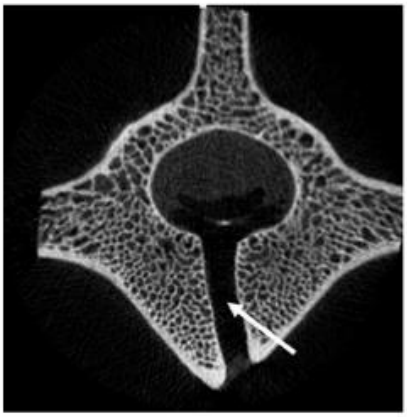

Fig. 7. Scan image of an ovine lumbar vertebra showing the wide nutritional foramen (white arrow).

Results and discussion

Ex vivo model

A known limitation of the ovine vertebral model is the anatomical differences from human vertebrae. Because of the orientation angle of the lumbar facet joints and pedicles, and the relatively short and sagittally oriented pedicles, a conventional transpedicular approach is associated with the risk of pedicle fracture and vertebral foramina disruption. Additionally, the access angle is limited, resulting in smaller and isolated defects.

Previous studies have detected cement leakage into the vertebral foramen in more than half the injected vertebrae [6]. To overcome these limitations, a parapedicular approach limited to the cranial hemivertebrae was developed [15], because the nutritional foramina are very prominent and act as low resistance accesses to the vertebral foramen. Precaution had to be taken to preserve vertebral and nutritional foramina to prevent neurologic and vascular complications.

The surgical limitations in this study were the high trabecular bone density; the hardness of the cortical bone of ovine lumbar vertebrae when compared with human; and the wide lumbar vertebrae nutritional foramina (Fig. 7). The L6 vertebrae, because of its shortness, may be more prone to vertebral foramina disruption with the described technique. The resulting interconnected bone defect is illustrated in Fig. 8, but minor cement leakage into the vertebral foramen was observed in two out of six vertebrae in the ex vivo study.

This model could potentially be used with alternative percutaneous vertebral augmentation techniques, most obviously kyphoplasty, as long as adequate-size instrumentation and suitable means for creating a bone defect in the highly dense trabecular network of the vertebral body was ensured. Application for SKyphoplasty would depend on the ability of the plastic device to break through the trabecular structure; however, because this technique demands a larger cannula and only a fixed degree of expansion of the devices is possible, its use would also be highly dependent on proper sizing of the instrumentation [4,20].

The mean total VBH (n=24) was 37.10±1.80 mm; the mean total BMD (n=24) was 0.3512±0.0493 gcm^{-3}; and the mean total defect VOI (n=18) was 1,275.46±219.29 mm^3. Individual group results are shown in Table 1, and the distribution of defect VOI values is shown in Fig. 9. Despite being randomly distributed into the groups, vertebrae from Group D showed lower VBH and lower BMD values. This may be explained because of individual anatomical differences between the vertebrae, which came from different sources with no

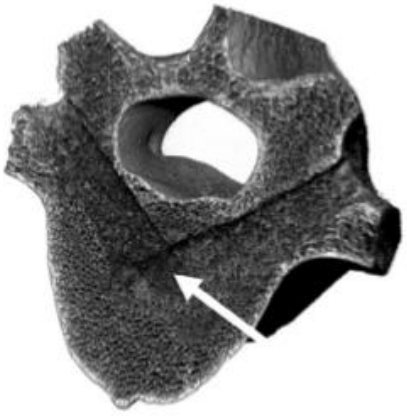

Fig. 8. 3D partial reconstructed L4 showing the interconnected defect (white arrow).

Table 1
Descriptive statistics analysis for vertebrae groups (n=24)

Vertebrae groups	N	VBH (mm)	BMD (gcm^{-3})	Defect VOI (mm^3)
A, intact vertebrae	6	38.13±2.01	0.397±0.010	—
B, vertebrae with empty defect	6	37.19±2.03	0.359±0.056	1,160.99±168.26
C, vertebrae with Cerament	6	37.23±1.61	0.358±0.029	1,308.03±312.36
D, vertebrae with Spine-Ghost	6	35.86±0.96	0.292±0.019	1,357.35±112.17

VBH, vertebral body height; BMD, bone mineral density; Defect VOI, defect volume of interest.

background information available. Besides that, defect VOI values from Group D showed less variance than those values from the other groups, perhaps due to the surgeon gaining more experience of the technique (as Groups B and C were completed before Group D), because this is a novel approach requiring high precision to manually drill the interconnected bilateral bone defects without disrupting the vertebral or nutritional foramina. No statistically significant differences were found between these three groups for defect VOI values. On the basis of the defect VOI and consistent defect morphology, the procedure is considered reproducible.

The micro-CT information of the distinctive characteristics of ovine vertebrae facilitated decisions regarding the surgical entry points and orientation angles for accessing each vertebral body. This enabled the creation of defects without disrupting cortical bone or the vertebral and nutritional foramina. On the other hand, micro-CT analysis revealed small disruptions of the vertebral foramen in 25% of the vertebrae (Fig. 10), which was expected to decrease with further training and with the use of slightly smaller instruments (which were chosen for the in vivo procedures).

Cerament was easy to handle, with 8–10 minutes setting time, good injectability, and a high radiopacity compared with bone (because of the presence of iohexol). Its higher radiopacity enabled visualization of the cement while being injected (Fig. 11) [21]. However, iohexol generates artifacts in the micro-CT images that prevent a correct evaluation of

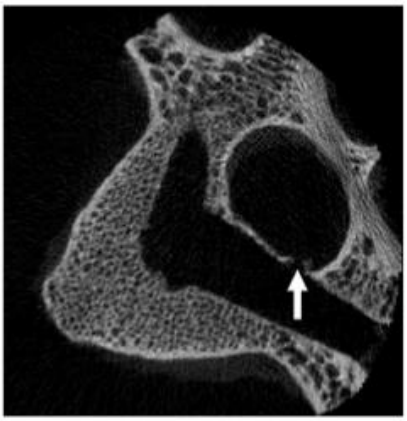

Fig. 10. Micro-computed tomography (micro-CT) scan image of an L4 showing the disrupted vertebral foramen (white arrow).

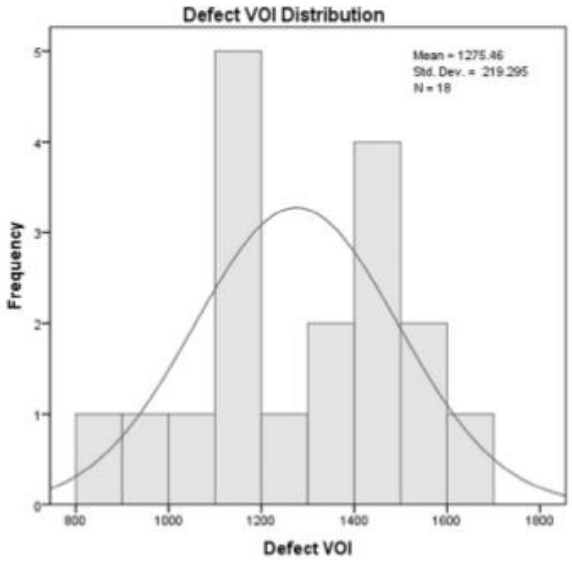

Fig. 9. Defect volume of interest (VOI)'s values distribution shown in a histogram with normal curve (SPSS 22 graph).

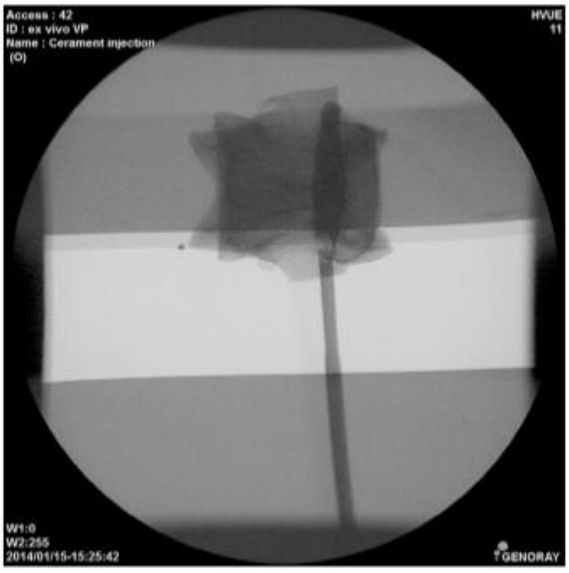

Fig. 11. C-Arm image showing an L4 with defect injected with Cerament in a dorsoventral projection.

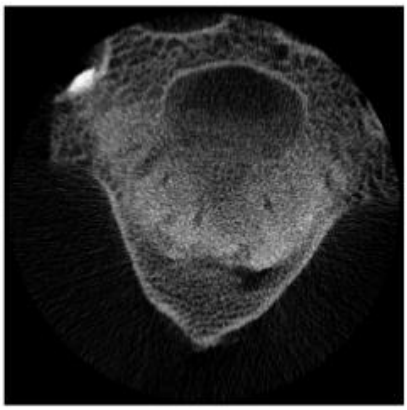

Fig. 12. Micro-computed tomography (micro-CT) scan image of an L4 showing the artifact caused by Cerament.

the cement inside the bone defect, impairing the evaluation of injected cement volume and the determination of possible leakage (Fig. 12).

Spine Ghost was also easy to handle, with a smaller setting time than that of Cerament's, and good injectability, but only moderate radiopacity (conferred by its bioactive glass-ceramic phase [22]). The micro-CT images had fewer artifacts, but the material was harder to visualize during injection.

A typical mechanical compression test trace is shown in Fig. 13, Top. All vertebrae withstood compressive loads much higher than the peak loads expected under physiological conditions (~1.3 kN). A vertebral stiffness was calculated from the slope of the linear section of the curve (typically this involved calculating the gradient at loads of between 2 and 5 kN). The net stiffnesses are shown in Fig. 13, Middle. As BMD values were significantly lower in Group D, and bone mass parameters (ie, BMD and Bone Volume/ Total Volume (Relative Bone Volume)) are strongly correlated with failure load, compressive stiffness, and work to failure [23], a normalized vertebral stiffness was calculated by dividing the vertebral stiffness by the BMD value of each vertebra, as shown in Fig. 13, Bottom. No statistically significant differences were found in stiffness or normalized stiffness between the different groups.

The developed model is reproducible and safe under much higher loads than would arise physiologically.

In vivo model

As noted previously, the *in vivo* procedure was performed informed by the ex vivo results. The chosen vertebra to create the bone defect was L4. The end plate height is higher, potentially permitting bigger defects than L6 would. In the second sheep intervened, from control Group E, rupture of the ventral cortical bone of the vertebral body occurred, with cement leakage to the vertebral body ventral surface. During the cement injection, an abrupt drop in the arterial blood pressure was observed (probably due to pulmonary fat embolism [24,25]), the animal went into cardiovascular arrest, and cardiopulmonary resuscitation maneuvers were performed. No secondary neurologic reactions were subsequently observed in this sheep. The fourth sheep (Group E) also suffered abrupt arterial blood pressure decrease during cement injection. To prevent any other cardiovascular changes in the other sheep, the injection speed was reduced, thus decreasing the cement injection force. No further cardiovascular changes were observed in the other animals. In two sheep from the control group, contact between the two bilateral connected defects was not wide enough, and the cement could only be injected from only one side without risking leakage. In these two cases the defect was filled bilaterally. All sheep remained anesthetized for 2 hours after injection, then recovered well and rapidly stood up and began to eat. One sheep of the first group that underwent surgery developed proprioceptive deficits of the hind limbs, due to cement leakage around the defect entry point affecting the spinal nerve roots, but the sheep remained ambulatory. After approximately 2 months the animal had fully recovered.

In vivo procedures were successful with all animals completing the 6 months implantation period. Ancillary imaging was crucial in offering visualization of vertebral landmarks and complementing the surgeon's visual and tactile control. It is also important to emphasize that constant anesthetic monitoring by a qualified veterinary enabled prompt intervention when necessary.

At the end of the in vivo study, micro-CT scanning was performed. The artifacts caused by iohexol in Cerament were less prominent because of cement resorption and new bone formation (Fig. 14). Iohexol may also cause hypersensitivity responses, and we suspect that it caused one of the animals to develop a transient mild angioedema after PVP. The micro-CT analysis revealed small disruptions of (1) the vertebral foramina in 26.7% of the vertebrae (Fig. 15), (2) the vertebral cortex in 13.3% of the vertebrae, and (3) the nutritional foramina in 20% of the vertebrae (n=15). Nevertheless, no cement leakage was observed into the vertebral foramina, which is in accordance with the low number of animals presenting postsurgical neurologic deficits, even if mild (1 out of 16), and with the high survival rate (100%) obtained.

Biological response and material integration were also assessed by histologic studies and reverse transcription-polymerase chain reaction.

Conclusions

A new ovine model for PVP has been developed. The surgical technique described, first developed ex vivo, is reproducible and safe under physiological loads. The model is innovative both in approach and design—interconnected defects created bilaterally in each cranial hemivertebra, allowing a controlled volume of cement to be injected with a low risk of leakage. This model enabled a much safer

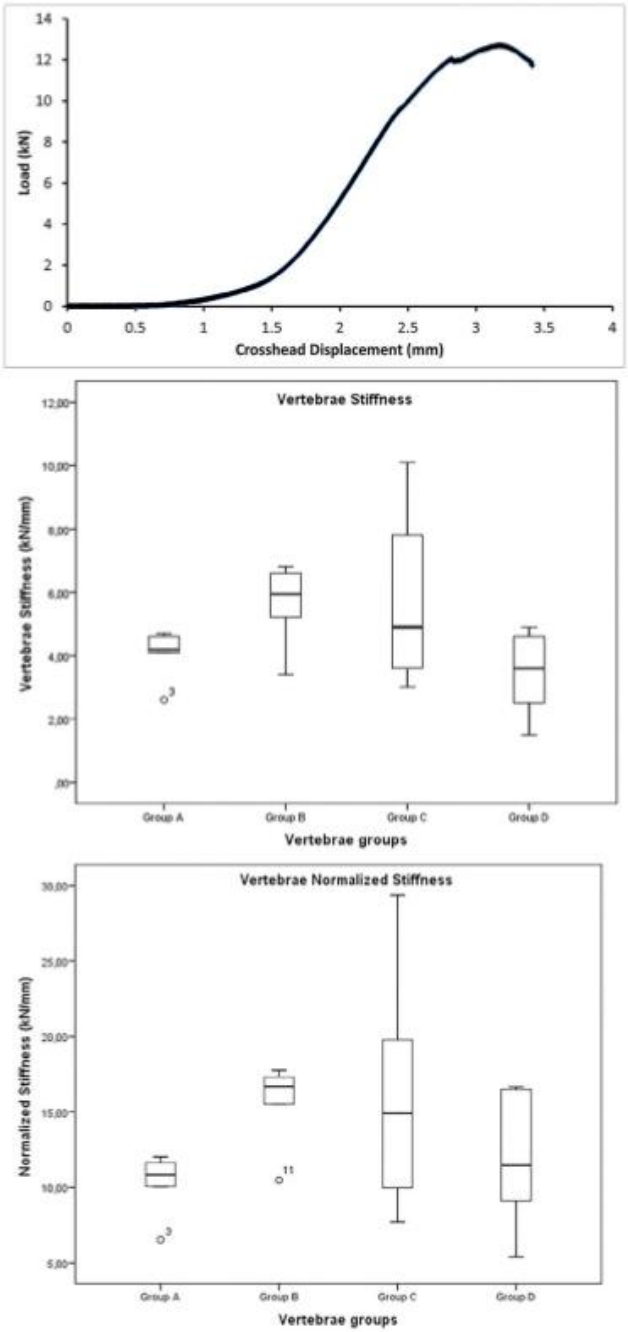

Fig. 13. (Top) Compression testing of vertebra with Cerament-filled defect. (Middle) Vertebrae stiffness (Groups A–D) (SPSS 22 graph). (Bottom) Vertebrae normalized stiffness (Groups A–D) (SPSS 22 graph).

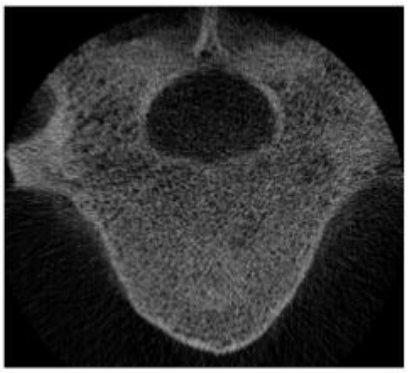

Fig. 14. Micro-computed tomography (micro-CT) scan image of an L4 injected with Cerament, from the in vivo study, showing cement resorption, new bone formation, and no artifact.

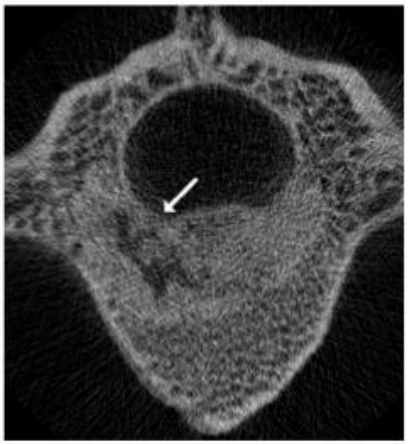

Fig. 15. Micro-computed tomography (micro-CT) scan image of an L4 injected with Cerament, from the in vivo study, showing a potential cortical disruption of the vertebral foramen (white arrow).

approach to the in vivo procedure with a survival rate of 100%. Although requiring surgical expertise, the procedure is suitable for preclinical in vivo studies, mimicking clinical applications.

Acknowledgments

This work has been supported by the European Commission under the Seventh Framework Programme through the project RESTORATION, under grant agreement 280575. The support from Medtronic Spine LLC Company, Portugal, in supplying surgical material is gratefully acknowledged. The support from Hamamatsu Photonics in supplying the Nanozoomer SQ is also gratefully acknowledged.

Appendix: Supplementary material

The following is the supplementary data to this article:

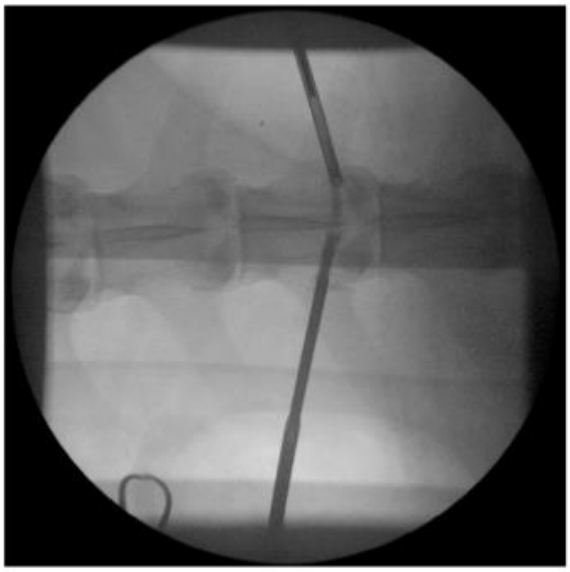

Video 1 C-Arm image showing Cerament filling the interconnected defects (in vivo study) in a dorsoventral projection.

References

[1] Savage JW, Schroeder GD, Anderson PA. Vertebroplasty and kyphoplasty for the treatment of osteoporotic vertebral compression fractures. J Am Acad Orthop Surg 2014;22:653–64.
[2] Santiago FR, Chinchilla AS, Álvarez LG, Abela ALP, García MDMC, López MP. Comparative review of vertebroplasty and kyphoplasty. World J Radiol 2014;6:329–43.
[3] Masala S, Mastrangeli R, Petrella MC, Massari F, Ursone A, Simonetti G. Percutaneous vertebroplasty in 1,253 levels: results and long-term effectiveness in a single centre. Eur Radiol 2009;19:165–71.
[4] Peh WCG, Munk PL, Rashid F, Gilula LA. Percutaneous vertebral augmentation: vertebroplasty, kyphoplasty and skyphoplasty. Radiol Clin North Am 2008;46:611–35.
[5] Voormolen MHJ, Mali WPTM, Lohle PNM, Fransen H, Lampmann LEH, van der Graaf Y, et al. Percutaneous vertebroplasty compared with optimal pain medication treatment: short-term clinical outcome of patients with subacute or chronic painful osteoporotic vertebral compression fractures. The VERTOS study. AJNR Am J Neuroradiol 2007;28:555–60.
[6] Benneker LM, Gisep A, Krebs J, Boger A, Heini PF, Boner V. Development of an in vivo experimental model for percutaneous vertebroplasty in sheep. Vet Comp Orthop Traumatol 2012;25:173–7.
[7] Alini M, Eisenstein SM, Ito K, Little C, Kettler AA, Masuda K, et al. Are animal models useful for studying human disc disorders/degeneration? Eur Spine J 2008;17:2–19.
[8] Potes JC, Reis J, Capela e Silva F, Relvas C, Cabrita AS, Simões JA. The sheep as an animal model in orthopaedic research. 2008. Available at: http://hdl.handle.net/10174/1548.
[9] Wilke H-J, Kettler A, Wenger KH, Claes LE. Anatomy of the sheep spine and its comparison to the human spine. Anat Rec 1997;247:542–55.

[10] Verron E, Pissonnier ML, Lesoeur J, Schnitzler V, Fellah BH, Pascal-Moussellard H, et al. Vertebroplasty using bisphosphonate-loaded calcium phosphate cement in a standardized vertebral body bone defect in an osteoporotic sheep model. Acta Biomater 2014;10:4887–95.

[11] Zhu XS, Zhang ZM, Mao HQ, Geng DC, Zou J, Wang GL, et al. A novel sheep vertebral bone defect model for injectable bioactive vertebral augmentation materials. J Mater Sci Mater Med 2011;22:159–64.

[12] Yang HL, Zhu XS, Chen L, Chen CM, Mangham DC, Coulton LA, et al. Bone healing response to a synthetic calcium sulfate/β-tricalcium phosphate graft material in a sheep vertebral body defect model. J Biomed Mater Res B Appl Biomater 2012;100:1911–21.

[13] Galovich LA, Perez-Higueras A, Altonaga JR, Gonzalo Orden JM, Marinoso Barba ML, Carrascal Morillo MT. Biomechanical, histological and histomorphometric analyses of calcium phosphate cement compared to PMMA for vertebral augmentation in a validated animal model. Eur Spine J 2011;20:376–82.

[14] Boger A, Benneker LM, Krebs J, Boner V, Heini PF, Gisep A. The effect of pulsed jet lavage in vertebroplasty on injection forces of PMMA bone cement: an animal study. Eur Spine J 2009;18:1957–62.

[15] Oliveira MT, Lucena S, Potes J, Queiroga MC, Rehman S, Dalgarno K, et al. *Ex vivo* model for percutaneous vertebroplasty. Key Eng Mater 2015;631:408–13.

[16] Vitale-Brovarone C, Pontiroli L, Novajra G, Tcacencu I, Reis J, Manca A. Spine-ghost: a new bioactive cement for vertebroplasty. Key Eng Mater 2015;631:43–7.

[17] EC. Directive 2010/63/EU of the European Parliament and the Council of 22 September on the protection of animals used for scientific purposes. Off J EU L 2010;276:33–79. http://eurlex.europa.eu/LexUriServ.

[18] Decreto-Lei n° 113/2013, de 7 de Agosto. Diário da República, 1.ª série—N.° 151. Ministério da Agricultura, do mar, do ambiente e do ordenamento do território, Lisboa.

[19] Mähler M, Berard M, Feinstein R, Gallagher A, Illgen-Wilcke B, Pritchett-Corning K, et al. FELASA recommendations for the health monitoring of mouse, rat, hamster, guinea pig and rabbit colonies in breeding and experimental units. Lab Anim 2014;48:178–92.

[20] Rashid F, Munk PL, Heran M, Malfair D, Chiu O. SKyphoplasty. Can Assoc Radiol J 2009;60:273–8.

[21] Marcia S, Boi C, Dragani M, Marini S, Marras M, Piras E, et al. Effectiveness of a bone substitute (CERAMENT™) as an alternative to PMMA in percutaneous vertebroplasty: 1-year follow-up on clinical outcome. Eur Spine J 2012;21:112–18.

[22] Vitale-Brovarone C, Bergui M, Onida B, Baino F, Miola M, Ferraris S, et al. Injectable osteoinductive bone cements. EP2569025. 2011.

[23] Roux JP, Wegrzyn J, Boutroy S, Bouxsein ML, Hans D, Chapurlat R. The predictive value of trabecular bone score (TBS) on whole lumbar vertebrae mechanics: an ex vivo study. Osteoporos Int 2013;24:2455–60.

[24] Aebli N, Krebs J, Davis G, Walton M, Williams MJA, Theis JC. Fat embolism and acute hypotension during vertebroplasty: an experimental study in sheep. Spine 2002;27:460–6.

[25] Benneker LM, Krebs J, Boner V, Boger A, Hoerstrup S, Heini PF, et al. Cardiovascular changes after PMMA vertebroplasty in sheep: the effect of bone marrow removal using pulsed jet-lavage. Eur Spine J 2010;19:1913–20.

Chapter 6

Novel mesoporous bioactive glass/calcium sulphate cement for percutaneous vertebroplasty and kyphoplasty: in vivo study

Submitted in December 2016

Novel mesoporous bioactive glass/calcium sulphate cement for percutaneous vertebroplasty and kyphoplasty: *in vivo* study

M.T. Oliveira[1,*], J. Potes[1], M.C. Queiroga[1], J.L. Castro[2], A.F. Pereira[2], J.C. Fragoso[3], A. Manca[4], C. Vitale-Brovarone[5], J.C. Reis[6].

[1]DMV, ECT, ICAAM, Universidade de Évora, Apartado 94, 7002-554, Évora, Portugal.

[2]DZ, ECT, ICAAM, Universidade de Évora, Portugal.

[3]ZEA – Sociedade Agrícola, Lda., Évora, Portugal.

[4]Interventional Radiology Team, Radiology Unit, Candiolo Cancer Institute– FPO, IRCCS Candiolo, Torino, Italy.

[5]Politecnico di Torino, Torino, Italy; COREP, Torino, Italy.

[6]DMV, ECT, Universidade de Évora, Portugal; CICECO, Universidade de Aveiro, Portugal.

*corresponding author: teresoliveira@uevora.pt, tel: +351266760859, fax: +351266760944

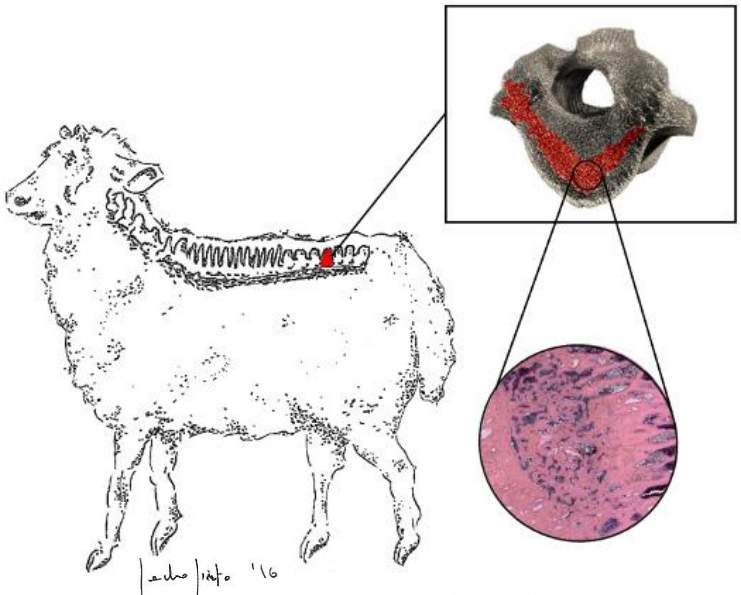

Testing a new bioactive composite – Spine-Ghost – for percutaneous vertebroplasty/ kyphoplasty. From the sheep to the slide.

Abstract

In the field of tissue engineering, synthetic cements are in expansion as valid alternatives to existing therapeutic options. To develop an innovative, resorbable and injectable composite cement – Spine-Ghost –, type III α-calcium sulphate hemihydrate was used as the bioresorbable matrix, while spray-dried mesoporous bioactive particles were added for high bioactivity, and a zirconia containing glass-ceramic was added to increase radiopacity. An injectable paste was obtained by adding water. To test the suitability of the injectable cement for percutaneous vertebroplasty, a sheep study was conducted, following a previously developed animal model. Two groups of mature Merino sheep were defined (n=8): A) the control group injected with a known commercial calcium sulphate-based biphasic cement; B) the experimental group injected with the novel cement. Bone defects were manually drilled percutaneously in the L4 vertebral bodies. Micro-CT overall mean tissue volume, an indicator of the injected defect volume, was 1.217±0.235 mL. All sheep survived and completed the 6-month implantation period. After sacrifice, the samples were assessed by micro-CT and by histological, histomorphometric, and immunohistological studies. There were no signs of infection or inflammation. Importantly, there was cement resorption and new bone formation. Spine-Ghost proved to be an adequate material for percutaneous vertebroplasty.

Keywords: Spine-Ghost; resorbable cement; percutaneous vertebroplasty; kyphoplasty; *in vivo* study; ovine.

1. Introduction

Vertebral compression fractures (VCFs) are the most frequent osteoporosis-related event in the elderly, especially in post-menopausal women [1-3]. Other causes, particularly in younger patients, include trauma [4] and cancer [5]. With the existing tendency of population ageing, the prevalence of VCFs will continue increasing [6]. VCFs not healing with conservative management and not demanding open surgery for spine instability, are currently treated through minimally invasive surgical techniques performed with radiological guidance: percutaneous vertebroplasty (PVP) and percutaneous kyphoplasty (PKP). Both techniques aim to augment and/or stabilize the defective vertebral body by percutaneously injecting a material that will interdigitate with the cancellous bone or fill the bone defect thus achieving immediate and lasting pain relief with functional recovery [7-9].

In the field of tissue engineering, synthetic materials composites are in expansion as valid bone graft alternatives. Optimal bone cement for vertebroplasty would show a reduced Young's modulus - around 120 MPa [10] –, comparable to that of the cancellous bone; a reduced polymerization temperature – approximately 40 ºC at most [10]; and an increased bioactivity and resorbability. Additionally, it should be injectable to enable percutaneous vertebral augmentation procedures; easy to handle and sterilize; and present high radiopacity to allow fluoroscopic guidance [11].

Presently, most of the cements used in percutaneous bone interventions are based on a polymeric matrix – polymethylmethacrylate (PMMA) –, provide immediate effect and safety and have been thoroughly used and investigated over the years. However, they can present some complications: 1) secondary fractures of the contiguous vertebral bodies due to the cement high elastic modulus [12]; 2) high polymerization temperatures: around 70 ºC [13], but can rise over 90 °C, as assessed by *in vivo* measurements [14], which can cause inflammation/ necrosis of the neighboring tissues; 3) excessive setting times; 4) low bioactivity and bioinertia [7]; 5) absence of resorbability, inhibiting the formation of new healthy tissue [15]; 6) pulmonary embolism and cardiorespiratory arrest due to PMMA leakage [16,17].

Calcium sulphate-based injectable ceramic cements, like Cerament™ (Bone Support, Lund, Sweden) are effective, well documented bone substitutes [18-20] since they are biocompatible, resorbable, and osteoconductive, displaying mechanical properties similar to those of cancellous bone, with reduced Young's Modulus [18], and a low risk of infection or donor site morbidity. Some disadvantages include their limited shear and compressive strength.

In order to overcome these limitations, ceramic biomaterials are most of the times combined with other composites [21].

To go beyond the state of art, a new bioactive injectable cement for percutaneous vertebroplasty was developed – Spine-Ghost – based on Vitale-Brovarone's patent (EP2569025), as described elsewhere [22]. It is composed of type III α-calcium sulphate hemihydrate combined with mesoporous particles of a bioactive glass (MBG), and a radiopaque glass-ceramic phase. MBG was used for its high bioactivity and ability to release silicon and calcium ions, which had been proven to be osteoinductive [23]. Arcos et al. reported the production of spherical mesoporous particles of bioactive glass by spray-drying [24] – to overcome the time-consuming sol-gel synthesis combined with an evaporation-induced self-assembly (EISA) process [25] –, and they were used as the dispersed phase in the calcium sulphate matrix to impart high bioactivity to the material. This allows a faster and more repeatable process [26]. An additional dispersed phase was added, consisting of a glass-ceramic bioactive phase containing zirconia (ZrO_2) to enhance the injectable cement's radiopacity.

Sheep are considered an appropriate large animal model for biomedical research, including orthopedic research [27], because of their anatomical similarities to human bones [28]. To date, most studies wherein a vertebral bone defect model was presented were executed using "open surgery" techniques [29,30]. Also, only a small number of percutaneous vertebroplasty preclinical studies have been performed in large animals, and those have faced several drawbacks, including cement leakage into the vertebral foramen [31], incomplete defect filling and lack of information on postoperative evolution [32,33]. To overcome these difficulties, we've previously developed a modified parapedicular approach model, wherein the overall mean tissue volume, an indicator of the injected defect volume, was 1.217±0.235 mL, maintaining a 100% survival rate [34].

In the present work, we report the *in vivo* results of Spine-Ghost implantation in a sheep vertebral defect model. The performance was compared to a commercial biphasic cement – Cerament™|Spine Support. Cerament™'s application for VCFs has been well documented [18-20]. After the 6 month-experimental period sheep were euthanized and the vertebrae (L4) were collected. Samples were assessed by micro-CT, histological, histomorphometric, and immunohistological methods, for osteointegration and cement resorbability evaluation purposes. After the implantation period, cement resorption with concomitant integration into the newly formed bone was observed, both in control and experimental groups.

Spine-Ghost seems a very promising material for vertebroplasty applications, showing an identical – if not superior – biological response to the one elicited by the commercial available control Cerament™.

2. Material and methods

2.1 Cement development and characterization

Spine-Ghost is a new bioactive injectable cement for percutaneous vertebroplasty that was developed based on Vitale-Brovarone's patent (EP2569025). As described elsewhere [22], a composite cement was obtained mixing four different phases. In particular, commercial type III dental α-calcium sulphate hemihydrate (CSH) was used as matrix that was enriched by spray-dried mesoporous bioactive particles (W-SC). CSH was used due to its well-known biocompatibility and ability to set upon mixing with water.

W-SC were produced through the water-based synthesis described in a previously submitted paper [35] and were used for their known high bioactivity and ability to release silicon and calcium ions, which have been proven to be osteoinductive [23]. A glass-ceramic radiopaque phase containing ZrO_2 (SiO_2/CaO/Na_2O/ZrO_2, 57/30/6/7 %mol) coded as SCNZgc was dispersed as a third phase to increase the mechanical properties of the cement and to impart a satisfactory radiopacity, in order to allow the radiological control of the cement injection. The different powders were mixed in the following proportion α-CSH/SCNZgc/W-SC: 70/20/10 %wt. and were then combined with water inside a syringe using an optimized liquid to powder ratio (L/P=0.4 ml/g), in order to obtain an injectable paste [22].

Prior to the *in vivo* study, the cement went through bioactivity and resorbability, *ex vivo* injection, mechanical and *in vitro* testing [22,36]. All the tests were carried out using a commercial reference as control prepared according to the manufacturer's instructions (Cerament™).

2.2 *In vivo* large animal model

Animal handling and surgical procedures were implemented following the European Community guidelines for the care and use of laboratory animals (Directive 2010/63/UE) and with the required legal consent from the national competent authorities [37,38]. Cerament™ and Spine-Ghost were implanted in a vertebral body defect (L4), according to the developed model [34]. 16 skeletally mature sheep, with an average body weight of 56.8±5.3 kg, were

randomly allocated into two groups: control group A, injected with Cerament™; and experimental group B, injected with Spine-Ghost. All underwent PVP. Prior to surgery the animals fasted for 24 hours. Following anesthesia pre-medication with atropine (0.05 mg/kg subcutaneous), xylazine (0.1 mg/kg intramuscular), butorphanol (0.01 mg/kg intravenous) and carprofen (2 mg/kg subcutaneous); induction was achieved with thiopental sodium 5% (5-10 mg/kg intravenous). After induction, the sheep were positioned and fixed on a radiolucent table in ventral decubitus with the hind limbs retracted caudally. Anesthesia maintenance was assured with isoflurane 1-2% under spontaneous ventilation. The surgical field was clipped and aseptically prepared. L4 was identified under tactile and fluoroscopic guidance (Digital C-Arm ZEN 2090 Pro, Genoray, Co., Ltd., Korea). A V-shaped defect was bilaterally manually drilled in the cranial hemivertebrae, in a modified parapedicular approach, as advocated in the formerly developed model [34]. Cerament™ and Spine-Ghost were prepared at room temperature, according to the manufacturers' instructions and were injected under fluoroscopic guidance into the defect, using a bone-filler system device (Medtronic Spine LLC, Portugal). The mean time of injection was one minute and the injected volume was approximately 1.2 mL. Both injected materials were allowed to set in the anaesthetized sheep for 2 hours. Amoxicillin and clavulanate acid (15 mg/kg, once a day, subcutaneous), carprofen (2 mg/kg, once a day, subcutaneous) and butorphanol (0.15 mg/kg, twice a day, intramuscular), were administered for 7 days after surgery. A fluorochrome (calcein green, 15 mg/kg) was also subcutaneously injected fifteen days after surgery. Sheep were released into the pasture the whole 6-month implantation period. Another fluorochrome (alizarin complexone 25 mg/kg) was subcutaneously injected two weeks before sacrifice. After the 6-months implantation period, the animals were sedated with xylazine and sacrificed by pentobarbiturate intravenous injection and the vertebrae explanted. Biological response and material integration were assessed firstly by micro-CT, and then by histological studies, as described below.

2.3. Assessment of tissue regeneration

a. Macroscopic inspection

All vertebrae were identified under tactile and fluoroscopic guidance. Vertebrae were assessed in situ for signs of soft tissue inflammation, of new bone formation and cement presence. Then the 16 vertebral segments (L4) were collected from the cadavers of the two groups. Soft tissue was extracted, and using a bone saw, the spinous and transverse processes were removed to fit the vertebrae into the micro-computed tomography (micro-CT) chamber

while preserving the vertebral arch. Vertebrae were stored immersed in 4% formaldehyde in phosphate buffered saline for two weeks, for fixation. After micro-CT scanning, vertebrae were divided in two parts, following their sagittal plane. Each sample was trimmed in order to exclude the vertebral canal and arch. Vertebral bodies' defects were evaluated macroscopically regarding cement integration/resorption, new bone formation and cortical disruptions.

b. Micro-CT assessment

All vertebrae underwent micro-CT scanning (Skyscan 1174, Kontich, Belgium) while still intact. The vertebrae were removed from 4% formaldehyde, rinsed with distilled water and coated with Parafilm M® (Sigma Aldrich, Missouri, USA), to avoid sample dehydration. Subsequently, vertebrae were posed in a rotation stage fixed by commercial play-dough, with their longitudinal axis matching the system's rotational axis. Scans were performed with 50-kVp, 800-µA, and a 1-mm aluminum filter. The pixel size was 62.08, exposure time 2,200 ms, rotation step 0.8°, full rotation over 360°, with 2 average frames per image. Each vertebra went through one scan, over approximately 59 minutes, assuring the imaging of the cranial hemivertebrae containing the bone defects, comprising 450 cross-sections. The cross-section images were reconstructed using N-Recon software (Skyscan, Kontich, Belgium). In the analyzer software (CTAn, Skyscan, Kontich, Belgium) two volumes of interest (VOIs) were defined for each vertebra: 1) VOI Defect, constituted by a set of regions of interest (ROIs), which outlined the defect (and residual cement), every other ten sections along the totality of the defect, and 2) VOI CHv, an elliptical VOI containing only intact trabecular bone, identical for all vertebrae, with 15 mm of length and 7 mm of height (100 cross-sections), defined within the caudal hemivertebrae. Next, the following 3D structural parameters were evaluated: relative bone volume (BV/TV), specific surface (BS/BV), trabecular thickness (Tb.Th), trabecular separation (Tb.Sp), trabecular number (Tb.N), and tissue volume (TV); this last one in an attempt to consistently characterize the volume of the injected defect. A uniform threshold method was applied.

c. Histology

i. Undecalcified histology

For qualitative evaluation of the slides and posterior histomorphometry, sections were included in resin. Initially the samples were fixed in 70% alcohol, followed by gradual dehydration with alcohol in increasing concentrations and defatting with xylol. Subsequently they were embedded in Technovit 9100 New® (Heraeus-Kulzer, Wehrheim, Germany), according to the manufacturer's instructions. From each resulting block, a minimum of three 70-80 µm slices was attained by the means of a Leica SP1600 Saw Microtome (Germany), at very low speeds. Sections were cut in such a way that the defective vertebral body with cement and adjoining bone were included. Samples were then processed for routine staining with Giemsa-Eosin and mounted for fluorescence microscopy.

For the slides observation and imaging, slides were digitized by means of the Nanozoomer SQ (Hamamatsu Photonics, Kyoto, Japan). For fluorescence microscopy, unstained resin sections of each sample were mounted in aqueous mounting medium; observation and pictures were done using an optic fluorescence microscope (Olympus BX41) equipped with a WB Fluorescence cube (Olympus U-LH100HG).

For histomorphometric studies, measurements were made with resource to Giemsa Eosin staining and fluorochromes labelling. NDP.2 View software (Nanozoomer Digital Pathology, Hamamatsu Photonics, Japan) was used. Two circular areas of interest (AOI), with the same diameter – 20 mm^2 –, were defined to evaluate the bone-cement interface: A) within the defect to evaluate new bone formation; and B) outside the bone defect to evaluate mature trabecular bone (Figure 1).

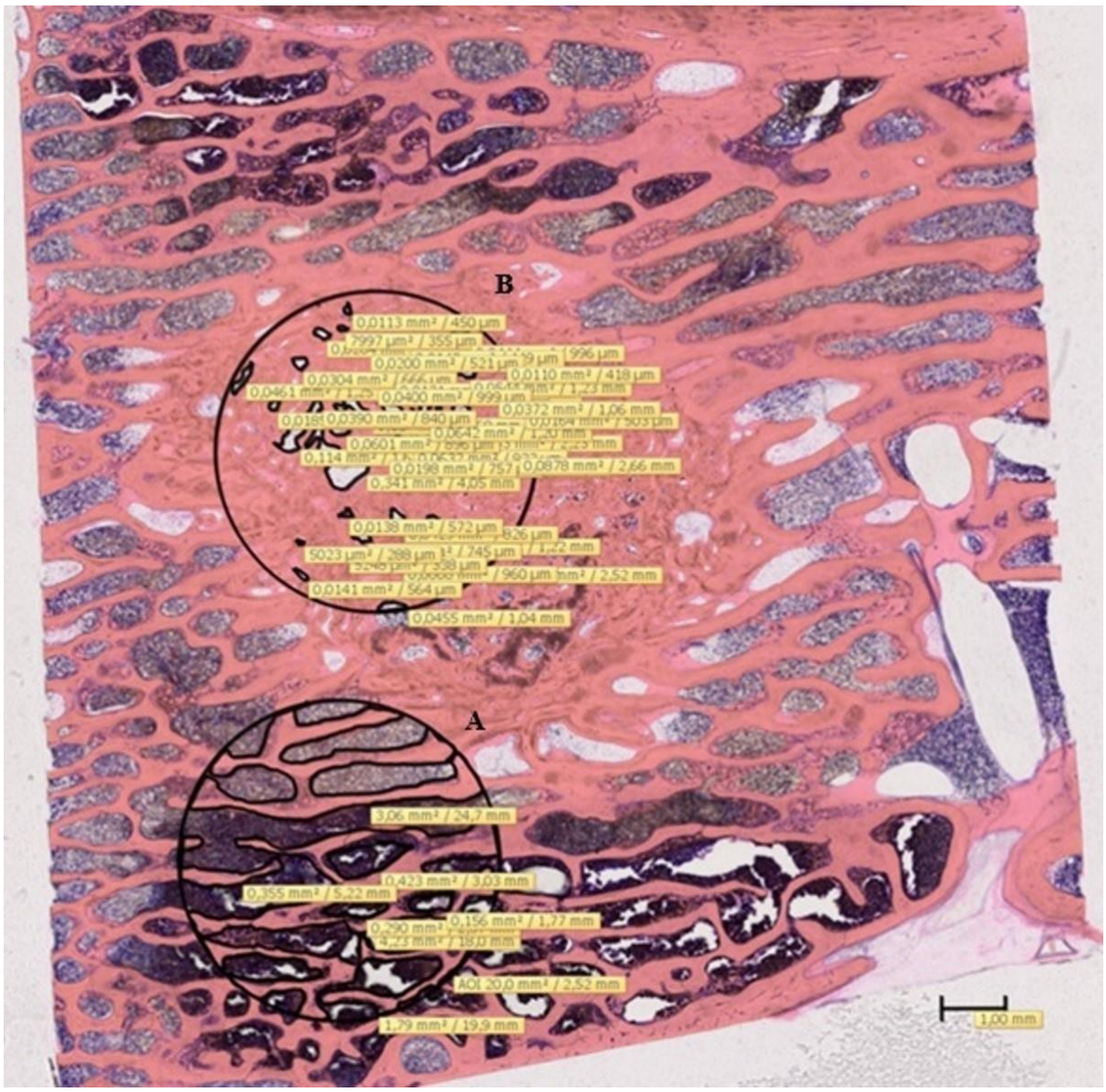

Figure 1. Histomorphometric study. Giemsa staining, 0.55x magnification; the circles are limiting the two areas of interest: A) newly formed trabecular bone within the defect; B) mature trabecular bone outside the defect. Scale bar on image.

The following bone parameters were assessed for each region of interest, following the guidelines of the American Society for Bone and Mineral Research (ASBMR): bone area (B.Ar, mm^2), relative bone volume (BV/TV, %) and trabecular thickness (Tb.Th, µm); mineral apposition rate (MAR) was also calculated for both groups through the fluorochromes labelling.

ii. Decalcified histology

For demineralization, samples were immersed in a formic acid 5% solution and subsequently followed routine processing and paraffin inclusion. Each paraffin block was cut into 4-5 µm slices for posterior histochemistry and immunohistochemistry processing.

For histochemistry sections were stained with Masson and Mallory Trichrome using Bio-Optica kits (Bio-Optica Milano, Milan, Italy), followed by dehydration and mounting, for better imaging of connective tissue. Again, slides were digitized using Nanozoomer SQ for ulterior observation and imaging.

For immunohistochemistry, the samples were checked for the expression of osteogenic differentiation markers (osteopontin, osteocalcin) and osteoclast differentiation markers (TRAP). An enzymatic antigen retrieval protocol was developed and applied. Incubation with a Trypsin-EDTA 0.5% solution at 37 ºC, followed by RT cooling of sections was performed. The positive controls consisted in slides containing bone, known to show positive reaction with osteocalcin and osteopontin, and lung, known to show positive reaction with TRAP. The negative control was prepared using thymus, lymph node and cerebellum. Additional controls were prepared with sample bone sections and the primary antibody omitted.

2.4 Statistical Analysis

Results from the micro-CT analysis and histomorphometry were analyzed using SPSS 22 for Windows (SPSS Inc., Chicago, IL). One way ANOVA analysis was performed, with means compared by the Tukey test (0.05 level), whenever assumptions were respected. Normality was verified using the Shapiro-Wilk test ($p < 0.05$), and homogeneity of variance was verified with resource to Levene's test for equality of variances. For variables that did not have a normal distribution, Kruskal-Wallis ANOVA was applied.

3. Results

3.1 Cement development and characterization

Prior to the *in vivo* study, the cement went through bioactivity, resorbability, *ex vivo* injection, mechanical, and *in vitro* testing, all of which with favorable results [22,36], qualifying it for further *in vivo* studies.

Injectability and radiopacity have been positively demonstrated in explanted vertebrae, using a 13-gauge vertebroplasty needle for injection. As can be seen in Figure 2A the cement could be easily injected without interruption and it showed a satisfactory radiopacity, assessed inside the interventional radiology operating room of the Candiolo Cancer Institute (Figure 2B). In comparison to the commercial reference, Spine-Ghost cement showed a high bioactivity

already after 8 hours of soaking in simulated body fluid (SBF), with the appearance of diffraction peaks identified with hydroxyapatite. In Figure 2C many cauliflower hydroxyapatite crystals can be observed after 7 days of soaking in SBF. Spine-Ghost showed mechanical properties comparable to the one of the healthy vertebral cancellous bone [22] and significantly higher (14 MPa-18MPa in wet and dry conditions respectively) than the commercial reference Cerament™. Spine-Ghost was able to harden completely in less than 1 hour in good agreement with the clinically used commercial reference and thus suitable for the vertebroplasty procedure.

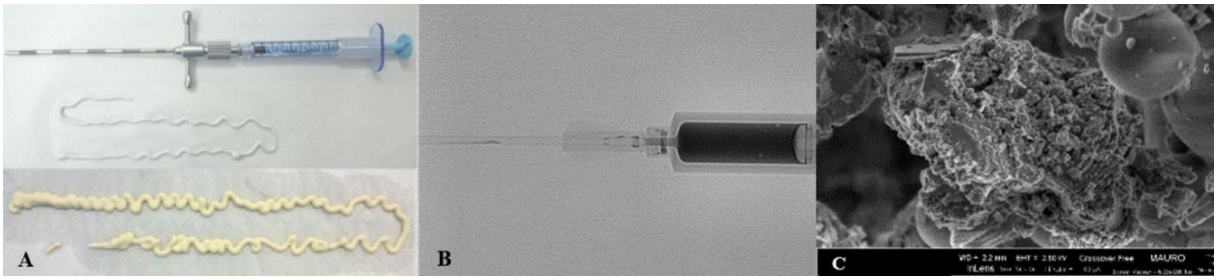

Figure 2. Cement characterization. A) Syringe after the injection of Spine-Ghost, coupled with a 13-gauge vertebroplasty needle and Spine-Ghost cement extruded on a paper sheet to prove its injectability; B) Spine-Ghost radiopacity assessment C) FE-SEM micrograph of precipitated HAp on Spine-Ghost after 7 days of immersion in SBF and relative EDS spectrum.

3.2 *In vivo* findings

All sheep remained anesthetized for 2 hours after injection and recovered well from surgery. Two sheep from group A experienced an abrupt drop in the arterial blood pressure during cement injections. No cardiovascular changes were observed in the other animals. In the second sheep intervened, from group A, rupture of the ventral cortical bone of the vertebral body was observed under the fluoroscope, with a minor leakage of cement to the ventral surface of the vertebral body. One sheep from group A developed proprioceptive deficits of the hind limbs, possibly due to cement leakage around the defect entry point, which affected the spinal nerve roots; nevertheless, this sheep remained ambulatory and had fully recovered after approximately 2 months. In two sheep from group A, the connection between the two bilateral defects was not wide enough so the cement was injected bilaterally to avoid leakage. *In vivo* procedures were successful with a survival rate of 100%, and all animals completed the 6-month implantation period. At the time of sacrifice all the animals presented a body condition score of 4/5, were alert and active and presented normal species behavior. All animals gained weight during the implantation period (an average increment of 6.4 kg with an initial body weight of 56.84±5.28 kg).

3.3 Assessment of tissue regeneration

a. Macroscopic

No sheep showed obvious signs of inflammation of the surrounding soft tissues and, under fluoroscopic guidance, radiopacity differences between the intervened vertebra and the adjoining vertebrae were not noteworthy (minimal to null). Explanted vertebrae from both groups had minimal to null signs of the PVP, with no signs of the cements or of the surgical instrumentation entry points, which were in all cases covered by newly formed cortical bone, showing in just a few cases a minor pale to rose discoloration (Figure 3A).

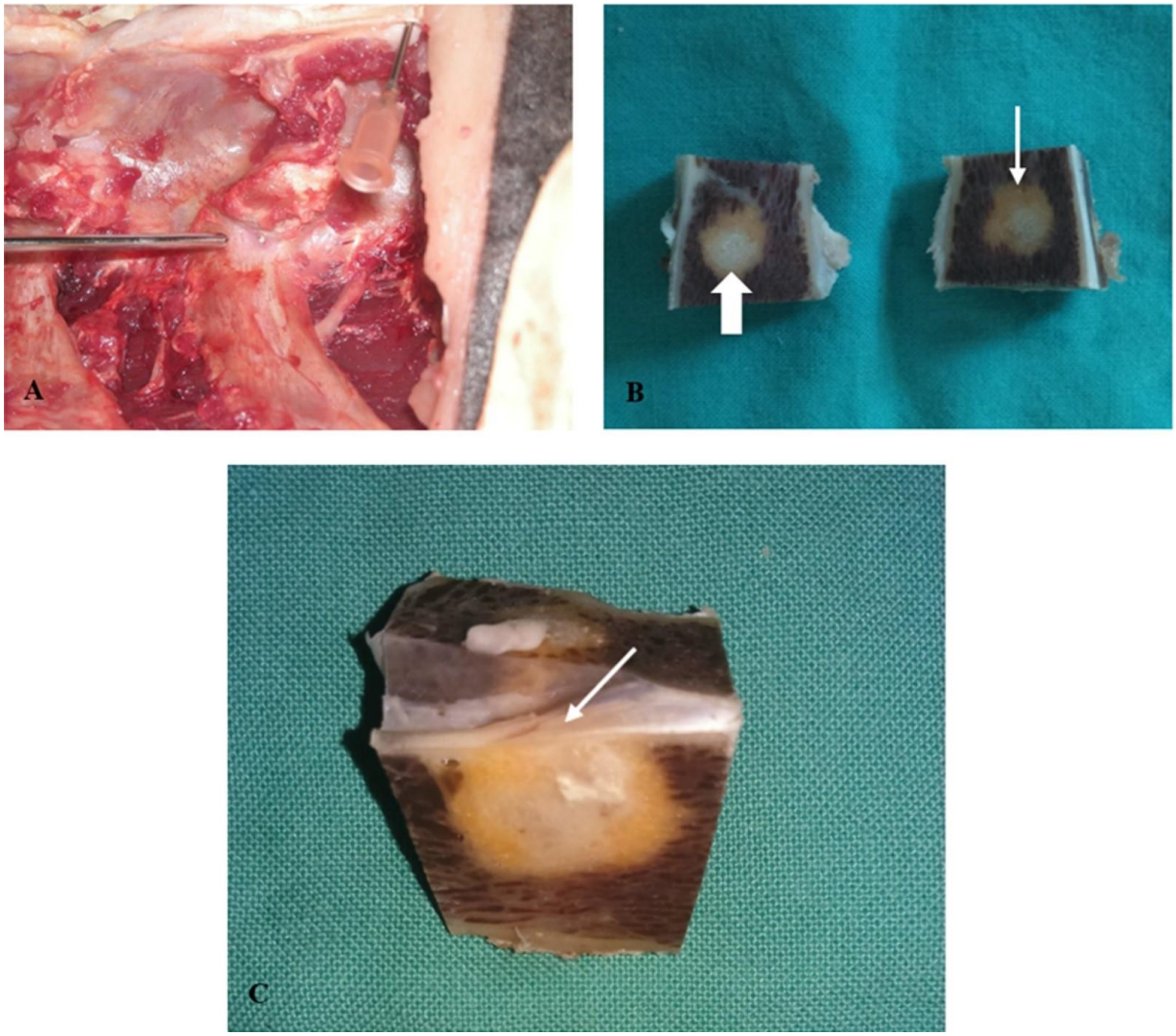

Figure 3. Macroscopic assessment. A) Instrumentation entry point with a pink discoloration pointed by the cannula; B) hemivertebra, after sagittal cut, with cement still evident (large white arrow) and adjoining newly formed bone (small white arrow); C) macroscopic evidence of cortical disruption of the vertebral canal.

After micro-CT scanning, vertebrae were cut along their sagittal plane and again macroscopically inspected. At this point, one vertebra from group A, belonging to the first sheep intervened, had to be discarded due to technical issues. Consequently, the rest of the study

and corresponding results are for n=7, when it comes to group A. All vertebrae, from groups A (n=7) and B (n=8), showed evident signs of cement resorption and new bone formation (Figure 3B), with no gaps between the cement and the bone. One vertebra from group A, belonging to the fifth sheep intervened, showed macroscopic signs of cortical disruption (Figure 3C). There was also evident in all samples an orange coloration over the newly formed bone, due to alizarin orange administration.

b. Micro-CT assessment

After the first macroscopic evaluation, micro-CT scanning of the intact vertebrae was performed. It presents the major advantage of enabling the sample evaluation without destroying it; however, in this study, it must be taken into consideration that the residual presence of the cements could not be separated from the new trabecular bone, due to the similar radiopacities in between them. Therefore, all further measurements and rendered models were attained and analyzed taking this fact into consideration.

The qualitative analysis of the reconstructed cross-section images, using CTAn (Skyscan, Kontich, Belgium), allowed the *in situ* comparison between the two injected cements resorption and new bone formation. In three of the samples (two controls and one Spine-Ghost augmented) the defect was hard to visualize clearly. Moreover, the evaluation of cases of disruption of the vertebral canal, the vertebral cortex, the nutritional foramina, and the interconnection of the defects was also enabled, as presented in the following graphic (Figure 4).

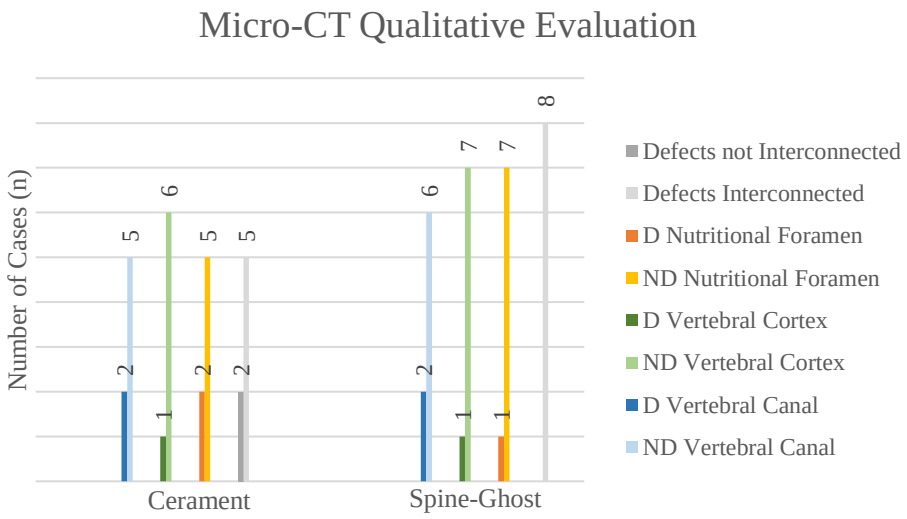

Figure 4. Clustered stacked chart presenting micro-CT qualitative evaluation. Data obtained from the injected vertebrae: group A (n=7) – Cerament™ –, and group B (n=8) – Spine-Ghost. Legend: ND – not disrupted; D – disrupted.

Still in CTAn (Skyscan, Kontich, Belgium) 3D structural parameters were calculated for the defect and the caudal hemivertebrae (CHv) areas, as shown in Table 1. Data are presented as mean ± standard deviation.

Table 1. Descriptive analysis of the 3D structural parameters

	Biomaterial	**Defect** [Mean±Std. Deviation]	**CHv** [Mean±Std. Deviation]
BV/TV %	Cerament	68.43±5.80	42.49±6.69
	Spine Ghost	79.00±10.24	40.20±9.97
BS/BVmm^2/mm^3	Cerament	9.54±2.03	14.36±2.20
	Spine Ghost	6.58±2.90	13.87±3.00
Tb.Th mm	Cerament	0.41±0.11	0.25±0.03
	Spine Ghost	0.58±0.21	0.25±0.04
Tb.Sp mm	Cerament	0.21±0.02	0.33±0.05
	Spine Ghost	0.24±0.17	0.39±0.04
Tb.N 1/mm	Cerament	1.77±0.35	1.72±0.15
	Spine Ghost	1.48±0,39	1.59±0.16
TV mm^3	Cerament	1299.51±291.21	510.72±0.00
	Spine Ghost	1146.36±158.92	510.72±0.00

Table 1. Descriptive analysis of the 3D structural parameters. Data acquihired from the injected vertebrae from group A (n=7) – Cerament™ –, and group B (n=8) – Spine-Ghost. Legend: BV/TV - relative bone volume; BS/BV – specific surface; Tb.Th - trabecular thickness; Tb.Sp - trabecular separation; Tb.N - trabecular number; and TV – tissue volume.

Mean trabecular thickness ($Tb.Th_{Defect}$) and mean trabecular separation ($Tb.Sp_{Defect}$) of the two groups, regarding the defect area, present no statistically significant differences; Spine-Ghost values are slightly superior.

Likewise, there is no statistically significant difference in the trabecular number ($Tb.N_{Defect}$) of the two cements, though Cerament™'s mean value is superior. On the contrary, the mean relative bone volume (BV/TV_{Defect}) was significantly higher in Spine-Ghost augmented vertebrae, when compared to Cerament™, and no significant differences were found in the caudal hemivertebra intact bone that could justify the higher bone volume ration found in the Spine-Ghost group. BS/BV or specific surface was significantly lower in Spine-Ghost samples when comparing to control. This suggests a thicker structure and might be related to a lower bone turn-over rate because bone resorption and formation occurs on bone surfaces. Moreover, when comparing the mean values of all structural parameters between the Defect and the CHv areas, mean trabecular number (Tb. N) is the only one that does not present

a statistically significant difference, indicating a normal tissue evolution, with an emergent open tissue structure.

3D models were also assembled in the rendering software (CTVol, Skyscan, Kontich, Belgium), enabling the visualization of the injected defects and the comparison between the two cements. Cement resorption was observed in both groups, with subsequent new bone formation filling the defects, which presents a porosity slightly closer than that of the normal trabecular bone observed in the caudal hemivertebrae (Figure 5). These images are in accordance to the abovementioned assumptions made based on the 3D structural parameters.

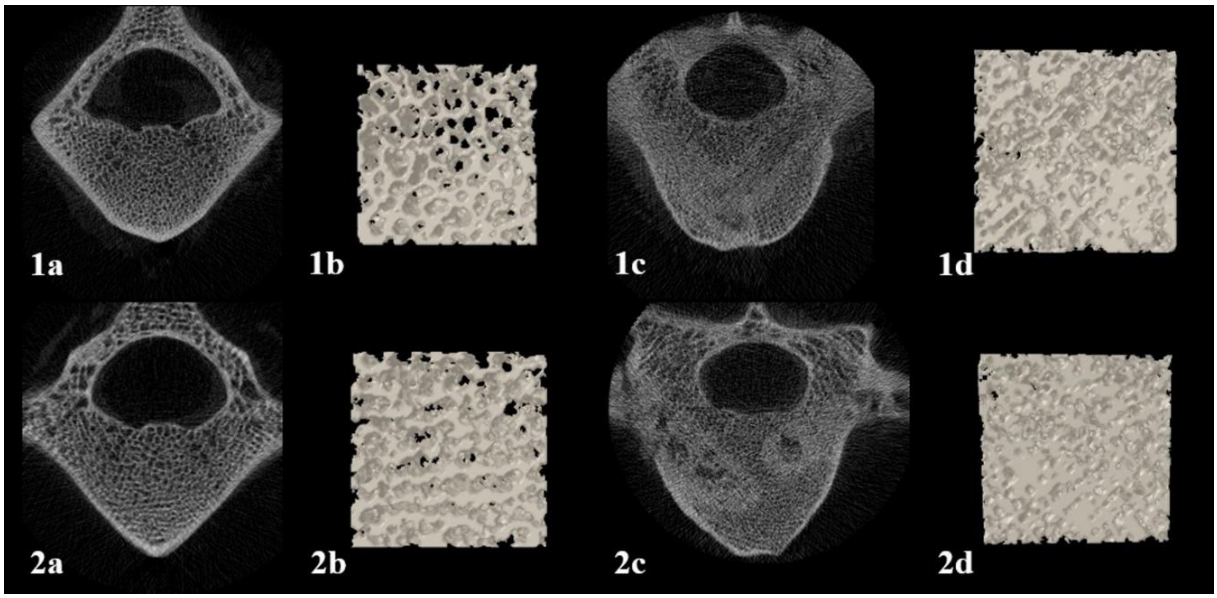

Figure 5. Micro-CT post-mortem assessment. Here it can be seen the reconstructed cross-section images and the 3D rendered models of 2 injected vertebrae – one from each group –, explanted from the sheep closest to the mean, when it comes to the trabecular bone mineral densities of the intact caudal hemivertebrae (BMD_{CHv}): 1) vertebra injected with Spine-Ghost, with a BMD_{CHv} of 0.45 gcm^{-3}; 2) vertebra injected with Cerament™, with a BMD_{CHv} of 0.50 gcm^{-3}; a) cross-section image of CHv; b) 3D rendered image of 30 cross-sections of VOI_{CHv}; c) cross-section image of the defect; d) 3D rendered image of 30 cross-sections of VOI_{Defect}.

c. Histology

i. Undecalcified histology

As described in the methods section, undecalcified sections were stained with Giemsa Eosin. Mature bone is stained in a darker shade of red/pink, whilst younger bone takes a lighter shade. Soft tissue and nuclei are stained in different shades of blue.

Qualitative evaluation of the slides showed new bone formation within the area of the defect for both groups in most of the vertebrae (13 out of 15); the pattern of long trabeculae, mostly parallel to the long axis of the vertebrae, was interrupted by a denser net of highly

interconnected trabeculae, in both groups (Figure 6A and B). In all sections bone was directly in contact with residual cements and no fibrous tissue or inflammatory reactions were observed. Also, the newly formed bone in the defect areas was mostly mature bone, with some areas of lighter pink stain where bone was more recently mineralized (Figure 6A). In the Spine-Ghost sections an affinity of Giemsa to the biomaterial was observed (Figure 6B).

In two samples from Cerament™ group and one from Spine-Ghost there were relatively large areas of defect yet to be occupied by bone (Figure 6C and 6D). The unoccupied area was larger in the Spine-Ghost single sample where this occurred (Figure 6D), whilst empty space areas were observed in three out of seven samples of the Cerament™ group (Figure 6C). In none of these sections a fibrous capsule was observed neither was inflammatory reaction.

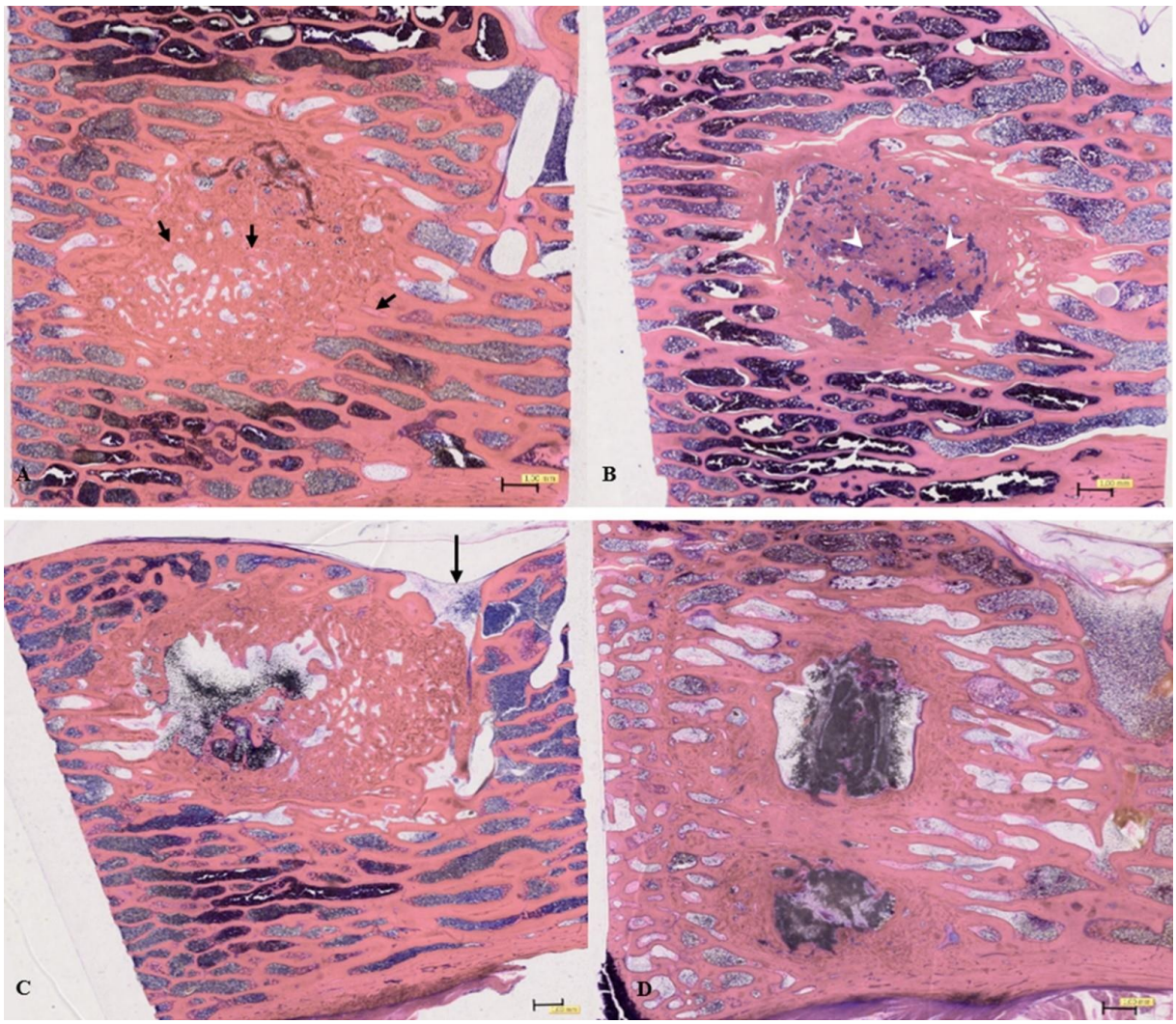

Figure 6. Undecalcified Technovitt 9100 sections of two vertebrae. A) Cerament™ augmented vertebra section (magnification 0.55x) with areas of lighter pink stain where bone was more recently mineralized (black arrows); B) Spine-Ghost augmented vertebra section (magnification 0.54x) showing the affinity of Giemsa to the biomaterial, which stains in shades of blue (white arrowheads). Both defect areas are fulfilled with an intricate network of trabeculae, with multiple directions, surrounding and penetrating the remains of the cements. In contrast, is evidenced the trabecular structure of intact tissue, mostly parallel to the long axis of the vertebrae. C) Cerament™ augmented vertebrae section (magnification 0.55x) where empty areas with some cement present

may be seen; it's also visible the disruption of the cortex of the vertebral canal (black arrow). This section belongs to same vertebra shown above in Figure 3. D) Spine-Ghost augmented vertebra section (magnification 0.55x) where an empty area with some cement present may be seen. This was the only section from this group where the defect cavity wasn't filled with trabeculae. Scale bar on images.

Histomorphometric results showed no statistically significant differences between the two groups regarding trabecular thickness within the defect and in the intact tissue. No statistically significant differences were found in the area occupied by bone and the relative bone volume, although they were higher in the defect Spine-Ghost sections (yet lower in the intact tissue). Results are summarized in Table 2.

Table 2. Descriptive analysis of the Histomorphometric Parameters

	Biomaterial	**Defect** [Mean±Std. Deviation]	**CHv** [Mean±Std. Deviation]
B.Ar mm^2	Cerament	13.51±3.78	8.51±0.87
	Spine Ghost	14.33±2.01	8.01±1.56
BV/TV %	Cerament	67.5	42.5
	Spine Ghost	71.65	40.1
Tb.Th mm	Cerament	0.21±0.09	0.20±0.09
	Spine Ghost	0.20±0.10	0.21±0.10

Table 2. Descriptive analysis of the histomorphometric parameters. Legend: B.Ar – trabecular bone area; BV/TV - relative bone volume; Tb.Th - trabecular thickness.

Since there was no fibrous capsule observed in any of the sections, the affinity index can be considered of 100%.

The data suggest that after 6-month implantation time, Spine-Ghost has a similar behavior when compared to control.

Unstained resin sections of each sample were mounted in aqueous mounting medium and observed using an optic fluorescence microscope. Observation of some of the sections suggests that new bone formation started closer to cement, since the red line – correspondent to the second fluorochrome injected (alizarin complexone) – is located further away from cement remains (Figure 7A), and also calcein green was the first label injected. However, this was not the only pattern of bone deposition observed, since there are areas in which the alizarin complexone appears limiting the trabeculae, and areas of bone remodeling within the trabecular structure are also apparent (Figure 7B). The mineral apposition rate (MAR) was calculated as

being of 1.60±0.27 µm/day in the control group and 1.39±0.54 µm/day in the experimental group.

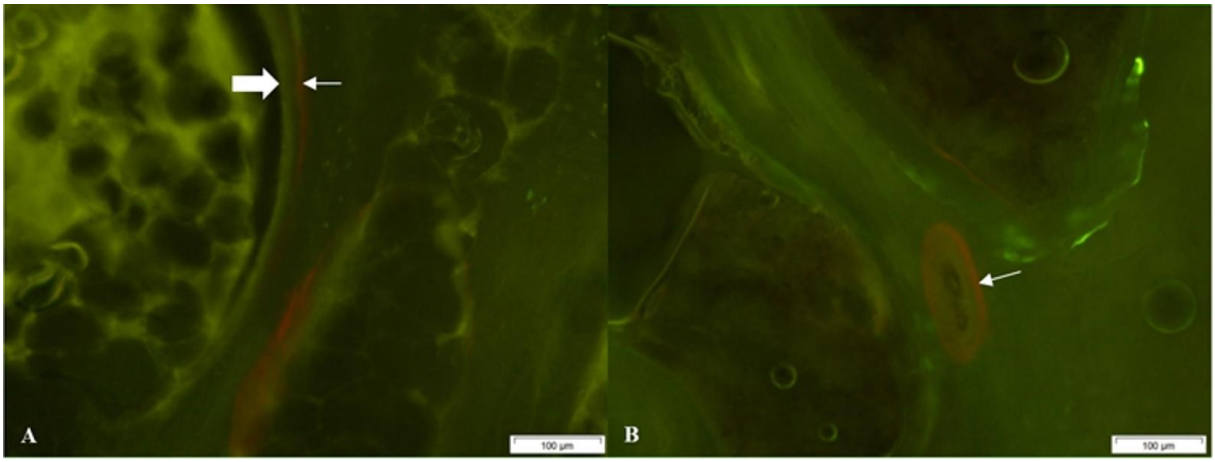

Figure 7. Spine-Ghost augmented vertebra section. A) double fluorochrome labelling obvious, with the calcein green line placed closer to material (large arrow) than alizarin complexone (small arrow); B) double fluorochrome marking showing different patterns of bone apposition and bone remodeling, with alizarin complexone (small arrow) encircling a trabecula. Scale bar on images.

ii. Decalcified histology

Histological observations were made on decalcified samples that followed routine processing and paraffin inclusion, and subsequently were cut into 4-5 µm slices (Figure 8). Mallory and Masson trichromes staining (Bio-Optica, Milan, Italy) allowed a more detailed observation.

In both groups, the vertebral body defects were being filled by an intricate network of trabeculae with neatly organized collagen fibres, as evidenced by Masson's trichrome (Figure 8A and 8C). It was also evident the presence of bone marrow within the trabeculae, and cement residues, which were integrated in the trabeculae themselves (Figure 8B and 8D). In Cerament™ group sections, larger quantities of cement are apparent within the trabeculae when compared to Spine-Ghost sections. Again, no inflammatory reaction, signs of increased bone resorption or fibrous encapsulation of both biomaterials were seen. Most of the sections (4 out of the 7 control samples and 7 out of 8 Spine-Ghost samples) showed complete filling of the defect area with new trabecular bone.

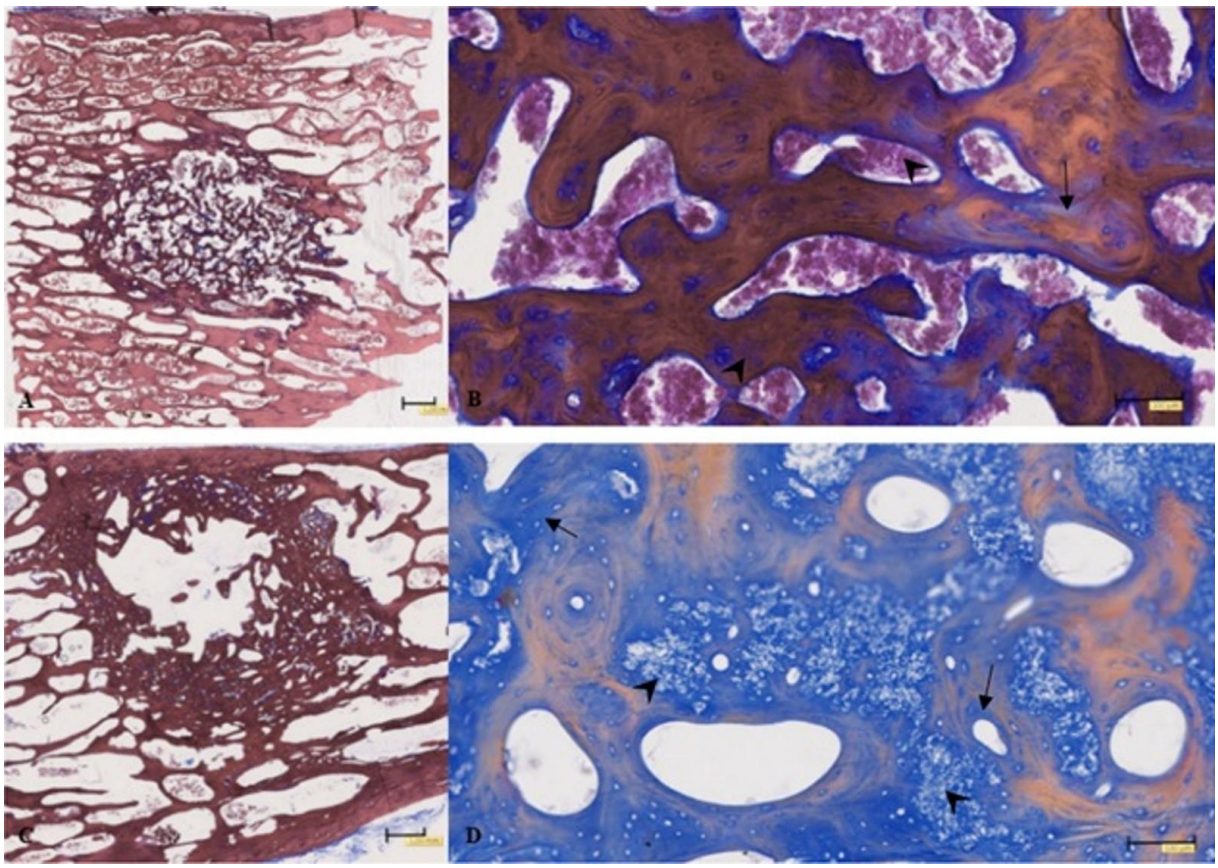

Figure 8. Sections of decalcified histology with Mallory and Masson trichromes staining. A) Spine-Ghost augmented vertebra demineralized section (Masson Trichrome with aniline blue), 0.5x magnification, showing the intricated net of trabecular bone within the defect area; B) and D) Spine-Ghost and Cerament™ augmented vertebrae demineralized sections, respectively (Mallory's trichrome), 10x magnification, showing biomaterial integration into the trabecular bone structure (arrowheads), blue staining of collagen fibres (small arrows); C) Cerament™ augmented vertebra demineralized section (Masson Trichrome with aniline blue), 0.58x magnification. Scale bar on images.

For immunohistochemistry, the samples were checked for the expression of osteogenic differentiation markers (osteopontin, osteocalcin) and osteoclast differentiation markers (TRAP). Antibodies were strongly adsorbed by cement particles, leading to ulterior staining by DAB chromogen (Figure 9A).

Apart from the TRAP adsorbed to the cement, no relevant TRAP detection was detected in Spine-Ghost sections. The same applies to Cerament™ sections. No osteoclasts were observed at the bone/cement interface (Figure 9B).

No relevant differences were found between the two groups.

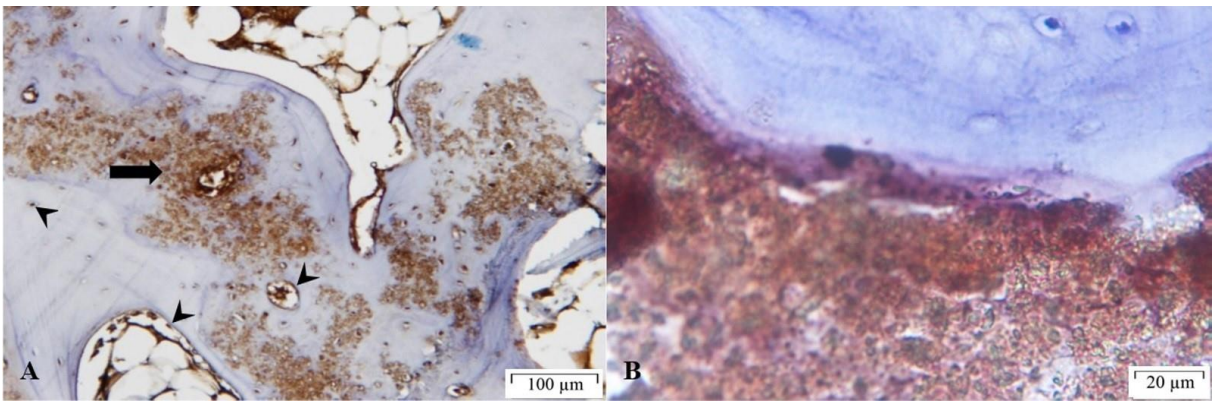

Figure 9. Sections of immunohistochemistry of Spine-Ghost augmented vertebra demineralized sections. A) 100x magnification, anti-osteopontin antibody, showing DAB stained biomaterial (large arrow); osteocytes, bone lining cells and cells within bone marrow are also positive (arrowheads). B) 1000x magnification, anti-TRAP antibody. The image shows an area of cement/bone interface. Scale bar on images.

4. Discussion

In vivo model was considered appropriate for preclinical studies, although requiring surgical expertise. No cement leakage was observed into the vertebral foramina, which is in accordance with the low number of animals presenting post-surgical neurologic deficits, even if mild (1 out of 16), and with the high survival rate (100%) obtained.

There were some limitations in the micro-CT quantitative analysis of new bone formation, namely the presence of residual cements within the defects. Cerament™'s radiopacity is conferred by the presence of iohexol in its constitution. Contrariwise, Spine-Ghost radiopacity is granted by the presence of zirconia oxide in the glass-ceramic phase (SCNZgc). At previous *ex vivo* studies, Cerament™ presented more image artefacts than Spine-Ghost, due to its greater initial radiopacity [36]. However, we have observed that at the end of the implantation this artefact was considerably reduced, not interfering significantly with the sample's image acquisition. On the contrary, due the radiodensity similarities between both of the residual cements and trabecular bone, as a result of the presence of calcium sulphate in their constitutions, we were not able to isolate the trabecular bone from the residual cements, at binary selection. To overcome this technical problem, we chose to use a global threshold method, to ensure that the differences between study groups were due to experimental effects rather than image processing effects, and we also analyzed an equal volume of interest (510.72053 mm^3) of normal trabecular bone for every caudal hemivertebrae (VOI_{CHv}). Regardless, this may be one of the reasons that explain the statistically significant differences in most of the 3D structural parameters when comparing between the defect area and the CHv area. The degree of this influence could not be determined.

Another concern is related to the nominal isotropic resolution of the equipment. The smallest feasible voxel size (i.e., highest scan resolution) was used. However, while it is generally considered that the highest ratio of voxels to object size is 2, this is associated with substantial local errors (fairly small when averaged over an entire structure) [39]. Ideally, the ratio should be higher for accurate morphologic measurements. When considering relatively large structures such as trabeculae in human and ovine bone (100 to 200 μm thick), small differences in voxel size (e.g., 10 to 20 μm) have little effect [39]. 3D micro-CT analysis data are known to be highly correlated with 2D histomorphometric data [40,41] and results from both methods should be interpreted in complement and bearing in mind advantages and limitations of both methods.

Finally, when intending to compare micro-CT 3D structural parameters with 2D histomorphometric measurements, it is recommended that the sample is scanned and posteriorly cut following the same plane. This was not possible in this study because of the vertebrae's geometry, which made them impossible to fix over the micro-CT rotation stage in any other way; on the other hand, two symmetric samples from every vertebrae were compulsory to histology. Therefore, in this particular study we chose to scan the vertebrae in a different plane from the histology cuts, in detriment to the comparison of the attained values in micro-CT *vs.* histomorphometry.

Histomorphometry is less sensitive in detecting global bone mass changes when compared to micro-CT. The limited number of sections observed in manual histomorphometric cannot illustrate as accurately as 3D micro-CT analysis volumetric changes. However, the overall results show a trend in BV/TV and bone occupied area that micro-CT data analysis reveal as significant. Differences in mean trabecular thickness values are harder to explain, but again, we believe there is an overestimation of the micro-CT mean trabecular thickness values in Defect areas due the presence of the residual cements. This also can be confirmed by looking at the 3D rendered models where we can see a more open trabecular net in the normal bone sites (CHv) rather than in the defect areas. Contrariwise, in histomorphometry, though a total of 525 trabeculae were hand measured, this was done in a limited number of sections. Nonetheless, though the mean trabecular thickness values are different, no statistically significant differences were found between the two groups with either of the methods.

At optic fluorescence microscopy, some degree of label escape was observed, probably due to the length of the interval between both labels, particularly regarding calcein green, and

a clear labelling line was not always seen. Another difficulty whilst analyzing the samples was the strong bone marrow auto fluorescence. Nevertheless, it allowed to observe not only new bone formation but also bone remodeling within the trabecular structure. Also, mineral apposition rate was calculated and presented no statistically significant differences between the two groups though Spine-Ghost presented a lower value, suggesting a slower resorption rate. In a future study of the same model it would be worthwhile to consider another fluorochrome labelling protocol or other data labelling method to overcome these difficulties.

Histological observations allowed a more detailed observation. Mallory and Masson trichromes staining (Bio-Optica, Milan, Italy) evidenced the neatly organized collagen fibres present in the newly formed bone, as well as the biomaterial integration into the trabecular bone structure. Nevertheless, no inflammatory reaction, signs of increased bone resorption or fibrous encapsulation of both biomaterials were seen in none of the groups and most of the sections (4 out of the 7 control samples and 7 out of 8 Spine-Ghost samples) showed complete filling of the defect area with new trabecular bone.

For immunohistochemistry, an enzymatic antigen retrieval protocol was applied. The size and nature of the samples posed technical difficulties for the completion of the standard thermal antigen retrieval step. Therefore, for the present samples an alternative method through incubation with a Trypsin-EDTA 0,5% solution at 37 ºC, followed by RT cooling of sections was applied. This allowed good epitope labelling, with no background and excellent tissue morphology preservation. Immunohistochemistry sections showed no relevant differences between the two groups and the relatively low levels of detected antigens were what would be expected to occur in mature, stable bone. No osteoclasts were observed at the bone/cement interface, though in a small part of the sections, a small number of osteoclasts-like cells, TRAP positive, were detected within the new trabeculae, suggesting that bone remodeling processes were in course, as it is to be expected.

To finish, it would be interesting to further investigate the potential of the test material in promoting new bone formation at different implantation times and different bone defect models, and to assess the *in vivo* mechanical strength of the filled vertebral body defect.

5. Conclusions

Spine-Ghost was successfully created as an injectable composite cement, presenting high bioresorbability and high bioactivity. It is particularly suited for vertebroplasty, since it proved to be radiopaque enough for fluoroscopy guided vertebral augmentation, and, once set, showed a mechanical strength comparable to the compressive strength of healthy vertebral trabecular bone and higher than the commercial reference. Moreover, it is easily injected into bone defects and presents an *ex vivo* reduced setting time, when compared to control cement. The new ovine model used, though requiring surgical expertise, is considered adequate for preclinical *in vivo* studies, simultaneously efficient and safe, with a survival rate of 100 percent in the present study.

Spine-Ghost demonstrated to be a very promising bone substitute biomaterial for vertebroplasty applications, with a biological response identical, if not superior – as suggested by the higher mean BV/TV measured – to the one elicited by the available commercial control. New bone formation was observed in every sheep, with concurrent cement resorption and integration into the new trabecular bone.

Acknowledgements: This work has been supported by the European Commission under the 7th Framework Programme through the project RESTORATION, grant agreement CP-TP 280575-2. The support from Medtronic Spine LLC Company, Portugal in supplying surgical material is gratefully acknowledged. The support from Hamamatsu, Portugal in supplying Nanozoomer is also gratefully acknowledged. Dr. Francesca Tallia, Dr. Lucia Pontiroli and Mehran Dadkah are kindly acknowledged for their support in developing the Spine-Ghost cement. To finish, we would like to thank Dr. José Abranches, for his selfless help and extensive knowledge, vital for our model development.

Conflicts of interest: The authors have no potential conflict of interest.

References

[1] D. Alexandru, & W. So, Evaluation and management of vertebral compression fractures, Perm. J. 16 (2012) 46-51. Doi: 10.7812/TPP/12-037.

[2] T. P. van Staa, E. M. Dennison, H. G. Leufkens, & C. Cooper, Epidemiology of fractures in England and Wales, Bone 29 (2001) 517–522. Doi:10.1016/S8756-3282(01)00614-7.

[3] The European Prospective Osteoporosis Study (EPOS) Group, Incidence of vertebral fracture in Europe: Results from the European Prospective Osteoporosis Study (EPOS). J Bone Miner Res 17 (2002) 716–724. Doi: 10.1359/jbmr.2002.17.4.716.

[4] Y. Katsuura, J. M. Osborn, & G. W. Cason, The epidemiology of thoracolumbar trauma: a meta-analysis, J. Orthopaed. 13 (2016) 383-388. Doi: 10.1016/j.jor.2016.06.019.

[5] Y.F. Gu, Y.D. Li, C.G. Wu, Z.K. Sun, & C.J. He, Safety and efficacy of percutaneous vertebroplasty and interventional tumor removal for metastatic spinal tumors and malignant vertebral compression fractures, Am. J. Roentgenol. 202 (2014) 298-305. Doi: 10.2214/AJR.12.10497.

[6] H.J. Jiang, J. Xu, Z.Y. Qiu, X.L. Ma, et al., Mechanical properties and cytocompatibility improvement of vertebroplasty pmma bone cements by incorporating mineralized collagen, Materials 8 (2015) 2616-2634. Doi: 10.3390/ma8052616.

[7] P.F. Heini, U. Berlemann, M. Kaufmann, K. Lippuner, et al., Augmentation of mechanical properties in osteoporotic vertebral bones–a biomechanical investigation of vertebroplasty efficacy with different bone cements, Eur. Spine J. 10 (2001) 164-171. Doi: 10.1007/s005860000204.

[8] W. Clark, P. Bird, P. Gonski, et al., Safety and efficacy of vertebroplasty for acute painful osteoporotic fractures (VAPOUR): a multicentre, randomised, double-blind, placebo-controlled trial, Lancet. 388 (2016):1408-1416. Doi: 10.1016/S0140-6736(16)31341-1.

[9] D. Wardlaw, S. R. Cummings, J. Van Meirhaeghe, et al., Efficacy and safety of balloon kyphoplasty compared with non-surgical care for vertebral compression fracture (FREE): a randomised controlled trial, Lancet. 373(2009) 1016-1024. Doi: 10.1016/S0140-6736(09)60010-6.

[10] A. Boger, A. Bisig, M. Bohner, P. Heini, & E. Schneider, Variation of the mechanical properties of PMMA to suit osteoporotic cancellous bone, J. Biomat. Sci. Polym. E. 19 (2008) 1125-1142. Doi: 10.1163/156856208785540154.

[11] D. Arens, S. Rothstock, M. Windolf, & A. Boger, Bone marrow modified acrylic bone cement for augmentation of osteoporotic cancellous bone, J. Mech. Behav. Biomed. Mater. 4 (2011) 2081-2089. Doi: 10.1016/j.jmbbm.2011.07.007.

[12] B.M. Frankel, T. Monroe, & C. Wang, Percutaneous vertebral augmentation: an elevation in adjacent-level fracture risk in kyphoplasty as compared with vertebroplasty, Spine J. 7 (2007) 575-582. Doi: 10.1016/j.spinee.2006.10.020.

[13] G. Lewis, Properties of acrylic bone cement: state of the art, J. Biomed. Mater. Res. 38 (1997) 155-182. Doi:10.1002/(SICI)1097-4636(199722)38:2<155::AID-JBM10>3.0.CO;2-C.

[14] G. C. Anselmetti, A. Manca, K. Kanika, et al., Temperature Measurement During Polymerization of Bone Cement in Percutaneous Vertebroplasty: An *In vivo* Study in Humans, Cardiovasc Intervent Radiol 32 (2009) 491-498. Doi: 10.1007/s00270-009-9509-7.

[15] J. Lieberman, & G. Friedlaender, Bone Regeneration and Repair: Biology and Clinical Applications, first ed., Humana Press, Totowa, New Jersey, 2005. Doi: 10.1385/1592598633.

[16] N. Aebli, D. Schwenke, G. Davis, T. Hii, et al., Polymethylmethacrylate causes prolonged pulmonary hypertension during fat embolism: A study in sheep, Acta orthopaed. 76 (2005) 904-911. Doi: 10.1080/17453670510045570

[17] L.M. Benneker, J. Krebs, V. Boner, A. Boger, et al., Cardiovascular changes after PMMA vertebroplasty in sheep: the effect of bone marrow removal using pulsed jet-lavage, Eur. Spine J. 19 (2010) 1913-1920. Doi: 10.1007/s00586-010-1555-y.

[18] S. Marcia, C. Boi, M. Dragani, S. Marini, et al., Effectiveness of a bone substitute (CERAMENT^{TM}) as an alternative to PMMA in percutaneous vertebroplasty: 1-year follow-up on clinical outcome, Eur. Spine J. 21 (2012) 112–118. Doi: 10.1007/s00586-012-2228-9.

[19] M. Rauschmann, T. Vogl, A. Verheyden, R. Pflugmacher, et al., Bioceramic vertebral augmentation with a calcium sulphate/hydroxyapatite composite (Cerament™ SpineSupport) in vertebral compression fractures due to osteoporosis, Eur. Spine J. 19 (2010) 887-892. Doi: 10.1007/s00586-010-1279-z.

[20] S. Masala, G. Nano, S. Marcia, M. Muto, et al., Osteoporotic vertebral compression fractures augmentation by injectable partly resorbable ceramic bone substitute (Cerament™| SPINE SUPPORT): a prospective nonrandomized study, Neuroradiology 54 (2012) 589-596. Doi: 10.1007/s00234-011-0940-5.

[21] A. Gupta, N. Kukkar, K. Sharif, B.J. Main, et al., Bone graft substitutes for spine fusion: A brief review, World J. Orthop., 6 (2015), 449-456. Doi: 10.5312/wjo.v6.i6.449.

[22] M. Dadkhah, L. Pontiroli, S. Fiorilli, A. Manca, F. Tallia, I. Tcacencu, C. Vitale-Brovarone, Preparation and characterisation of an innovative injectable calcium sulphate based bone cement for vertebroplasty application, J. Mater. Chem. B. 5 (2017) 102-115.

[23] L.L. Hench, Genetic design of bioactive glass, J. Eur. Ceram. Soc. 29 (2009) 1257-1265. Doi: 10.1016/j.jeurceramsoc.2008.08.002

[24] D. Arcos, A. López-Noriega, E. Ruiz-Hernández, O. Terasaki, M. Vallet-Regí, Ordered mesoporous microspheres for bone grafting and drug delivery, Chem. Mater. 21 (2009) 1000-1009. Doi: 10.1021/cm801649z

[25] X. Yan, C. Yu, X. Zhou, J. Tang, & D. Zhao, Highly Ordered Mesoporous Bioactive Glasses with Superior *In Vitro* Bone-Forming Bioactivities, Angew. Chem. Int. Ed. 43 (2004) 5980-5984. Doi: 10.1002/anie.200460598

[26] A.B.D. Nandiyanto, & K. Okuyama, Progress in developing spray-drying methods for the production of controlled morphology particles: From the nanometer to submicrometer size ranges, Adv. Powder Tech. 22 (2011) 1-19. Doi: 10.1016/j.apt.2010.09.011.

[27] M. Alini, S.M. Eisenstein, K. Ito, C. Little, et al., Are animal models useful for studying human disc disorders/degeneration? Eur. Spine J. 17 (2008) 2-19. Doi: 10.1007/s00586-007-0414-y.

[28] H.-J. Wilke, A. Kettler, K.H. Wenger, & L.E. Claes, Anatomy of the sheep spine and its comparison to the human spine, Anat. Rec. 247 (1997) 542-555. Doi: 10.1002/(SICI)1097-0185(199704)247:4<542::AID-AR13>3.0.CO;2-P.

[29] E. Verron, M.L. Pissonnier, J. Lesoeur, V. Schnitzler, et al., Vertebroplasty using bisphosphonate-loaded calcium phosphate cement in a standardized vertebral body bone defect in an osteoporotic sheep model, Acta biomater. 10 (2014) 4887-4895. Doi: 10.1016/j.actbio.2014.07.012.

[30] H.L. Yang, X.S. Zhu, L. Chen, C.M. Chen, et al., Bone healing response to a synthetic calcium sulphate/β-tricalcium phosphate graft material in a sheep vertebral body defect model, J. Biomed. Mater. Res. B Appl. Biomater. 100 (2012) 1911-1921. Doi: 10.1002/jbm.b.32758.

[31] L.M. Benneker, A. Gisep, J. Krebs, A. Boger, et al., Development of an *in vivo* experimental model for percutaneous vertebroplasty in sheep, Vet. Comp. Orthop. Traumatol. V.C.O.T. 25 (2012) 173-177. Doi: 10.3415/VCOT-11-02-0026.

[32] L.A. Galovich, A. Perez-Higueras, J.R. Altonaga, J.M. Gonzalo Orden, et al., Biomechanical, histological and histomorphometric analyses of calcium phosphate cement compared to PMMA for vertebral augmentation in a validated animal model, Eur. Spine J. 20 (2011) 376-382. Doi: 10.1007/s00586-011-1905-4.

[33] A. Boger, L.M. Benneker, J. Krebs, V. Boner, et al., The effect of pulsed jet lavage in vertebroplasty on injection forces of PMMA bone cement: an animal study, Eur. Spine J. 18 (2009) 1957-1962. Doi: 10.1007/s00586-009-1079-5.

[34] M.T. Oliveira, J. Potes, M.C. Queiroga, J.L. Castro, et al., Percutaneous vertebroplasty: a new animal model, Spine J. 16 (2016) 1253–1262, Doi: 10.1016/j.spinee.2016.06.011.

[35] L. Pontiroli, M. Dadkhah, G. Novajra, I. Tcacencu, S. Fiorilli, C. Vitale-Brovarone, An aerosol-spray-assisted approach to produce mesoporous bioactive glass microspheres under mild acidic aqueous conditions, Matter. Lett. (unpublished results).

[36] M.T. Oliveira, S. Lucena, J. Potes, M.C. Queiroga, et al., *Ex vivo* model for percutaneous vertebroplasty, Key Eng. Mater. 631 (2015) 408–413. Doi: 10.4028/www.scientific.net/KEM.631.408.

[37] Directive 2010/63/EU, Official Journal of the European Union, L276/33-79, 2010, ISSN 1725-2601.

[38] Decreto-Lei nº 113/2013, de 7 de Agosto. Diário da República, 1.ª série — N.º 151. Ministério da Agricultura, do mar, do ambiente e do ordenamento do território, Lisboa.

[39] M.L. Bouxsein, S.K. Boyd, B.A. Christiansen, R.E. Guldberg, et al., Guidelines for assessment of bone microstructure in rodents using micro–computed tomography, J. Bone Miner. Res. 25 (2010), 1468-1486. Doi: 10.1002/jbmr.141.

[40] R. Müller, H. Van Campenhout, B. Van Damme, G. Van der Perre, et al., Morphometric analysis of human bone biopsies: a quantitative structural comparison of histological sections and micro-computed tomography, Bone 23 (1998) 59-66. Doi: 10.1016/S8756-3282(98)00068-4.

[41] T. Uchiyama, T. Tanizawa, H. Muramatsu, N. Endo, et al., A morphometric comparison of trabecular structure of human ilium between microcomputed tomography and conventional histomorphometry, Calcif. Tissue. Int. 61 (1997) 493-498. Doi: 10.1007/s002239900373.

Chapter 7

Discussion

7. Discussion

7.1. Welfare and analgesia in animal models

When assembling a team, one must be conscious of the responsibility of each researcher for reinforcing the 3R's concept. From the breeding farms' conditions, to transportation, accommodation, and the experiment itself, it is the responsibility of all the research members in the team to minimize each animal's pain, suffering and distress (Decreto-Lei no. 113/2013; European Directive 2010/63). The multidisciplinarity of the research team was considered of extreme importance, creating the specific knowledge confluence needed for the developed project. The actions pertaining animal welfare include those of a) choice of the flock and latency period; b) providing husbandry conditions – adequate accommodation and food supply, according to the local climate –; c) developing an optimized experimental design – conscientious number of cases, *ex vivo* training, suitable radiologic ancillary means and fluorochromes, minimally invasive procedures, adjusted anaesthetic protocols and postoperative care –; and d) establishing clear "humane endpoints", from which the experiment would be terminated, ending the animal's suffering and/ or distress.

One of the main difficulties when working with sheep is the recognition of pain and/or distress signs. Sheep are very stoic animals, which will uneasily show evident signs of pain. It is of utmost importance for the researcher to know the normal individual and herd behaviour, thus being able to analyse subtle deviations of posture, appetite, urination, or defecation from normal, which can be caused by pain (Plummer *et al.*, 2008; Lizarraga & Chambers, 2013).

In this field veterinarians have an added responsibility towards animal physical integrity, welfare, and – particularly – health, as they are supposedly the most apt team members to correct pain and/ or illness, as well as to ensure good pre-emptive analgesia and anaesthesia protocols – with minimal side effects –, and to develop refinement techniques – such as better surgical models –, when required.

For the present study, the anaesthetic protocol included, as pre-medication, drugs to provide pre-emptive analgesia and sedation: 1) an α2-agonist – xylazine – for its well-recognized sedation, analgesia and muscle relaxant effects (Kästner, 2006; Moolchand *et al.*, 2014); 2) an opioid – butorphanol – to control postoperative acute pain; and 3) a cyclooxygenase-2 (COX-2)-specific NSAID – carprofen – for postoperative pain, due to its long-acting analgesic properties with minimal adverse effects (DiVincenti *et al.*, 2014). Atropine was administered as needed for its anticholinergic action, to decrease saliva secretion;

although several authors have reported its limited use (Galatos, 2011; Flecknell, 2015; Seddighi & Doherty, 2016), as large and repeated doses are often needed (0.5 mg/kg intramuscular) to achieve and maintain the desired effects, and also because of the secondary increase of saliva's viscosity, impairing the cleansing of the pharyngeal area (Flecknell, 2015; Seddighi & Doherty, 2016). Induction was achieved with intravenous thiopental sodium, and anaesthesia maintenance was ensured by the volatile anaesthetic agent – isoflurane 1-2.5% – in oxygen under spontaneous ventilation.

Several other drugs could have been used. For instance, to replace xylazine, other α2-agonists – medetomidine, dexmedetomidine or detomidine – are available; yet, xylazine is known to provide better sedative and analgesic effects than the other drugs in sheep (Kästner, 2006; Moolchand *et al.*, 2014). Attention must be taken when using α2-agonists, because of the risk of hypoxemia – secondary to alveolar edema and pulmonary congestion –, hypotension and decrease in gastrointestinal motility. Nevertheless, α2-agonists actions can be reversed by their antagonists, such as atipamezole, yohimbine and tolazoline. Benzodiazepines, like diazepam and midazolam, are good alternatives as tranquilizers, also leading to muscle relaxation; however, they have no analgesic effect and should be used in combination with other agents, because they can cause transient excitation when administered alone (Seddighi & Doherty, 2016). Likewise, phenothiazines – e.g. acepromazine – can be used as sedatives, but have no analgesic effect.

Opioids are effective analgesics, but analgesia has a short duration in sheep. The combination of some opioids – such as tramadol, methadone and morphine – with the α2-agonist xylazine is known to improve sedation when compared with administration of the α_2-agonist alone, allowing to reduce the α2-agonist's dose and, subsequently, the incidence and severity of side effects (de Carvalho *et al.*, 2016). For the present study, an opioid with agonist-antagonist activity – butorphanol – was the chosen opioid, for its efficacy in sheep (Waterman *et al.*, 1991), availability and cost-effectiveness. Other possible agents would have been morphine, pethidine, buprenorphine, fentanyl, hydromorphone, and oxymorphone (Galatos, 2011; Lizarraga *et al.*, 2012). Some authors support the use of fentanyl patches for pain management, in sheep used for orthopaedic studies (Ahern *et al.*, 2009; Christou *et al.*, 2014). Moreover, a comparison between transdermally administered fentanyl and intramuscular administered buprenorphine showed that the first one was superior for alleviation of postoperative orthopedic pain in sheep (Ahern *et al.*, 2009). Nevertheless, recent studies support the use of sustained-release buprenorphine as a mean of providing effective, long-acting analgesia in sheep (Walkowiak & Graham, 2015; Zullian *et al.*, 2016).

Also for analgesia, NSAIDs are used to induce long-acting analgesia. Combined with other analgesics, they are effective in providing pre-emptive and long-lasting postoperative analgesia in small ruminants (Galatos, 2011). NSAIDs are known to reduce inflammation through inhibition of COX enzymes and prostanoid production in the periphery, thus preventing peripheral sensitisation (Welsh & Nolan, 1995; Colditz *et al.*, 2011); moreover, it is also acknowledged NSAIDs' efficacy in reducing central sensitisation (Lizarraga & Chambers, 2006). The main side effect of NSAIDs is the abomasal ulceration (Lizarraga & Chambers, 2006), thus, their use should be cautious. For this study, the drug of choice was carprofen, for its long-acting analgesic properties in sheep, with a plasma half-life of 48-72 hours, and its lower ulcerogenic effect, when compared to most other NSAIDs (Welsh *et al.*, 1992). Flunixin would also have been a good alternative, as it has already been recognized its efficacy at increasing the thresholds to noxious mechanical stimulation after just one day of treatment in sheep suffering from footrot (Welsh & Nolan, 1995). However, it can cause myonecrosis and injection site inflammation, so it should be administered intravenously (Pyörälä *et al.*, 1999).

As injectable anaesthetics, ketamine or propofol would have been valid alternatives to thiopental (Gatson *et al.*, 2015). Ketamine has the advantage of compensating the negative cardiorespiratory effects of both α2-agonists and benzodiazepines, as it possesses incremental effects on the heart rate, blood pressure and respiratory rate. A recent study by Özkan *et al.* (2010), showed that the combinations xylazine-ketamine and diazepam provide sufficient anaesthesia for minor procedures. The same study concluded that for major surgeries, e.g. maxillofacial surgery, the combination xylazine-ketamine would present better results, with faster inductions, better pain control, stable depth of anaesthesia and faster recoveries. Likewise, propofol is characterized by smooth inductions, effective surgical anaesthesia and rapid recoveries (Correia *et al.*, 1996), presenting better results, when administered through a constant rate infusion, than a multimodal protocol using xylazine, thiopental and halothane (Lin *et al.*, 1997). More recently a synthetic neuroactive steroid – alfaxalone – has also been studied as an injectable agent for the induction and/ or maintenance of anaesthesia, in total intravenous anaesthesia (TIVA) protocols; by interacting with the gamma-aminobutyric acid (GABA) receptor, this hypnotic agent induces mild to moderate anaesthesia and muscle relaxation, with no clinically significant alterations in cardiovascular function and mild respiratory depression (Moll *et al.*, 2013). The use of a constant rate infusion of alfaxalone is known to decrease the needed dose of the volatile anaesthetic agent, desflurane (Granados *et al.*, 2012). Another recent study in goats supports the combined use of alfaxalone and fentanyl, to reduce alfaxalone's dose and minimize adverse cardiopulmonary effects during anaesthesia. (Dzikiti *et al.*, 2016).

Isoflurane was the volatile agent used for convenience. Other agents, such as sevoflurane and desflurane would have been effective alternatives, presenting cardiopulmonary effects similar to those elicited by isoflurane, and allowing faster recoveries (Mohamadnia *et al.*, 2008; Okutomi *et al.*, 2009). However, sevoflurane is known to induce higher cerebral cortical spike activity in sheep (Voss *et al.*, 2006), consistent with the poor recoveries – with excitation and restlessness – obtained by the aforesaid authors (Mohamadnia *et al.*, 2008). Halothane has fallen in disuse, for its more patent cardiopulmonary effects and slower recoveries (Gençcelep *et al*., 2004).

7.2. *Ex vivo* model development

To reliably test the new cement for VCFs and reproduce the procedure in humans while reducing the discomfort and pain caused in the experimental animals, the chosen technique was the minimally invasive PVP. At the time the project started, few techniques had been described in sheep. Several studies were found with reproducible vertebral bone defect models in sheep; yet, the authors used "open" lateral approaches to the vertebral bodies (Kobayashi *et al.*, 2007; Zhu *et al.*, 2011; Verron *et al.*, 2014).

At that time, only two percutaneous vertebroplasty models in sheep were found in the scientific literature. Galovich *et al.* (2011) developed a sheep PVP model for biocements testing, in which a lateral approach to the vertebral body was performed; still, the created bone defects were small, making the model not suitable for biomechanical analysis of biocements. Likewise, Benneker *et al.* (2012) developed a model with a para- to transpedicular approach, aiming towards the cranial- and caudal hemivertebra; however, cement leakage into the vertebral foramen was observed in 19 of the 33 vertebrae studied. Moreover, as this was a terminal study, the authors weren't able to present any information regarding the clinical condition of the animals in the postsurgical period. Consequently, for the present project, the development of a new animal model was mandatory.

The developed new model is innovative in the sense that two interconnected bone defects in the cranial hemivertebrae – with a mean volume of 1.234±0.240 mL (n=12) – were created, through a bilateral modified parapedicular approach, therefore avoiding the wide lumbar nutritional foramen, which is a potential point of cement leakage into the circulation. This approach also reduces the risks of pedicle's fracture and vertebral foramina's disruption verified in the transpedicular approach (Benneker *et al*., 2012), enabling the creation of larger defects.

More recently, another model has been developed and described by Bungartz *et al.* (2016), who also referred several setbacks, including the sacrifice of two animals after surgery, secondary to cement leakage into the vertebral foramina.

Like the aforementioned authors (Galovich *et al.*, 2011; Benneker *et al.*, 2012; Bungartz *et al.*, 2016) some difficulties were felt in avoiding the disruption of either the vertebral foramina or the ventral cortex of the vertebral bodies, while trying to create a wide enough vertebral body bone defect. This was mostly because of some of the anatomical peculiarities of ovine vertebrae – e.g. the orientation angle of the lumbar facet joints and pedicles (less than 30° to the frontal plane, compared to over 60° in humans) and the relative short and sagitally oriented pedicles (Wilke *et al.*, 1997; Mageed *et al.*, 2013). The right orientation angle of the surgical instrumentation at the entry point proved fundamental. Consequentially, the extreme value of fluoroscopy for this procedure should be acknowledge.

Another difficulty was to breach the hard cortical bone of the ovine lumbar vertebrae to create the trabecular defect. As advocated by Benneker *et al.* (2012), the use of the surgical high speed drill – instead of the manual drill – would have been an alternative; however, to reproduce more consistently the surgical technique used in humans (Mathis & Wong, 2003) the manual drill was used.

At the time, the new model was developed, L4, L5 and L6 were the chosen vertebrae for manipulation. At the end of the experiment, the hypothesis of using L6 was discarded, due to its short vertebral body, which led to smaller defects than the defects created in the other vertebrae. In a future study, L1-L3 vertebrae should also be considered, due to their similarities to L4-L5, as observed in studies by Mageed *et al.* (2013) and Wilke *et al.* (1997).

One limitation of this study was regarding the mechanical tests. The intact thawed vertebrae were mounted in parallel flat PMMA (Vertex, Cure) plates, adapting some previously published protocols (Buckley *et al.*, 2009; Tarsuslugil *et al.*, 2013; Fang *et al.*, 2014). Still, when the axial compression load was applied, the plates fractured and failed before the vertebrae, which prevented the calculation of the compressive strength of vertebrae. Nonetheless, vertebrae stiffness and corrected vertebrae stiffness values were obtained.

This limitation was caused by the great trabecular bone density of sheep vertebrae, and consequently the high mechanical stiffness and strength of vertebral bodies (Keller, 1994; Mitton *et al.*, 1997; Liebschner, 2004). In comparison, several large animal species, like the

dog, the pig, the sheep, the goat, and the calf present higher BMDs than humans – with the sheep having the highest one and the pig the lowest one (closer to human's BMD). This occurs because of the constant forces generated by the support of the large muscle bulk along the quadruped animals' backs, which expose them to higher axial compression stresses (Aerssens *et al.*, 1998; Reinwald & Burr, 2008). Moreover, Aerssens *et al.* (1998), showed that the fracture stress was lowest in the samples from human and pig, intermediate in dog and cow samples, and highest in sheep samples.

Another important remark regarding the mechanical testing is that all vertebrae were conserved by freezing at -18 ºC and went through the same number of freezing/ thawing cycles, during the experimental period. Panjabi *et al.* (1985) made a long-term study on vertebrae frozen at -18 °C, where they found no significant differences in the mechanical properties of vertebrae tested on the first day and vertebrae tested after long-term freezing. Another study by Borchers *et al.* (1995) showed that repeated freezing-thawing cycles at -20 ºC did not compromise the structural integrity and compressive mechanical properties of trabecular bone. Other possibilities for conservation of the vertebrae would be ethanol or buffered formalin. However, a recent study by Stefan *et al.* (2010) showed that these two conservation methods alter significantly the plastic mechanical properties of cortical bovine bone and therefore should not be used when biomechanical testing to evaluate the failure load of a new orthopaedic implant is in view. Another study by Wieding *et al.* (2015) yielded the same conclusions regarding ovine cortical bone; moreover, in this study, freezing had no influence on the mechanical properties of the ovine cortical bone. Finally, a study by Nazarian *et al.* (2009), conducted in murine femurs and vertebral bodies, showed that bone preservation by freezing and formalin fixation over a 2-week period did not alter the elastic mechanical properties; however, formalin fixation weakened the viscoelastic properties of murine bone.

All vertebrae were tested under the same conditions – at room temperature, in air –, as it has already been proven that different test conditions could lead to different results: for instance, a study from Mitton *et al.* (1997) showed that the shear strength of a sample of cancellous bone from the lumbar vertebrae of ewes was higher when the tests were conducted at room temperature in air than when they were conducted with a sample in physiological saline bath regulated at 37 °C.

Finally, considering the bone anatomy, structure, modelling and remodelling processes, close to human's, the pig would have been an alternative – as a large animal model for testing

new composites – to sheep (Mosekilde *et al.*, 1993; Turner, 2002; Thorwarth *et al.*, 2005; Schlegel *et al.*, 2006). Nevertheless, commercial pigs are rarely chosen as models for implant biomaterial research because of their large growth rates and very high body weight (Li *et al*., 2015); moreover, they are considered difficult to handle, noisy, aggressive, and expensive, and are often disregarded in favour of sheep and goat (Turner, 2007). Also the dog, due to its similarities regarding the bone composition (ash weight, hydroxyproline, extractable proteins and IGF-1 content) and easy handling, has been commonly acknowledged as a large animal model for orthopaedic research (Aerssens *et al.*, 1998; Pearce *et al.*, 2007); however, its use is in decline because of the higher cost, the interspecies difference in the rate of bone remodelling, and the existent social concerns, since it is seen as a companion animal.

7.3. *In vivo* study

Regarding the *in vivo* procedures, there were some issues – cardiovascular changes and/ or arrest – during the cement injection, which were overcome simply by increasing the time of injection. These changes are most likely due to fat pulmonary embolism, as previously described by Aebli *et al.* (2002) and Benneker *et al.* (2010), being a potential life-threatening complication of the procedure. The same complication is frequently observed in humans (Saracen & Kotwica, 2016) and a recent study has shown that it can be prevented by performing vertebral body lavage prior to cement augmentation (Hoppe *et al.*, 2016).

In accordance with what was observed in the *ex vivo* study, another surgical difficulty was the orientation angle of the surgical instrumentation, which if it was not correct it would have hindered the defect creation, and eventually it would have led to cortical disruption. During the present study, ventral cortical disruption occurred in one sheep and cortical disruption of the vertebral foramen occurred in two sheep. Just one of those animals developed neurological signs – moderate proprioceptive deficits of the hind limbs –, probably due to the cement leakage around the defect entry point affecting the spinal nerve roots; nonetheless, the sheep remained ambulatory and after approximately two months with conservative therapy for an initial period the animal had fully recovered.

Also noteworthy is the two sheep in which the cement couldn't be injected only from one side. At the time of the surgery, the defects appeared interconnected, due to the data obtained from fluoroscopy and also from the instrumentation manipulation; however, as the cement was injected, only one half of the defect was being filled and resistance was felt upon injection, which compelled the surgeon to fill the contralateral defect.

It's important to note that all these setbacks occurred during the first group of four surgeries performed. Thereafter, with the natural progression of the surgeon's learning curve, the procedure become safer and no more problems were observed in later surgeries.

Concerning the biomaterials, they are of utmost importance for this kind of surgeries. As referred before, beside the osteoconductive/ osteoinductive and bioactivity features, they should assemble several physical characteristics that enable their usage during surgery. According to Lewis (2006), the key properties for injectable bone cements are: 1) easy injectability (with adequate viscosity), 2) high radiopacity, which allow their visualization during injection, and 3) a resorption rate that is neither too high nor too low. The cements should present high porosities – microporosity with mean pore diameter <10 μm, to allow circulation of body fluid and macroporosity with mean pore diameter >100 μm, to provide a scaffold for blood–cell colonization –, rapid setting times, easy preparation and handleability, appropriate adhesiveness and viscosity (initially relatively low, to allow injection without extravasation, and constant after the setting time). Finally, the biomaterials should have the requisite mechanical properties – e.g. values of modulus of elasticity and mechanical strength similar to those of the healthy cancellous bone, which is in the range of 2-12 MPa – that would allow for immediate reinforcement of the vertebral body with ensuing normal function and pain relief (Lewis, 2006; Campana *et al.*, 2014).

Relatively to the used biomaterials, a few remarks should be made. Both Cerament™ (control group) and Spine-Ghost (experimental group) are calcium sulphate (CaS)-based injectable cements (Rauschmann *et al.*, 2010; Dadkhah *et al.*, 2017). However, while Cerament™ is a biphasic cement consisting of 60% α-CaS hemihydrates – known for its biocompability – and 40 % hydroxyapatite (HA) – to provide long-term support, with its radiopacity conferred by the presence of the non-ionic contrast agent iohexol (Rauschmann *et al.*, 2010), Spine-Ghost is a biphasic cement consisting of 70% α-CaS hemihydrate, 20% glass-ceramic radiopaque phase and 10% mesoporous particles of a bioactive glass (MBG) – used for its high bioactivity and osteoinductive properties (Hench *et al.*, 2009), which combined with water results in an injectable paste (Dadkhah *et al.*, 2017). Spine-Ghost's radiopacity was similar to that of the soft tissues, which made it difficult to visualize the cement during injection; nevertheless, Spine-Ghost's radiopacity is long-lasting and will keep the bone cement visible until its complete resorption, as it is conferred by its glass-ceramic phase, while Cerament™'s radiopacity fade away over time, hindering the visualization of the bone cement at follow-ups (Dadkhah *et al.*, 2017). Both the materials have proved to be bioactive and resorbable (Marcia

et al., 2012; Dadkhah *et al.*, 2017). Both cements were easy to handle and have adequate injectabilities; regardless, Spine-Ghost was less viscous than Cerament, so easier to be injected (Dadkhah *et al.*, 2017). Cerament's working/ hardening time is 7 minutes (Abramo *et al.*, 2010), while Spine-Ghost's is 8-20 minutes (Dadkhah *et al.*, 2017), both being sufficient for the procedure. Both cements present final setting times within 1 hour (Rauschmann *et al.*, 2010; Dadkhah *et al.*, 2017); however, for reasons of safety, Cerament™'s manufacturers instruct the surgeons to maintain the patients at rest for two hours (Rauschmann *et al.*, 2010), which obliged the surgical team to keep all sheep anaesthetized for that long after the procedure was concluded. The same anaesthetic times were observed for Spine-Ghost. Finally, both cements showed adequate properties in terms of stiffness and strength, with Spine-Ghost presenting a higher compressive strength in both wet and dry conditions compared to Cerament™, ensuring an enhanced mechanical support when compared to control (Rauschmann *et al.*, 2010; Dadkhah *et al.*, 2017).

Micro-CT assessment was considered essential for the *ex vivo* and *in vivo* studies. In the *ex vivo* study, micro-CT allowed, among other things, to visualize in 3D rendered models the specificities of the sheep vertebrae. Moreover, during the *in vivo* study, it enabled qualitative evaluation of the vertebrae, like the visualization of cortical disruptions – confirming our suspicions at surgery – and the calculation of 3D structural parameters, without destroying the samples (Guldberg *et al.*, 2008; Peyrin, 2011; Apple *et al.*, 2013). This non-destructive visualization and quantification of the 3D structure of trabecular bone is perhaps one of micro-CT's greater advantage, when compared to the more conventional histology, since the 3D structural parameters – e.g. bone mineral density, relative bone volume, structural model index – obtained are correlated with the trabecular bone mechanical properties (Mittra *et al.*, 2005; Teo *et al.*, 2007).

Even so, there are some limitations in the micro-CT quantitative analysis of new bone formation. In the present study, the main difficulty was the accurate segmentation of mineralized tissue from the biomaterials within the cross-section images. This is particularly relevant when using bioceramics, due to the radiodensities' similarities between the bone and the materials (Guldberg *et al.*, 2008; Apple *et al.*, 2013), rather than, for instance, with metallic implants. Thus, the contact surface and integration of bone around the scaffold can not be accurately calculated. As recommended by several authors, we chose to use the global threshold method (Rajagopalan *et al.*, 2005; Brun *et al.*, 2011). Nonetheless, other authors recommend more sophisticated segmentation algorithms to separate materials with overlapping density

distributions (Hilldore *et al.*, 2007; Guldberg *et al.*, 2008). Another major limitation was related to the equipment itself. When intending to calculate the structural parameters, high resolutions (small voxel sizes) should be attempted. Large structures such as trabeculae in human and ovine bone (100 to 200 μm thick) should be scanned with voxel sizes never more than 60 μm (Thomsen *et al.*, 2005), as it is generally considered that the ratio of voxels to object size should be 2 (Bouxsein *et al.*, 2010). The voxel size used was borderline with this limit – 62 μm –; however, if considering the 100 μm-thick trabeculae, these resolution values become low, as the maximum voxel size used should be 50 μm. Despite this fact, the 3D structural parameters were calculated so that the results could be compared with the 2D morphologic measurements obtained in histomorphometry, as it is acknowledged that these data are highly correlated (Müller *et al.*, 1998; Chappard *et al.*, 2005; Park *et al.*, 2011). Nevertheless, these methods are known to be complementary and the results should be interpreted bearing in mind the advantages and limitations of both methods. To try to minimize the equipment's limitations internal controls were used – the caudal hemivertebrae with intact trabecular bone – to be able to appreciate the significant differences within groups. The planes used for the sample's scanning and cutting were different, due to the vertebrae geometry – which hinders the vertebrae's positioning at the micro-CT rotation stage – and the requirement of having two symmetric hemi-samples for histology (undecalcified and decalcified bone samples).

Concerning the micro-CT analysis of the *in vivo* study presented in this project, the following results were observed: regarding the defect augmented area, the mean relative bone volume (BV/TV) was significantly higher in Spine-Ghost augmented vertebrae, when compared to Cerament™, and no significant differences were found in the caudal hemivertebrae area – which contains only intact trabecular bone – that could justify the higher bone volume ration found in the Spine-Ghost group. Contrariwise, the specific surface (BS/BV) was significantly lower in Spine-Ghost samples when compared to Cerament™. A lower BS/BV may suggest a thicker structure of the Spine-Ghost augmented vertebrae and might be related to a lower bone turn-over rate, because bone resorption and formation occurs on bone surfaces. The remaining parameters – mean trabecular thickness (Tb.Th), mean trabecular separation (Tb.Sp) and trabecular number (Tb.N) – presented no statistically significant differences between the two groups – Spine-Ghost and Cerament™ –, though the first two parameters presented slightly superior values in the Spine-Ghost group. To finalize, when comparing the mean values of all the structural parameters between the defect augmented area and the caudal hemivertebrae area, the only value that presented no statistically significant difference was the mean trabecular number (Tb.N), indicating a normal tissue evolution, with

an emergent open tissue structure, for both cements. Micro-CT assessment also enabled the reconstruction and visualization of the injected vertebrae, through the rendering software. This option enabled the visual comparison between the two cements and the confirmation of the data obtained through the analysis software. Thus, cement resorption was observed in both groups followed by new bone formation, which presented a slightly closer porosity than the intact trabecular bone from the caudal hemivertebrae.

Histomorphometry or quantitative histology is a time-consuming, laborious and destructive method. Histomorphometry is also less sensitive in detecting global bone mass changes when compared to micro-CT, because of the limited number of sections observed in manual histomorphometric. Nonetheless, histology is still the gold standard for bone remodelling processes evaluation, as it is the only method that enables the visualization of bone microstructure – bone cells and their activities (Iwaniec *et al.*, 2008; Brandi *et al.*, 2009). Several authors refer to the imperative use of the conventional method to overcome micro-CT's technical difficulties, like for example the impossibility of distinguish between woven from lamellar bone (Rühli *et al.*, 2007; Tamminen *et al.*, 2011). In the *in vivo* study, the obtained histomorphometric results showed no statistically significant differences between the two groups – Spine-Ghost and Cerament™ – regarding trabecular thickness, relative bone volume and bone area within the defect and in the intact tissue. Since there was no fibrous capsule observed in any of the sections, the affinity index can be considered of 100%. In accordance to the abovementioned, these results were compared with the results obtained through micro-CT analysis, and though there were differences, they were not statistically significant and the same trend was shown. The main difference was in the mean Tb.Th, which was overestimated by micro-CT. This is a recognized feature of the micro-CT analysis (Chappard *et al.*, 2005); additionally, there is possibly a potential overestimation of the micro-CT values in the defect augmented areas due the presence of the residual cements, as confirmed by looking at the 3D rendered models.

The optic fluorescence microscopy is considered an indispensable tool for bone tissue engineering studies, as it enables the determination of the onset time and location of osteogenesis (van Gaalen *et al.*, 2010), without sacrificing the animal, thus serving the ideal of the 3R's concept. However, protocols' standardization is not a current reality (van Gaalen *et al.*, 2010). The protocol used for this project – adapted from the protocols advocated by other authors (Lee *et al.*, 2003; Pautke *et al.*, 2005; van Gaalen *et al.*, 2010) – presented some flaws, for instance, some degree of label escape, probably due to the length of the interval between

the labels, and also the strong bone marrow auto fluorescence. Still, the labelling was sufficient to enable MAR calculation (1.60±0.27 µm/day in the control group and 1.39±0.54 µm/day in the experimental group). The strong bone marrow fluorescence is common in fluorochrome labelling and it's hardly a problem as it is distributed throughout all the bone regions and can then easily be distinguished from the fluorochrome labelling (van Gaalen *et al.*, 2010). Nevertheless, in a future study it should be considered the use of another fluorochrome labelling protocol or other data labelling method to overcome these difficulties.

The qualitative observation of the slides was performed for both undecalcified and decalcified samples. The evaluation of the undecalcified samples showed new bone formation within the area of the defect for both groups in most of the vertebrae, with the pattern of long trabeculae, mostly parallel to the long axis of the vertebrae interrupted by a denser net of highly interconnected trabeculae. Also, in both groups the bone was in direct contact with residual cements and no fibrous tissue or inflammatory reactions were observed. Most of the newly formed bone was mature. Three vertebrae – two from Cerament™ group and one from Spine-Ghost – showed relatively large areas of defect yet to be occupied by bone. Moreover, empty space areas were observed in three out of seven samples of the Cerament™ group. Histological observations on decalcified samples allowed a more detailed observation. Thus, Masson's trichrome evidenced the precisely organized collagen fibres in the newly formed trabecular network in the defect area. And both trichromes confirmed the presence of bone marrow within the trabeculae, and cement residues, which were integrated in the trabeculae themselves. In Cerament™ group sections, larger quantities of cement are apparent within the trabeculae when compared to Spine-Ghost sections. Again, no inflammatory reaction, signs of increased bone resorption or fibrous encapsulation of both biomaterials were seen.

Immunohistochemistry is considered an essential technique when testing new biomaterials, as it allows to evaluate the cell activity at the bone-biomaterial interface, thus providing information about the osteogenic potential of the biomaterial and its effect on osteoblastic differentiation. Most of the available information on immunohistochemical detection of osteogenic markers in decalcified bone sections in sheep is scarce and vague (Haque *et* al., 2006; Adeyemo *et al.*, 2008). The main limitations are technical, as the size and nature of the samples posed difficulties associated with the sectioning of calcified tissue, preservation of tissue morphology and remaining antigen integrity (Klein & Memoli, 2011). A recent study by Katoh *et al.* (2016) advocate the use of microwave to assist tissue fixation and staining and presents several protocols using microwave irradiation found in literature. Another

study recommended the use of hyaluronidase and pepsin for predigestion of the bone sample combined with alkaline phosphatase-mediated chromogenic detection (Li *et al.*, 2015). To overcome these difficulties an enzymatic antigen retrieval protocol was developed and applied, which allowed good epitope labelling, with no background and excellent tissue morphology preservation. Immunohistochemistry sections showed no relevant differences between the two groups – Cerament™ and Spine-Ghost – and the relatively low levels of detected antigens were what would be expected to occur in mature, stable bone. No osteoclasts were observed at the bone/cement interface, though in a small part of the sections, a small number of osteoclasts-like cells, TRAP positive, were detected within the new trabeculae, suggesting that bone remodeling processes were in course, as it was expected.

7.4. References

Abramo, A., Geijer, M., Kopylov, P., & Tägil, M. (2010). Osteotomy of distal radius fracture malunion using a fast remodeling bone substitute consisting of calcium sulphate and calcium phosphate. *Journal of Biomedical Materials Research Part B: Applied Biomaterials, 92*(1), 281-286.

Adeyemo, W. L., Reuther, T., Bloch, W., Korkmaz, Y., Fischer, J. H., Zöller, J. E., & Kuebler, A. C. (2008). Healing of onlay mandibular bone grafts covered with collagen membrane or bovine bone substitutes: a microscopical and immunohistochemical study in the sheep. *International journal of oral and maxillofacial surgery, 37*(7), 651-659.

Ahern, B. J., Soma, L. R., Boston, R. C., & Schaer, T. P. (2009). Comparison of the analgesic properties of transdermally administered fentanyl and intramuscularly administered buprenorphine during and following experimental orthopedic surgery in sheep. *American journal of veterinary research, 70*(3), 418-422.

Appel, A. A., Anastasio, M. A., Larson, J. C., & Brey, E. M. (2013). Imaging challenges in biomaterials and tissue engineering. *Biomaterials, 34*(28), 6615-6630.

Baroud, G., Bohner, M., Heini, P., & Steffen, T. (2004). Injection biomechanics of bone cements used in vertebroplasty. *Biomedical materials and engineering, 14*(4), 487-504.

Borchers, R. E., Gibson, L. J., Burchardt, H., & Hayes, W. C. (1995). Effects of selected thermal variables on the mechanical properties of trabecular bone. *Biomaterials, 16*(7), 545-551.

Bouxsein, M. L., Boyd, S. K., Christiansen, B. A., Guldberg, R. E., Jepsen, K. J., & Müller, R. (2010). Guidelines for assessment of bone microstructure in rodents using micro–computed tomography. *Journal of bone and mineral research, 25*(7), 1468-1486.

Brun, F., Turco, G., Accardo, A., & Paoletti, S. (2011). Automated quantitative characterization of alginate/hydroxyapatite bone tissue engineering scaffolds by means of micro-CT image analysis. Journal of Materials Science: *Materials in Medicine, 22*(12), 2617-2629.

Buckley, J. M., Parmeshwar, R., Deviren, V., & Ames, C. P. (2009). An improved metric for quantifying the stiffnesses of intact human vertebrae. Proceedings of the Institution of Mechanical Engineers, Part H: *Journal of Engineering in Medicine, 223*(5), 537-543.

Bungartz, M., Maenz, S., Kunisch, E., Horbert, V., Xin, L., Gunnella, F., & Sachse, A. (2016). First-time systematic postoperative clinical assessment of a minimally invasive approach for lumbar ventrolateral vertebroplasty in the large animal model sheep. *The Spine Journal*, *16*(10), 1263-1275.

Campana, V., Milano, G. I. U. S. E. P. P. E., Pagano, E., Barba, M., Cicione, C., Salonna, G. & Logroscino, G. (2014). Bone substitutes in orthopaedic surgery: from basic science to clinical practice. *Journal of Materials Science: Materials in Medicine*, *25*(10), 2445-2461.

de Carvalho, L. L., Nishimura, L. T., Borges, L. P., Cerejo, S. A., Villela, I. O., Auckburally, A., & de Mattos-Junior, E. (2016). Sedative and cardiopulmonary effects of xylazine alone or in combination with methadone, morphine or tramadol in sheep. *Veterinary anaesthesia and analgesia*, *43*(2), 179-188.

Chappard, D., Retailleau-Gaborit, N., Legrand, E., Baslé, M. F., & Audran, M. (2005). Comparison insight bone measurements by histomorphometry and μCT. *Journal of Bone and Mineral Research*, *20*(7), 1177-1184.

Christou, C., Rawlinson, J., Mitchell, G., Oliver, R., & Walsh, W. (2014). The use of fentanyl patches for sheep in orthopaedic research. *Bone Joint Journal*, *96*(Supp 11), 215-215.

Correia, D., Nolan, A. M., & Reid, J. (1996). Pharmacokinetics of propofol infusions, either alone or with ketamine, in sheep premedicated with acepromazine and papaveretum. *Research in veterinary science*, *60*(3), 213-217.

Cremers, S., Garnero, P., & Seibel, M. J. (2008). Biochemical markers of bone metabolism. In: Bilezikian, J. P., Raisz, L. G., & Martin, T.J. (Eds), Principles of Bone Biology, 3rd Ediction, San Diego: Academic Press, p.1857-1881.

Dadkhah, M., Pontiroli, L., Fiorilli, S., Manca, A., Tallia, F., Tcacencu, I., & Vitale-Brovarone, C. (2017). Preparation and characterisation of an innovative injectable calcium sulphate based bone cement for vertebroplasty application, *J. Mater. Chem. B.* *5*(1) 102-115.

Decreto-Lei nº 113/2013, de 7 de Agosto. Diário da República, 1.ª série — N.º 151. Ministério da Agricultura, do mar, do ambiente e do ordenamento do território, Lisboa.

Directive 2010/63/EU, *Official Journal of the European Union*, L276/33-79, 2010, ISSN 1725-2601.

DiVincenti, J., Westcott, R., & Lee, C. (2014). Sheep (Ovis aries) as a model for cardiovascular surgery and management before, during, and after cardiopulmonary bypass. *Journal of the American Association for Laboratory Animal Science, 53*(5), 439-448.

Dzikiti, B. T. (2013). Intravenous anaesthesia in goats: A review. *Journal of the South African Veterinary Association, 84*(1), 1-8.

Dzikiti, B. T., Ndawana, P. S., Zeiler, G., Ferreira, J. P., & Dzikiti, L. N. (2016). Determination of the minimum infusion rate of alfaxalone during its co-administration with fentanyl at three different doses by constant rate infusion intravenously in goats. *Veterinary anaesthesia and analgesia, 43*(3), 316-325.

Fang, Z., Giambini, H., Zeng, H., Camp, J. J., Dadsetan, M., Robb, R. A., An, K. N., Yaszemski, M. J., & Lu, L. (2014). Biomechanical evaluation of an injectable and biodegradable copolymer P (PF-co-CL) in a cadaveric vertebral body defect model. *Tissue Engineering Part A, 20*(5-6), 1096-1102.

Flecknell, P. (2015). Laboratory animal anaesthesia. Academic Press.

Gatson, B. J., Pablo, L., Plummer, C. E., & Granone, T. D. (2015). Effects of premedication with sustained-release buprenorphine hydrochloride and anesthetic induction with ketamine hydrochloride or propofol in combination with diazepam on intraocular pressure in healthy sheep. *American journal of veterinary research, 76*(9), 771-779.

Gençcelep, M., Atasoy, N., & Tas, A. (2004). The effects of inhalation anaesthetics (halothane and isoflurane) on certain clinical and haematological parameters of sheep. *Small Ruminant Research, 53*(1), 157-160.

Granados, M. M., Domínguez, J. M., Fernández-Sarmiento, A., Funes, F. J., Morgaz, J., Navarrete, R., Carrillo, J. M., Rubio, M., Muñoz-Rascón, P., Gómez de Segura, I. A., & Gómez-Villamandos, R. (2012). Anaesthetic and cardiorespiratory effects of a constant-rate infusion of alfaxalone in desflurane-anaesthetised sheep. *Veterinary Record*, *171*(5), 125.

Guldberg, R. E., Duvall, C. L., Peister, A., Oest, M. E., Lin, A. S., Palmer, A. W., & Levenston, M. E. (2008). 3D imaging of tissue integration with porous biomaterials. *Biomaterials, 29*(28), 3757-3761.

Heini, P., & Berlemann, U. (2001). Bone substitutes in vertebroplasty. *European Spine Journal, 10*(2), S205-S213.

Hench, L. L. (2009). Genetic design of bioactive glass. *Journal of the European Ceramic Society, 29*(7), 1257-1265.

Hilldore, A., Wojtowicz, A., & Johnson, A. W. (2007). Micro-CT based quantification of non-mineralized tissue on cultured hydroxyapatite scaffolds. *Journal of Biomedical Materials Research Part A, 82*(4), 1012-1021.

Hoppe, S., Elfiky, T., Keel, M. J. B., Aghayev, E., Ecker, T. M., & Benneker, L. M. (2016). Lavage prior to vertebral augmentation reduces the risk for cement leakage. *European spine journal, 25*(11), 3463-3469.

Iwaniec, U. T., Wronski, T. J., & Turner, R. T. Histological analysis of bone. Methods Mol Biol 2008; 447:325-41.Brandi, M. L. (2009). Microarchitecture, the key to bone quality. *Rheumatology, 48*(suppl 4), iv3-iv8.

Katoh, K. (2016). Microwave-Assisted Tissue Preparation for Rapid Fixation, Decalcification, Antigen Retrieval, Cryosectioning, and Immunostaining. *International Journal of Cell Biology, 2016* (9), 1-9.

Kästner, S. B. (2006). A2-agonists in sheep: a review. *Veterinary anaesthesia and analgesia, 33*(2), 79-96.

Keller, T. S. (1994). Predicting the compressive mechanical behavior of bone. *Journal of biomechanics, 27*(9), 1159-1168.

Klein, M. J., & Memoli, V. A. (2011, February). Orthopaedic specimen preparation: what pathologists should know and do. In Seminars in diagnostic pathology (Vol. 28, No. 1, pp. 4-12). WB Saunders.

Kobayashi, N., Ong, K., Villarraga, M., Schwardt, J., Wenz, R., Togawa, D., Fujishiro, T., Turner, A. S., Seim, H. B. 3rd, & Bauer, T. W. (2007). Histological and mechanical

evaluation of self-setting calcium phosphate cements in a sheep vertebral bone void model. *Journal of Biomedical Materials Research Part A, 81*(4), 838-846.

Lee, T. C., Mohsin, S., Taylor, D., Parkesh, R., Gunnlaugsson, T., O'Brien, F. J., Giehl, M., & Gowin, W. (2003). Detecting microdamage in bone. *Journal of Anatomy, 203*(2), 161-172.

Li, S., Liu, B., Tian, M., Zhang, L., Tickner, J., Xu, J., & Rong, L. (2015). An effective and practical immunohistochemical protocol for bone specimens characterized by hyaluronidase and pepsin predigestion combined with alkaline phosphatase-mediated chromogenic detection. *Histology and histopathology*, *30*(3), 331-343.

Li, Y., Chen, S. K., Li, L., Qin, L., Wang, X. L., & Lai, Y. X. (2015). Bone defect animal models for testing efficacy of bone substitute biomaterials. *Journal of Orthopaedic Translation, 3*(3), 95-104.

Liebschner, M. A. (2004). Biomechanical considerations of animal models used in tissue engineering of bone. *Biomaterials*, *25*(9), 1697-1714.

Lin, H. C., Purohit, R. C., & Powe, T. A. (1997). Anesthesia in sheep with propofol or with xylazine-ketamine followed by halothane. *Veterinary Surgery*, *26*(3), 247-252.

Lizarraga, I., & Chambers, J. P. (2012). Use of analgesic drugs for pain management in sheep. *New Zealand veterinary journal, 60*(2), 87-94.

Mageed, M., Berner, D., Jülke, H., Hohaus, C., Brehm, W., & Gerlach, K. (2013). Morphometrical dimensions of the sheep thoracolumbar vertebrae as seen on digitised CT images. *Laboratory animal research, 29*(3), 138-147.

Marcia, S., Boi, C., Dragani, M., Marini, S., Marras, A., Piras, E., Anselmetti, G., & Masala, S. (2012). Effectiveness of a bone substitute (CERAMENT^{TM}) as an alternative to PMMA in percutaneous vertebroplasty: 1-year follow-up on clinical outcome, *Eur. Spine J. 21* 112–118.

Mathis, J. M., & Wong, W. (2003). Percutaneous vertebroplasty: technical considerations. *Journal of vascular and interventional radiology, 14*(8), 953-960.

Mitton, D., Rumelhart, C., Hans, D., & Meunier, P. J. (1997). The effects of density and test

conditions on measured compression and shear strength of cancellous bone from the lumbar vertebrae of ewes. *Medical engineering & physics, 19*(5), 464-474.

Mittra, E., Clinton, R., & Qin, Y. X. (2005). Interrelationship of trabecular mechanical and microstructural properties in sheep trabecular bone. *Journal of biomechanics, 38*(6), 1229-1237.

Mohamadnia, A. R., Hughes, G., & Clarke, K. W. (2008). Maintenance of anaesthesia in sheep with isoflurane, desflurane or sevoflurane. *The Veterinary Record, 163*(7), 210-215.

Moll, X., Santos, L., García, F., & Andaluz, A. (2013). The effects on cardio-respiratory and acid–base variables of a constant rate infusion of alfaxalone–HPCD in sheep. *The Veterinary Journal, 196*(2), 209-212.

Moolchand, M., Kachiwal, A. B., Soomro, S. A., & Bhutto, Z. A. (2014). Comparison of sedative and analgesic effects of xylazine, detomidine, and medetomidine in sheep. *Egyptian Journal of Sheep & Goat Sciences, 9*(2), 43-48.

Mosekilde, L., Weisbrode, S. E., Safron, J. A., Stills, H. F., Jankowsky, M. L., Ebert, D. C., Danielsen, C. C., Sogaard, C. H., Franks, A. F., Stevens, M. L., Paddock, C. L., & Boyce, R. W. (1993) Calcium-restricted ovariectomized Sinclair S-1 minipigs: an animal model of osteopenia and trabecular plate perforation. *Bone, 14*, 379-382.

Müller, R., Van Campenhout, H., Van Damme, B., Van Der Perre, G., Dequeker, J., Hildebrand, T., & Rüegsegger, P. (1998). Morphometric analysis of human bone biopsies: a quantitative structural comparison of histological sections and micro-computed tomography. *Bone; 23*, 59–66.

Nazarian, A., Hermannsson, B. J., Muller, J., Zurakowski, D., & Snyder, B. D. (2009). Effects of tissue preservation on murine bone mechanical properties. *Journal of Biomechanics, 42*(1), 82-86.

Okutomi, T., Whittington, R. A., Stein, D. J., & Morishima, H. O. (2009). Comparison of the effects of sevoflurane and isoflurane anesthesia on the maternal-fetal unit in sheep. *Journal of anesthesia, 23*(3), 392-398.

Ozkan, F., Cakir-Ozkan, N., Eyibilen, A., Yener, T., & Erkorkmaz, U. (2010). Comparison of

ketamine-diazepam with ketamine-xylazine anesthetic combinations in sheep spontaneously breathing and undergoing maxillofacial surgery. *Bosnian journal of basic medical sciences/Udruzenje basicnih mediciniskih znanosti= Association of Basic. Journal of Medical Sciences, 10*(4), 297-302.

Panjabi, M. M., Krag, M., Summers, D., & Videman, T. (1985). Biomechanical time-tolerance of fresh cadaveric human spine specimens. *Journal of Orthopaedic Research, 3*(3), 292-300.

Park, S. Y., Kim, K. H., Koo, K. T., Lee, K. W., Lee, Y. M., Chung, C. P., & Seol, Y. J. (2011). The evaluation of the correlation between histomorphometric analysis and micro-computed tomography analysis in AdBMP-2 induced bone regeneration in rat calvarial defects. *Journal of periodontal & implant science, 41*(5), 218-226.

Pautke, C., Vogt, S., Tischer, T., Wexel, G., Deppe, H., Milz, S., ... & Kolk, A. (2005). Polychrome labeling of bone with seven different fluorochromes: enhancing fluorochrome discrimination by spectral image analysis. *Bone, 37*(4), 441-445.

Pearce, A. I., Richards, R. G., Milz, S., Schneider, E., & Pearce, S. G. (2007). Animal models for implant biomaterial research in bone: a review. *European Cells & Materials, 13*(1), 1-10.

Plummer, P. J., & Schleining, J. A. (2013). Assessment and management of pain in small ruminants and camelids. *Veterinary Clinics of North America: Food Animal Practice, 29*(1), 185-208.

Pyörälä, S., Laurila, T., Lehtonen, S., Leppä, S., & Kaartinen, L. (1999). Local Tissue Damage in Cows after Intramuscular Administration of Preparations Containing Phenyl. *Acta veterinaria scandinavica, 40*(2), 145-150.

Rajagopalan, S., Lu, L., Yaszemski, M. J., & Robb, R. A. (2005). Optimal segmentation of microcomputed tomographic images of porous tissue-engineering scaffolds. *Journal of Biomedical Materials Research Part A, 75*(4), 877-887.

Rauschmann, M., Vogl, T., Verheyden, A., Pflugmacher, R., Werba, T., Schmidt, S., & Hierholzer, J. (2010). Bioceramic vertebral augmentation with a calcium sulphate/hydroxyapatite composite (Cerament™ SpineSupport) in vertebral compression

fractures due to osteoporosis. *European Spine Journal, 19*(6), 887-892.

Reinwald, S., & Burr, D. (2008). Review of nonprimate, large animal models for osteoporosis research. *Journal of Bone and Mineral Research, 23*(9), 1353-1368.

Rühli, F. J., Kuhn, G., Evison, R., Müller, R., & Schultz, M. (2007). Diagnostic value of micro-CT in comparison with histology in the qualitative assessment of historical human skull bone pathologies. *American journal of physical anthropology, 133*(4), 1099-1111.

Saracen, A., & Kotwica, Z. (2016). Complications of percutaneous vertebroplasty: An analysis of 1100 procedures performed in 616 patients. *Medicine, 95*(24), e3850.

Schlegel, K. A., Lang, F. J., Donath, K., Kulow, J. T., & Wiltfang, J. (2006). The monocortical critical size bone defect as an alternative experimental model in testing bone substitute materials. *Oral Surgery, Oral Medicine, Oral Pathology, Oral Radiology, and Endodontology, 102*(1), 7-13.

Seddighi, R., & Doherty, T. J. (2016). Field Sedation and Anesthesia of Ruminants. *Veterinary Clinics of North America: Food Animal Practice, 32*(3), 553-570.

Stefan, U., Michael, B., & Werner, S. (2010). Effects of three different preservation methods on the mechanical properties of human and bovine cortical bone. *Bone, 47*(6), 1048-1053.

Tamminen, I. S., Isaksson, H., Aula, A. S., Honkanen, E., Jurvelin, J. S., & Kröger, H. (2011). Reproducibility and agreement of micro-CT and histomorphometry in human trabecular bone with different metabolic status. *Journal of bone and mineral metabolism, 29*(4), 442-448.

Tarsuslugil, S. M., O'Hara, R. M., Dunne, N. J., Buchanan, F. J., Orr, J. F., Barton, D. C., & Wilcox, R. K. (2013). Development of calcium phosphate cement for the augmentation of traumatically fractured porcine specimens using vertebroplasty. *Journal of biomechanics, 46*(4), 711-715.

Teo, J., Wang, S. C., & Teoh, S. H. (2007). Preliminary study on biomechanics of vertebroplasty: a computational fluid dynamics and solid mechanics combined approach. *Spine, 32*(12), 1320-1328.

Thomsen, J. S., Laib, A., Koller, B., Prohaska, S., Mosekilde, L. I., & Gowin, W. (2005).

Stereological measures of trabecular bone structure: comparison of 3D micro computed tomography with 2D histological sections in human proximal tibial bone biopsies. *Journal of Microscopy, 218*(2), 171-179.

Thorwarth, M., Schultze-Mosgau, S., Kessler, P., Wiltfang, J., & Schlegel, K. A. (2005). Bone regeneration in osseous defects using a resorbable nanoparticular hydroxyapatite. *Journal of oral and maxillofacial surgery, 63*(11), 1626-1633.

Turner, A. S. (2002). The sheep as a model for osteoporosis in humans. *The Veterinary Journal, 163*(3), 232-239.

Turner, A. S. (2007). Experiences with sheep as an animal model for shoulder surgery: strengths and shortcomings. *Journal of shoulder and elbow surgery, 16*(5), S158-S163.

van Gaalen, S. M., Kruyt, M. C., Geuze, R. E., de Bruijn, J. D., Alblas, J., & Dhert, W. J. (2010). Use of fluorochrome labels in *in vivo* bone tissue engineering research. *Tissue engineering Part B: Reviews, 16*(2), 209-217.

Voss, L. J., Ludbrook, G., Grant, C., Sleigh, J. W., & Barnard, J. P. M. (2006). Cerebral cortical effects of desflurane in sheep: comparison with isoflurane, sevoflurane and enflurane. *Acta anaesthesiologica scandinavica, 50*(3), 313-319.

Walkowiak, K. J., & Graham, M. L. (2015). Pharmacokinetics and Antinociceptive Activity of Sustained-Release Buprenorphine in Sheep. *Journal of the American Association for Laboratory Animal Science, 54*(6), 763-768.

Waterman, A. E., Livingston, A., & Amin, A. (1991). Analgesic activity and respiratory effects of butorphanol in sheep. *Research in veterinary science, 51*(1), 19-23.

Welsh, E. M., Baxter, P., & Nolan, A. M. (1992). Pharmacokinetics of carprofen administered intravenously to sheep. *Research in veterinary science, 53*(2), 264-266.

Welsh, E. M., & Nolan, A. M. (1995). Effect of flunixin meglumine on the thresholds to mechanical stimulation in healthy and lame sheep. *Research in Veterinary Science, 58*(1), 61-66.

Wieding, J., Mick, E., Wree, A., & Bader, R. (2015). Influence of three different preservative techniques on the mechanical properties of the ovine cortical bone. *Acta of Bioengineering and Biomechanics, 17*(1), 137-146.

Wilke, H. J., Kettler, A., Wenger, K. H., & Claes, L. E. (1997). Anatomy of the sheep spine and its comparison to the human spine. *The Anatomical Record, 247*(4), 542-555.

Zullian, C., Lema, P., Lavoie, M., Dodelet-Devillers, A., Beaudry, F., & Vachon, P. (2016). Plasma concentrations of buprenorphine following a single subcutaneous administration of a sustained release formulation of buprenorphine in sheep. *Canadian Journal of Veterinary Research, 80*(3), 250-253.

Chapter 8

Conclusions and future perspectives

8.1. Conclusions

Multimodal analgesia, with low doses of multiple agents, like sedatives, NSAIDs, and opioids, seems to provide sufficient postoperative pain relief with minimal adverse effects. The advocated protocol was considered suitable – regarding the described surgical techniques – for controlling orthopaedic and neuropathic pain, as demonstrated by rapid animal recovery, with almost immediate food demand and herd behaviour. Nevertheless, other protocols may be adequate.

The developed PVP model, using a bilateral modified parapedicular approach, was considered appropriate for preclinical studies; still, it requires expertise and training. The designed defect is innovative regarding the approach. *Ex vivo* training revealed to be essential, as it allowed the surgeon to feel comfortable with the technique, and so to avoid the use of more living, sentient animals. *In vivo* procedures were successful with a high survival rate (100%) obtained.

Ancillary imaging – fluoroscopy and micro-CT – were crucial both in developing and applying the model and, regarding micro-CT, in further assessing the obtained samples. Micro-CT is a powerful tool that enables the analysis of the bone structure without destroying the sample, complementing histology and other means. Moreover, micro-CT gives the researcher the opportunity of predicting the bone behaviour, through the calculation of the structural parameters and mechanical strength and stiffness prediction. Researchers should always look for the best ancillary means (within reasonable economical limits) and techniques that provide as much information as possible without increasing the number of experimental units.

Spine-Ghost was successfully created as an injectable composite cement, presenting high bioresorbability and high bioactivity. It is particularly suited for vertebroplasty, since it is radiopaque, easily injected, it has a reduced setting time, and, once set, showed a mechanical strength comparable to the compressive strength of healthy vertebral trabecular bone. Moreover, *in vivo* it presented a biological response identical, if not superior, to the one elicited by the available commercial control, after a 6-month implantation time.

8.2. Future perspectives

In the line of the experimental work developed for this project several other ideas emerged.

Concerning the developed model, besides the obvious utility of testing other materials, it also should be of interest considerer the modified parapedicular approach for testing other surgical techniques like, for instance, kyphoplasty. Moreover, considering the well-known setbacks of using a sheep model – the hard cortical and trabecular bone –, but acknowledging the surplus benefits, in a next occasion the same model could be tested on long-term steroid-induced or ovariectomy-induced osteoporotic sheep, eventually fed with calcium-restricted diets, like preconized by several authors (Aldini *et al.*, 2002; Turner, 2002; Wu *et al.*, 2008, Ding *et al.*, 2010; Oheim *et al.*, 2012; Verron *et al.*, 2014). The major disadvantage of these animals is the time-consuming process to obtain them.

It would be interesting to further investigate, at different implantation times, the potential of the experimental material in promoting new bone formation. To do so, other imaging techniques could be use, like for instance, *in vivo* computer tomography or magnetic resonance imaging. Other alternative would be to alter the experimental design and choose different time intervals to sacrifice different animals, keeping in mind that this option must also comply with the 3R's concept and be very well justified.

Likewise it would be beneficial to predict – through the correlation with the 3D structural parameters – the mechanical strength and stiffness of the filled vertebral body defect, both *post-mortem* – which would require the animal sacrifice at different time intervals, if the model was the sheep – and *in vivo* – through an *in vivo* computer tomography; or, less factual but even so very accurate, through a micro-CT based finite element modelling (Jaecques *et al.*, 2004; Wirth *et al.*, 2010; Watson *et al.*, 2014).

Another technique that could have been explored to further assess the biological response of sheep vertebrae to the biomaterial was the reverse transcription-polymerase chain reaction (rt-PCR). An essential key for long-term survival and function of biomaterials is their bioactivity and the fact that they do not elicit a negative immune response. After a biomaterial is implanted into the body, the immune system initiates an immune response sequence, largely mediated by the local inflammatory microenvironment. Rt-PCR would allow to access this inflammatory response. This is of utmost interest regarding the developing of future

biomaterials, as it allows to improve biomaterials' integration and diminish the risk of chronic inflammation and/ or foreign body reaction, and ultimately to create biomaterials that are able to trigger the desired immunological outcomes and thus support the healing processes (Franz *et al.*, 2011; Olivares-Navarrete *et al.*, 2015).

Likewise, the measurement of serum, urine and saliva biomarkers is a non-invasive technique that can be used to complement imaging and histological analyses to assess the bone turnover, wherein specific antibodies are used to detect proteins (biomarkers) in cells within a chosen tissue. For that reason, it should be considered an asset when developing research projects involving animal models, as it allows the researcher to obtain more information from a given animal, at different time points, without sacrificing the same. According to Leeming *et al.* (2006) bone biomarkers can be divided in three groups: 1) bone formation markers; 2) bone resorption markers; and 3) osteoclast regulatory proteins. They are considered particularly useful in medicine to assess metabolic skeletal diseases, such as Paget's disease, osteoporosis, and other types of bone disorders, such as metastatic bone cancer (Leeming *et al.*, 2006). The main limitation of biomarkers to measure bone metabolism is their biological variability, dependent on numerous factors like age, gender, and disease, which hinders the establishment of reference values for serum and urine biomarkers levels (Seibel *et al.*, 2005); nevertheless, a recent study by Sousa *et al.* (2013) support the use of bone biomarkers to provide information regarding bone cellular activity in real time.

Finally, Spine-Ghost would benefit to be tested in different bone defect animal models or sites, thus extending its use to other applications. For instance, currently calcium sulphate injectable cements are described as good alternatives for vertebral compression fractures (Masala *et al.*, 2012) and augmentation around pedicle screws in the osteoporotic spine (Yi *et al.*, 2008), femoral neck fractures (Patel & Kamath, 2016) and femoral head osteonecrosis (Civinini *et al.*, 2012), tibial plateau fractures (Iundusi *et al.*, 2015), calcaneal fractures (Bibbo *et al.*, 2006; Chen *et al.*, 2011), distal radial fractures (Abramo *et al.*, 2010), proximal humerus fractures (Somasundaram *et al.*, 2013) and osteomyelitis (Karr *et al.*, 2011). These would possibly be good alternative applications to test the novel composite since favourable outcomes are predictable.

8.3. References

Abramo, A., Geijer, M., Kopylov, P., & Tägil, M. (2010). Osteotomy of distal radius fracture malunion using a fast remodeling bone substitute consisting of calcium sulphate and calcium phosphate. *Journal of Biomedical Materials Research Part B: Applied Biomaterials, 92*(1), 281-286.

Aldini, N. N., Fini, M., Giavaresi, G., Giardino, R., Greggi, T., & Parisini, P. (2002). Pedicular fixation in the osteoporotic spine: a pilot *in vivo* study on long-term ovariectomized sheep. *Journal of orthopaedic research, 20*(6), 1217-1224.

Bibbo, C., & Patel, D. V. (2006). The effect of demineralized bone matrix-calcium sulfate with vancomycin on calcaneal fracture healing and infection rates: a prospective study. *Foot & ankle international, 27*(7), 487-493.

Chen, L., Zhang, G., Hong, J., Lu, X., & Yuan, W. (2011). Comparison of percutaneous screw fixation and calcium sulfate cement grafting versus open treatment of displaced intra-articular calcaneal fractures. *Foot & ankle international, 32*(10), 979-985.

Civinini, R., De Biase, P., Carulli, C., Matassi, F., Nistri, L., Capanna, R., & Innocenti, M. (2012). The use of an injectable calcium sulphate/calcium phosphate bioceramic in the treatment of osteonecrosis of the femoral head. *International orthopaedics, 36*(8), 1583-1588.

Ding, M., Cheng, L., Bollen, P., Schwarz, P., & Overgaard, S. (2010). Glucocorticoid induced osteopenia in cancellous bone of sheep: validation of large animal model for spine fusion and biomaterial research. *Spine, 35*(4), 363-370.

Franz, S., Rammelt, S., Scharnweber, D., & Simon, J. C. (2011). Immune responses to implants–a review of the implications for the design of immunomodulatory biomaterials. *Biomaterials, 32*(28), 6692-6709.

Iundusi, R., Gasbarra, E., D'Arienzo, M., Piccioli, A., & Tarantino, U. (2015). Augmentation of tibial plateau fractures with an injectable bone substitute: CERAMENT™. Three-year follow-up from a prospective study. *BMC musculoskeletal disorders, 16*(1), 1-5.

Jaecques, S. V. N., Van Oosterwyck, H., Muraru, L., Van Cleynenbreugel, T., De Smet, E.,

Wevers, M., Naert, J., & Vander Sloten, J. (2004). Individualised, micro CT-based finite element modelling as a tool for biomechanical analysis related to tissue engineering of bone. *Biomaterials*, *25*(9), 1683-1696.

Karr, J. C. (2011). Management in the wound-care center outpatient setting of a diabetic patient with forefoot osteomyelitis using Cerament Bone Void Filler impregnated with vancomycin: off-label use. *Journal of the American Podiatric Medical Association*, *101*(3), 259-264.

Leeming, D. J., Alexandersen, P., Karsdal, M. A., Qvist, P., Schaller, S., & Tanko, L. B. (2006). An update on biomarkers of bone turnover and their utility in biomedical research and clinical practice. *European Journal* of *Clinical Pharmacology*, *62*(10), 781–792.

Lewis, G. (2006). Injectable bone cements for use in vertebroplasty and kyphoplasty: State-of-the-art review. *Journal of Biomedical Materials Research Part B: Applied Biomaterials*, *76*(2), 456-468.

Masala, S., Nano, G., Marcia, S., Muto, M., Fucci, F. P. M., & Simonetti, G. (2012). Osteoporotic vertebral compression fractures augmentation by injectable partly resorbable ceramic bone substitute (Cerament™| SPINE SUPPORT): a prospective nonrandomized study. *Neuroradiology*, *54*(6), 589-596.

Olivares-Navarrete, R., Hyzy, S. L., Slosar, P. J., Schneider, J. M., Schwartz, Z., & Boyan, B. D. (2015). Implant materials generate different peri-implant inflammatory factors: poly-ether-ether-ketone promotes fibrosis and microtextured titanium promotes osteogenic factors. *Spine*, *40*(6), 399-404.

Oheim, R., Amling, M., Ignatius, A., & Pogoda, P. (2012). Large animal model for osteoporosis in humans: the ewe. *European Cells & Materials*, *24*, 372-385.

Patel, H. M., & Kamath, A. F. (2016). Subchondral Insufficiency Fracture of the Femoral Head treated with Core Decompression and Bone Void Filler Support. *The Archives of Bone and Joint Surgery*, *4*(3), 264-268.

Seibel, M. J. (2005). Biochemical markers of bone turnover part I: biochemistry and variability. *The Clinical biochemist. Reviews/Australian Association of Clinical Biochemists.*, *26*(4), 97-122.

Somasundaram, K., Huber, C. P., Babu, V., & Zadeh, H. (2013). Proximal humeral fractures: the role of calcium sulphate augmentation and extended deltoid splitting approach in internal fixation using locking plates. *Injury*, *44*(4), 481-487.

Sousa, C. P., De Azevedo, J. T., Reis, R. L., Gomes, M. E., & Dias, I. R. (2013). Short-term variability in biomarkers of bone metabolism in sheep. *Lab animal*, *43*(1), 21-26.

Verron, E., Pissonnier, M. L., Lesoeur, J., Schnitzler, V., Fellah, B. H., Pascal-Moussellard, H., Pilet, P., Gaulthier, O., & Bouler, J. M. (2014). Vertebroplasty using bisphosphonate-loaded calcium phosphate cement in a standardized vertebral body bone defect in an osteoporotic sheep model. *Acta biomaterialia*, *10*(11), 4887-4895.

Turner, A. S. (2002). The sheep as a model for osteoporosis in humans. The Veterinary Journal, 163(3), 232-239.

Watson, N. A. D., Gandhi, A. A., Fredericks, D. C., Smucker, J. D., & Grosland, N. M. (2014). Sheep cervical spine biomechanics: A finite element study. *The Iowa orthopaedic journal*, *34*, 137-143.

Wirth, A. J., Mueller, T. L., Vereecken, W., Flaig, C., Arbenz, P., Müller, R., & Van Lenthe, G. H. (2010). Mechanical competence of bone-implant systems can accurately be determined by image-based micro-finite element analyses. *Archive of applied mechanics*, *80*(5), 513-525.

Wu, Z. X., Lei, W., Hu, Y. Y., Wang, H. Q., Wan, S. Y., Ma, Z. S., Sang, H. X., Fu, S. C., & Han, Y. S. (2008). Effect of ovariectomy on BMD, micro-architecture and biomechanics of cortical and cancellous bones in a sheep model. *Medical engineering & physics*, *30*(9), 1112-1118.

Yi, X., Wang, Y., Lu, H., Li, C., & Zhu, T. (2008). Augmentation of pedicle screw fixation strength using an injectable calcium sulfate cement: an *in vivo* study. *Spine*, *33*(23), 2503-2509.